

---

Insulin nanocomplexes formed by self-assembly from  
amine-modified poly(vinyl alcohol)-graft-poly(L-Lactide)  
for non-invasive mucosal delivery:  
Preparation, characterization and in vivo investigations

---

## **DISSERTATION**

zur Erlangung des Doktorgrades  
der Naturwissenschaften  
(Dr. rer. nat.)

dem Fachbereich Pharmazie  
der Philipps-Universität Marburg

vorgelegt von  
Michael Simon  
aus Ossendorf/Westfalen

Marburg/Lahn 2005

Vom Fachbereich Pharmazie der Philipps-Universität Marburg als Dissertation  
am 28.Oktober 2005 angenommen

Erstgutachter: Prof. Dr. T. Kissel

Zweitgutachter: Prof. Dr. U. Bakowsky

Tag der mündlichen Prüfung: 05.Dezember 2005

Die vorliegende Arbeit  
entstand auf Anregung und unter der Leitung von

*Herrn Prof. Dr. Thomas Kissel*

am Institut für Pharmazeutische Technologie und Biopharmazie  
der Philipps-Universität Marburg

## **Danksagung**

Mein besonderer Dank gilt meinem Doktorvater und Lehrer Herrn Prof. Dr. Thomas Kissel für die Betreuung der Arbeit und sein in mich gesetztes Vertrauen. Seine große Erfahrung und die stete Aufforderung zur Präsentation und Diskussion haben maßgeblich zum Gelingen der Arbeit, sowie zu meiner wissenschaftlichen Ausbildung beigetragen. Eine bessere Vorbereitung auf das Arbeitsleben in der pharmazeutischen Industrie könnte ich mir nicht vorstellen.

Für die Zusammenarbeit bei den in-vivo Untersuchungen an der medizinischen Poliklinik III in Giessen, schulde ich Herrn Prof. Dr. Thomas Linn und seinen Mitarbeiterinnen Frau Doris Erb und Gundula Hertel großen Dank. Die langjährige klinische Erfahrung von Prof. Linn auf dem Gebiet der diabetologischen Forschung und die hohe Motivation seiner Mitarbeiter, haben den Erfolg der Tierversuche sichergestellt.

Darüberhinaus danke ich Herrn Prof. Dr. Udo Bakowsky für die zahlreichen Untersuchungen am Rasterkraftmikroskop und die Gastfreundschaft am Institut in Saarbrücken. Seine sofortige Bereitschaft an der Darstellung und der Strukturaufklärung der Komplexe mitzuwirken, waren eine große Hilfe.

Für die Einarbeitung in die Titrationskalorimetrie und die Diskussion der Daten danke ich Herrn Dr. Frank Dullweber, Frau Dr. Jasmine Fokkens und Herrn Prof. Dr. Gerhard Klebe.

Allen Kollegen und Freunden, die mich während des Institutsalltages unterstützt und begleitet haben, danke ich für die Zusammenarbeit und das hervorragende Arbeitsklima.

Besonders möchte ich Herrn Dr. Matthias Wittmar erwähnen, der die untersuchten Polymere synthetisiert und charakterisiert hat. Ohne seine fachliche Kompetenz und seine Hilfsbereitschaft bei zahllosen Soft- und Hardware-Problemen, wäre vieles nicht so reibungslos abgelaufen. Desweiteren danke ich Frau Dr. Lea Ann Dailey und Frau Dr. Isabel Behrens für die Unterstützung bei den Zellversuchen und den Untersuchungen am konfokalen Mikroskop. Auch danke ich Frau Dr. Christine Oster und Herrn Dr. Ulrich Westedt für die vielen fachlichen Diskussionen und Kaffeepausen, die mir oft neue Impulse bzw Koffein für die weitere Forschungsarbeit gegeben haben.

Nicht zuletzt gilt ein Dank meinen Eltern und besonders meiner Freundin Melanie, die in den vergangenen Jahren wegen dieser Arbeit auf so manches verzichten musste. Ihr Beistand hat mich durch alle Höhen und Tiefen begleitet.

"Es ist nicht gut, vor Wirklichkeiten zu tun,  
als ob sie nicht wären, sonst rächen sie sich"

*(Romano Guardini)*

## Table of contents

### Chapter 1: Introduction

1.1. Rationale of systemic delivery of peptides and proteins across absorptive mucosae	8-9
1.2. Non-invasive insulin delivery across mucosal surfaces	
1.2.1 The most important therapeutic protein: Insulin	10-11
1.2.2 Major types of Diabetes mellitus	11-12
1.2.3 Conventional insulin therapy	12-14
1.2.4 Strategies of noninvasive insulin delivery	14-17
1.2.5 Focus: Nasal insulin delivery	17-20
1.3. A novel nasal insulin delivery system for insulin	
1.3.1 Multifunctional polymers: Bioadhesive and biodegradable	20-21
1.3.2 Self-assembly with insulin to nanocomplexes	22
1.3.3 A novel class: Watersoluble DEAPA polymers	23
1.4. Objectives of the work	24
1.5. References	25-27

### Chapter 2: Self-Assembling Nanocomplexes from Insulin and Water-Soluble Branched Polyesters, Poly[(vinyl-3-(diethylamino)-propyl-carbamate-co-(vinyl acetate)-co-(vinyl alcohol)]-graft-poly(L-lactic acid): A Novel Carrier for Transmucosal Delivery of peptides

2.1. Abstract	29
2.2. Introduction	30-32
2.3. Materials and Methods	32-36
2.4. Results and Discussion	
2.4.1 Synthesis and structural characterization of the Copolymers	37-40
2.4.2 Formation of nanocomplexes with insulin	41-44
2.4.3 Nanocomplex Characterization	45-46
2.4.4 Microcalorimetry	46-48
2.4.5 Visualization of nanocomplexes	49-52
2.5. Conclusion	53
2.6. References	54-57

**Chapter 3:** Insulin containing nanocomplexes formed by self-assembly from biodegradable amine-modified poly(vinyl alcohol)-graft-poly(L-lactide): Bioavailability and nasal tolerability in rats

<b>3.1. Abstract</b>	59
<b>3.2. Introduction</b>	60-61
<b>3.3. Materials and Methods</b>	61-64
<b>3.4. Results and Discussion</b>	
<b>3.4.1 Non Diabetic Rats</b>	64-69
<b>3.4.2 Diabetic rats</b>	69-
<b>3.4.3 Histological Studies</b>	732
	74-76
<b>3.5. Conclusion</b>	77
<b>3.6. References</b>	78-80

**Chapter 4:** Nanosized carriers for insulin based on amine-modified graft polyesters: Protection from enzymatic degradation, interaction with Caco-2 cell monolayers, peptide transport and cytotoxicity

<b>4.1. Abstract</b>	82
<b>4.2. Introduction</b>	83-84
<b>4.3. Materials and Methods</b>	85-89
<b>4.4. Results and Discussion</b>	
<b>4.4.1 Preparation of nanocomplexes and nanoparticles</b>	89-90
<b>4.4.2 Protection from enzymatic degradation of insulin in NC</b>	90-93
<b>4.4.3 In vitro cytotoxicity studies</b>	94-98
<b>4.4.4 Confocal laser scanning miocrosopy</b>	98-100
<b>4.4.5 Transport studies</b>	100-101
<b>4.5. Conclusion</b>	102
<b>4.6. References</b>	103-105

**Chapter 5:** Summary and Outlook

106 -114

**Appendices**

115 -119

# **Chapter 1**

## Introduction

Parts Published in “Away with the needle. Noninvasive administration routes for insulin: improved quality of life for diabetics”

Pharmazie in unserer Zeit  
Deutsche Pharmazeutische Gesellschaft, DPhG  
Volume 30(2) 136-141, 2001

## **1.1. Rationale of Systemic Delivery of Peptides and Proteins Across Absorptive Mucosae**

Advances in biotechnology have accelerated the economical, large-scale production of therapeutically active peptides and proteins, making them readily available for therapeutic use. In most cases such compounds are indicated for chronic therapy, and they will need to be administered by an appropriate delivery system. Although the oral route is preferred for the administration of drugs, particularly those required in chronic therapies, this is not feasible for the systemic delivery of most peptide and protein drugs (1). Their rapid hydrolytic and enzymatic degradation in the hepatogastrointestinal “first-pass” elimination renders oral administration impractical. The general approach to deliver peptides and proteins has been parenteral administration, which is invasive and inconvenient. As a result, transmucosal delivery of peptide- and protein-based pharmaceuticals has been actively investigated in recent years, and some products are already available on the market. This route offers the advantage of being non-invasive, and it holds great potential for the application of rate-modulated delivery systems.

Two major barriers a.) the physicochemical barrier, stemming from the physiology and histology of the various mucosae and b.) the enzymatic barrier, impede successful transmucosal delivery (2). The former effectively deters permeation of large macromolecules, while the latter works in tandem to break down peptides and proteins of any sizes. Thus, bioavailabilities of peptides and proteins are usually less than 1% on transmucosal administration if no other adjuvants are added. To counter these barriers and to increase bioavailability, several approaches have been used. Enzyme inhibitors and permeation enhancer represent two classes of adjuvants that have been used effectively, albeit not always safely. The present popular approach has been to use biodegradable polymers for nano-/microparticles, which stabilize the peptide and allow for a controlled-release delivery system.

## 1.2. Non-invasive insulin delivery across mucosal surfaces

### 1.2.1. The most important therapeutic protein: Insulin

Insulin is synthesized in humans and other mammals in beta cells (B-cells) of the islets of Langerhans in the pancreas. One to three million islets of Langerhans (pancreatic islets) form the endocrine part of the pancreas, which is primarily an exocrine gland. The endocrine part accounts for only 2% of the total mass of the pancreas. Within the islets of Langerhans, beta cells constitute 60-80% of all the cells. Insulin comprises 51 amino acids and is one of the smallest proteins known; shorter 'proteins' are usually referred to as (poly)peptides. Beef insulin differs from human insulin in two amino acids, and pork insulin in one. Fish insulins are resembling human insulin and show hormonal activity in man.

Insulin is structured as 2 polypeptide chains linked with 2 sulfur bridges and has a molecular weight of about 5.7 kDa (see figure 1).

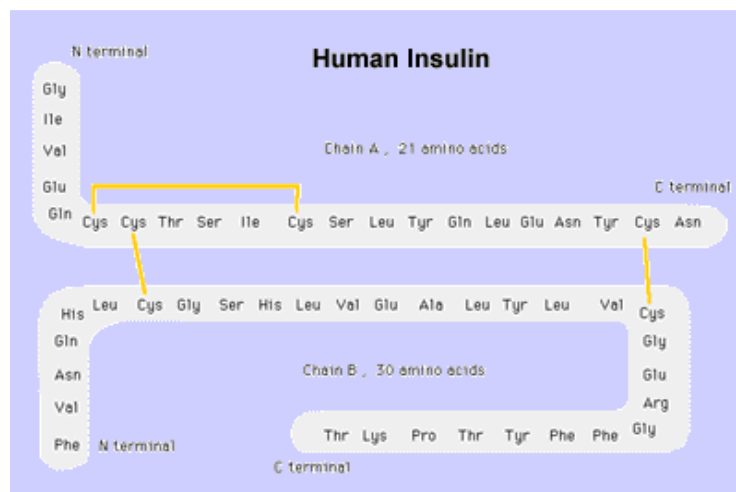


Figure 1.

Chain A consists of 21, and chain B of 30 amino acids. Insulin is produced as a prohormone - proinsulin that is later transformed by proteolytic action into the active hormone.

The actions of insulin on the human metabolism level include:

- cellular uptake of certain substances, most prominently glucose
- increase of DNA replication and protein synthesis
- modification of the activity of numerous enzymes (allosteric effect)
- increased glycogen synthesis → causes storage of glucose in liver (and muscle) cells in the form of glycogen
- increased fatty acid synthesis → causes fat cells to take up glucose which is converted to fatty acids
- increased esterification of fatty acids → causes adipose tissue to make fats (triglycerides) from fatty acid esters
- decreased proteinolysis → causes reduction of protein degradation
- decreased lipolysis → causes reduction in conversion of fat cell lipid stores into blood fatty acids
- decreased gluconeogenesis → decreases production of glucose from various substrates in liver

An insufficient insulin production, a resistance to insulin or a combination of both, causes a serious disease: Diabetes mellitus.

### **1.2.2. Major types of Diabetes mellitus**

#### **Type 1 Diabetes**

Type 1 diabetes can develop at any age; however, it usually develops in children and young adults, which is why it was formerly designated juvenile diabetes. The classification was previously based on the need for insulin (insulin-dependent diabetes mellitus, IDDM), because insulin injections must be taken daily. Now, the type of diabetes is determined by the etiological process rather than the treatment modality. Type 1 diabetes is thus characterized by islet cell destruction and type 2 diabetes by a combination of defects in insulin secretion and action. About 5% to 10% of all people with diabetes have type 1 diabetes. Type 2 diabetes is the most common type of diabetes, and gestational and secondary diabetes are other forms of the disease. Type 1 diabetes develops because of an autoimmune response in which the body destroys its own pancreatic beta cells. What causes the autoimmune response is

unknown. However, it is discussed that the disease may not develop without the presence of environmental factors, such as exposure to certain viral infections (Coxsackie B). People who have first grade relatives with type 1 diabetes are more likely to develop the disease; however, most people with type 1 do not have a family history of the disease. Other factors that increase a person's risk are being white and having islet cell antibodies in the blood.

### **Type 2 Diabetes**

Type 2 diabetes is a lifelong disease that develops when the pancreas cannot produce enough insulin or when the body's tissues become resistant to insulin. Blood sugar can rise to an unsafe level even before diabetes symptoms occur. Type 2 diabetes can develop at any age, although it usually develops in adults (adult-onset diabetes). It was also called non-insulin-dependent diabetes mellitus (NIDDM), because it can often be treated without using insulin. Between 90% and 95% of all diabetics have type 2 diabetes. Some people believe, incorrectly, that type 2 diabetes is a milder form of the disease than type 1 diabetes, but it can cause the same harmful effects as type 1. Type 2 diabetes is caused by insulin resistance, which occurs when the body's cells and tissues do not respond properly to insulin. Weight, level of physical activity, and family history affect how the body responds to insulin. People who are overweight, get little or no exercise, or have diabetes in their family have an increased risk of developing type 2 diabetes. The conventional treatment of typ 2 diabetes includes a balanced diet, oral anti-diabetics and if necessary insulin substitution.

#### **1.2.3. Conventional insulin therapy**

The subcutaneous route, requiring single or multiple daily injections, is the mainstay of conventional insulin therapy. There are numerous disadvantages to injectable insulin therapy:

Poor patient compliance due to pain or discomfort, inconsistent pharmacokinetics, adipolysis at the site of injection and social stigma.

For no other protein, such an enormous research effort was spent in the last decades, on academic as well as industrial level, to develop non-invasive delivery systems. Not at least do to the increasing number of people worldwide affected by diabetes, e.g. 2002 in the US 13,0 million people with diagnosed diabetes (American Diabetes Association), a huge commercial potential for a non-invasive insulin delivery system can be assumed.

The therapeutic insulin era began in 1922 with the first clinical use of insulin by Banting and Best. In the ensuing 80 years, scientists uncovered the basic pathophysiology of diabetes, gradually elucidated insulin structure and focused their attention on developing better insulin formulations (e.g. NPH, lente). Despite these advances, mimicking physiological patterns of insulin secretion has proven to be virtually impossible and the goal of restoring and maintaining blood glucose and other metabolic parameters at near normal levels in diabetic patients are elusive (3). Vascular complications due to the long-term dysmetabolic milieu remain a major cause of morbidity and mortality among diabetic patients. The administration of insulin in the form of a bolus subcutaneous injection has been the basis of insulin therapy since its introduction. However, this feature is central to the problem of glycaemic control since the pharmacokinetics of conventional insulin preparations given by this route make it virtually impossible to replicate the physiological pattern of nutrient-related and basal insulin secretion. Improvements in glycaemic control are expected with the combined use of rapid-acting (e.g. lispro, aspart, glulisine) and long-acting insulin analogues (e.g. glargine, detemir) given by the s.c. route (4,5). However, dependence on s.c. administration of insulin to improve glycaemic control has resulted in increasingly complex and intensive insulin regimes involving multiple daily injections, or continuous insulin infusion using a variety of pumps aided by increasingly sophisticated glucose monitoring devices. Attempts to develop alternative routes of administering insulin began soon after the introduction of insulin therapy

in the 1920s. Since then, almost every conceivable route has been studied, including rectal, ocular and vaginal delivery, but these with limited success. Some of the most promising routes, strategies and commercial developments, particular in phase III clinical trials, are shortly reviewed in the following chapter.

#### **1.2.4. Strategies of non-invasive insulin delivery**

##### **Peroral (enteric-gastrointestinal)**

From all possible application routes, the oral administration of insulin provides by far the greatest challenge. Polypeptides are degraded in the acidic environment of the stomach and by digestive enzymes, especially in the small intestine. Numerous individual and combined strategies have been devised to enhance insulin absorption. These include the co-administration of insulin with enzyme inhibitors and/or permeation enhancer, methods designed to improve insulin chemical stability and the use of muco-bioadhesives, liposomes, emulsions and polymer-based delivery systems. Coating with a pH dependent acrylic based polymer and its encapsulation in microspheres and nanoparticles (6-10). The most promising approach to date is hexyl-insulin-monoconjugate-2 (HIM2), a native recombinant insulin with a small polyethylene glycol 7-hexyl group attached to the position B29 amino acid lysine, currently in development (Nobex Cooperation and Glaxo Smith Kline). Preclinical and pharmacokinetic and safety data for HIM2 are running. Ongoing phase I and II clinical trials suggest that oral HIM2 has a bioavailability of ~ 5% and may result in an acceptable glucose-lowering effect (11). While the concept is promising, its far away from approval and still faces significant hurdles.

## **Oral-buccal sublingual**

The oral mucosa offers a number of attractive features for administration of polypeptide drugs. The oral cavity is easily accessible, has a large surface area (100-200 cm<sup>2</sup>) with little proteolytic activity and is highly vascularized. However, in practice the multilayered structure of the squamous epithelium of the buccal and sublingual mucosae combined with the continuous but highly variable flow of saliva in the mouth constitutes an effective barrier to absorption. The use of absorption enhancer (surfactants, bile salts, chelators, alcohol and fatty acids), alone or combined with bioadhesive delivery systems (gels, films, patches) has been extensively tested in animal studies. Furthermore the addition of enzyme inhibitors and/or molecular modifications to increase the lipophilicity of the insulin molecule (conjugation with various polymers, acylation, methylation) and the use of prodrugs (12,13). Further efforts have been made to develop mucoadhesive delivery systems (14) and liposomal formulations, including highly deformable lipid vesicles (transferosomes) (15). A liquid aerosol formulation comprising mixed micelles made from a combination of absorption enhancers has been developed by Genex Biotechnology Cooperation (Toronto, Canada), the Oralin™ (oral insulin spray) is delivered by the RapidMist™ metered-dose applicator (16). Local tolerability appears acceptable, but bioavailability remains low, necessitating repeated administrations.

## **Transdermal**

Although the skin is easily accessible and has a large surface area (1-2 m<sup>2</sup>), it is relatively impermeable to large, hydrophilic polypeptides such as insulin. Attempts to optimize transdermal insulin delivery have involved breaking down or removing the lipid barrier, the stratum corneum by a variety of chemical, electrical or physical methods. Iontophoresis (17), low- frequency ultrasound, phonophoresis (18) and/or the use of drug carrier agents (19) are the main methodologies being explored. Apart from the issue of safety of the various chemical and physical pretreatments used, the long-term biophysical impact of iontophoresis

remains uncertain. Altea Therapeutics (Atlanta, USA) has developed a transdermal patch (AT 1391) that delivers basal insulin over a 12h period. It consists of a reusable disk-shaped device powered by a small battery, creating micropores by generating an electric pulse that vaporizes the epidermis. The second component is a patch that delivers insulin through the microscopic pores. Steady-state insulin levels occur within a couple of hours. The Altea system recently entered phase 1 clinical trials.

## **Pulmonary**

The respiratory tract, with an estimated surface area of 140 m<sup>2</sup>, offers great potential for the delivery of polypeptide drugs. The alveolar surface, which accounts for > 95% of the absorptive area, is lined by a very thin (0.1-0.2 μm) vesiculated and richly perfused monolayer of epithelial cells, which allow for a rapid uptake and a fast onset of action after inhalation. Of the entirely new insulin delivery systems, the inhaled insulin is the most likely to make it to the marketplace. The breakthrough for pulmonary peptide delivery was in the 1990's when the importance of aerosol dynamics was recognized. Many factors are known to influence the site of deposition of inhaled particles, including size, aerodynamic diameter, surface morphology, charge, solubility and hygroscopicity (20). For optimal deep lung deposition efficacy, particles should have low velocity and a size between 1 and 3 μm in diameter. In this regard, the specific device has a major impact on the metabolic effect and on reproducibility of the applied insulin (21). Current pulmonary drug delivery systems include a variety of pressurized metered dose inhalers (pMDI), dry powder inhalers (DPI), nebulizers and aqueous mist inhalers (AMI). Most of the recent clinical experience with inhaled insulin has been obtained using a dry powder formulation in the Nektar/Exubera® device (Nektar Therapeutics Inc., San Carlos, CA, Aventis, Bridgewater, NJ, Pfizer, NY), or liquid aerosols formulations in the AERx® Insulin Diabetes Management System (Aradigm Corp., Hayward, CA, NovoNordisk A/S, Copenhagen, Denmark) and in the Aerodose® Inhaler (Aerogen Inc.,

Sunnyvale, CA, USA). Other delivery technologies include the use of modified particles in the AIR™ Pulmonary Drug Delivery System (Advanced Inhalation research Alkermes, Cambridge, MA, Eli Lilly, Indianapolis) and in the form of Technosphere™ insulin (Mannkind Biopharmaceuticals, NY, USA) (8,22,23). Concerns still exist about side effects like cough caused by use of the inhalant devices, an increase of insulin antibodies and scarring in the lungs. Although several of these devices are well into phase III trials, application for FDA approval is not expected this year as studies continue to verify the safety of these products .

### **1.2.5. Focus: Nasal insulin delivery**

Even if the emphasis of current efforts is concentrated on pulmonary insulin delivery, there is also the nasal application of insulin in form of nosedrop/-spray still highly interesting. The nasal application of peptides is the only route of administration from the mentioned non-parenteral delivery concepts, that has gained numerous regulatory approvals so far:

- *Miacalcin*®: Calcitonin,  $M_w$  3500 (Novartis)
- *Synarel*®: Nafarelin acetate ( $M_w$  1322), Gonadotropin releasing hormone GnRH (Pharmacia/Pfizer)
- *DDAVP*®: Desmopressin,  $M_w$  1068 (Ferring)
- *Suprefact*®: Buserelin,  $M_w$  1300 (Aventis)
- *Syntocinon*®: Oxytocin,  $M_w$  1007 (Novartis)

These drugs are characterized by a low molecular weight and a high potency. Thus, therapeutic plasma concentrations of these drugs can be achieved at relatively low doses. In contrast, a marketable insulin preparation would require much higher bioavailabilities. A nasal insulin delivery is therefore a much greater challenge.

The nasal cavity offers an epithelial surface of approximately 150 cm<sup>2</sup> but the main barriers include the very active mucociliary clearance mechanism and the presence of proteolytic enzymes. As early as 1923, Woodyatt attempted to administer insulin intranasally and in

1932, Collins and Goldzieher achieved sufficient insulin absorption across the nasal mucosa to produce a hypoglycaemic effect in subjects with diabetes mellitus. Progress in intranasal application of insulin has been dependent on the use of safe absorption promoters, which are able to enhance the absorption of insulin in clinically relevant doses (24). Table 2 summarizes insulin nasal absorption promoting systems. An extensive range of enhancer has been used to increase the absorption of insulin across the nasal mucosa. These include bile salts and their derivatives, surfactants, fatty acids and their derivatives and cyclodextrins (25-27). Other methods used to improve insulin absorption involve inhibiting nasal proteases and/or retarding the removal of insulin with bioadhesives (26-28). The bioavailability of intranasal insulin varies according to the type, volume and concentration of both the enhancer and the insulin. Furthermore can the size, density, shape and hygroscopicity of the particles, the nasal airflow characteristics and the presence of any nasal pathology be of significant influence. In humans, when compared with s.c. route, nasal insulin absorption is much quicker, but the bioavailability is lower, at less than 20% (29), and the variability is higher (30). Clinical studies in patients with type 1 and type 2 diabetes have revealed a rapid but relatively short-lived increase in plasma insulin following nasal administration with multiple doses required to control postprandial hyperglycaemia (31,32). However, metabolic control was frequently inferior to s.c. insulin and many patients suffered local nasal irritation (32,33). More recently, a lyophilized nasal insulin preparation containing sodium glycocholate given preprandially achieved glycaemic control equivalent to a regimen of twice daily NPH insulin in patients with type 2 diabetes over a 4-month period (34). A gel formulation developed subsequently was found to have equivalent efficacy to s.c. insulin and improved nasal tolerance in type 1 diabetes patients treated over a 6-month period (35). To date, the relatively limited clinical experience with intranasal insulin demonstrates a need for high and repeated doses to achieve glycaemic control.

Type of compound	Enhancer/promoter	Example	F <sub>ab</sub> /F <sub>rel</sub> (%) <sup>1</sup>	Reference	Possible mechanism of action of each class
<i>Absorption enhancers</i>					
Bile salts (and derivatives)	Sodium deoxycholate/ -glycocholate/ -taurodihydrofusidate	1% SDC spray 1% SGC spray 4% SGC spray 1% STDHF spray 1% STDHF spray	20 12-12.5 67.5 11.4 7.1-9.2	Pontiroli A.E., Br. Med. J. 284 (1982) 303-306 Moses A.C., Diabetes 32 (1983) 1040-47 Pozza G., Clin. Pharm. 17 (1989) 209-307 Nolte M.S., Horm. Metab. Res. 22 (1990) 170-174	Disrupt membranes, open tight junctions, enzyme inhibition, mucolytic activity
Surfactants	Sodium lauryl sulphate, saponin, polyoxyethylene-9-lauryl ether	0.8% Laureth-9 spray	21.6	Pontiroli A.E., Diabet. Metabol. 13 (1987) 441-443	Disrupt membranes
Chelating agents	Ethylenediaminetetraacetic acid, salicylates		-	Aungst B. J., Pharm Res. 5 (1986) 305-308	Open tight junctions
Fatty acids (and derivatives)	Sodium caprylate, sodium laurate, phospholipids (e.g. didecanoylphosphatidylcholine, lysophosphatidylcholine)	2% DDPC spray 2% DDPC spray	6.4-11.2 / 20 8.8-13.2 / 9.9-14.8	Drejler K., Diabet. Med. 9 (1992) 335-340 Jacobs M.A., Diabetes 42 (1993) 1649-55	Disrupt membranes
Enzyme inhibitors	Bestatin, amastatin, aprotinin		-	Morimoto K., Int. J. Pharm. 113 (1995) 1-8	Enzyme inhibition
Miscellaneous	Cyclodextrins, N-acetyl cystein,	DM-βCD powder (0.25 mg/kg)	3.4-5.1	Merkus F.W., J. Control. Rel. 41 (1996) 69-75	Disrupt membranes, open tight junctions
<i>Bioadhesive materials</i>					
Powders	Carbopol, starch microspheres, chitosan, albumin, starch	Starch microspheres Starch microspheres  Chitosan powder  Maize starch/ Carbopol 974P powder	30 4.5  17.0  9.9-14.4	Bjork E., Int. J. Pharm. 47 (1988) 233-238 Illum L., Int. J. Pharm. 57 (1989) 49-54 Dyer A.M., Pharm. Res. 19 (2002) 998-1008 Callens C., J. Control. Rel. 66 (2000) 215-220	Reduce nasal clearance, open tight junctions,
Liquids, Gels	Chitosan, carbopol, carboxy-methylcellulose, hydroxypropyl-cellulose	Carbopol gel	20.6	Najafabadi A.R., Drug Deliv. 11 (5) 295-300 (2004). Illum L., Pharm. Res. 11 (1994) 1186-9 Morimoto K., J. Pharm. Pharmacol. 37 (1985) 134-136	

**Table 2.** Nasal absorption promoting systems

<sup>1</sup> F<sub>ab</sub>: absolute bioavailability, F<sub>rel</sub>: relative bioavailability (to subcutaneous route)

The occurrence of nasal irritation and the potential for damage to the nasal mucosa and nasal-ciliary function (36) are a cause for concern, especially when viewed in the context of the need for long-term exposure. In order for intranasal insulin to become a clinical viable alternative to s.c. insulin, major obstacles still remain to be overcome.

### **1.3. A novel nasal insulin delivery system for insulin**

#### **1.3.1. Multifunctional polymers: Bioadhesive and biodegradable**

Bioadhesive polymers - multifunctional macromolecules which are able to increase the permeability of epithelial tissues and to simultaneously inhibit proteolytic enzymes. By virtue of mucoadhesive properties these polymers make close contact to mucosa, thereby exerting such effects at locally high concentrations in a limited area. Desirable features: (a) no irritation or cell sensitivity, (b) sufficiently adhesive, (c) easily removable. In the case of bioadhesive particulate drug delivery systems, the term bioadhesion is typically used to describe the adhesion between polymeric nanoparticles, either synthetic or natural, and soft tissues (i.e., gastrointestinal mucosa). Although the target of many bioadhesive delivery systems may be a soft tissue cell layer (i.e., epithelial cells), the actual adhesive bond may form with either the cell layer, a mucous layer, or a combination of the two. The process involved in the formation of such bioadhesive bonds has been described in two major steps (37): 1. Contact stage: An intimate contact is formed between the mucoadhesive and mucous membrane. 2. Consolidation stage: Various physicochemical interactions occur to consolidate and strengthen the adhesive joint, leading to prolonged adhesion.

It has been stated that at least one of the following polymer characteristics are required to obtain adhesion:

- (a) sufficient quantities of hydrogen-bonding chemical groups ( $\text{—OH}$ ) and ( $\text{—COOH}$ )
- (b) anionic/cationic surface charges
- (c) high molecular weight
- (d) high chain flexibility
- (e) surface tensions that will induce spreading into the mucous layer

Each of these characteristics favors the formation of bonds that are either chemical or mechanical in origin. Types of chemical bonds include strong primary as well as weaker secondary forces such as ionic bonds, van der Waals interactions, and hydrogen bonds. Although individually these forces are very weak, strong adhesions can be produced through numerous interaction sites. Therefore polymers with numerous reactive, polar groups such as carboxy- or hydroxyl-groups tend to develop intense mucoadhesive bonds.

For the nanocomplexes we employ polyvinylalcohol as basis, a polymer which exhibits a large quantity of such groups. In addition, a further synthetic modification through grafting with hydrophobic lactide groups or the charge modification by introduction of anionic sulfobutyl- or cationic amine-groups, favor and strengthen the bioadhesive character. Potential advantages of nanoparticulate systems based on mucoadhesive polymers in drug delivery:

- Prolong delivery of drugs in all non-parenteral routes of administrations
- Localization for purposes of local therapy
- Targeting to specific diseased tissues
- Localization for purposes of
  - permeability modification
  - protease and other enzyme inhibition
  - modulations of immunologic expression
- Improve the viability of non-parenteral, non oral routes of drug administration

### **1.3.2. Self-assembly with insulin to nanocomplexes (NC)**

Colloidal carriers may take many forms: liposomes, niosomes, nanoparticles and microemulsions. The conventional preparation techniques to manufacture nanoparticulate systems are based on emulsification, evaporation, solvent displacement and salting out procedures. Commonly however these methods have the disadvantage of involving heat, sonication, organic solvents or toxic chemical crosslinking agents (38). Each of these factors can alter the delicate structure of insulin, resulting in its loss of bioactivity. Therefore a spontaneous self-assembly between insulin and a polymer to defined complexes, under gentle conditions, would be a promising approach.

The different amino acids side chains of insulin possess a variety of chemical and physical properties, which result in a behaviour far more complex than those of small ligands. All the interactions important for bioadhesion (electrostatic, hydrophobic, hydrogen bonds, steric effects) can occur simultaneously among insulin and segments of the polymer, directing both protein folding and complexation. The two most important parameters governing polymer/protein assembling in water are hydrophobic and electrostatic interactions. The association of both partners results in soluble species, including complexes with insoluble proteins such as membrane proteins, complex coacervation, precipitation, or gelation. In the case of soluble species the complexation possibly stops at an optimum size that is usually thought to be a balanced structure in equilibrium. Roughly summarized, three types of soluble mixed compounds have been observed (39): small “hairy” proteins (i.e. surrounded by many synthetic polymer chains), long “necklaces” containing several proteins along one polymer chain, and aggregates of both partners that did not sediment.

### 1.3.3. A novel class: watersoluble DEAPA polymers

In our working group a novel class of biodegradable polymers was synthesized and characterized (40). The polymers based on poly(vinyl alcohol) were charged modified, grafted with D,L-lactide and -glycolide and utilized e.g. for tetanus parenteral vaccination (41). The second generation of these graft polymers were composed of amine modified components (*diethylamino-propylamine*, *dimethylamino-propylamine*, *diethylamino-ethylamin*) and proved to be useful for DNA delivery (42,43). This work focus on the water soluble polymers of this class, which are characterized by short lactide side chains. (see figure 2).

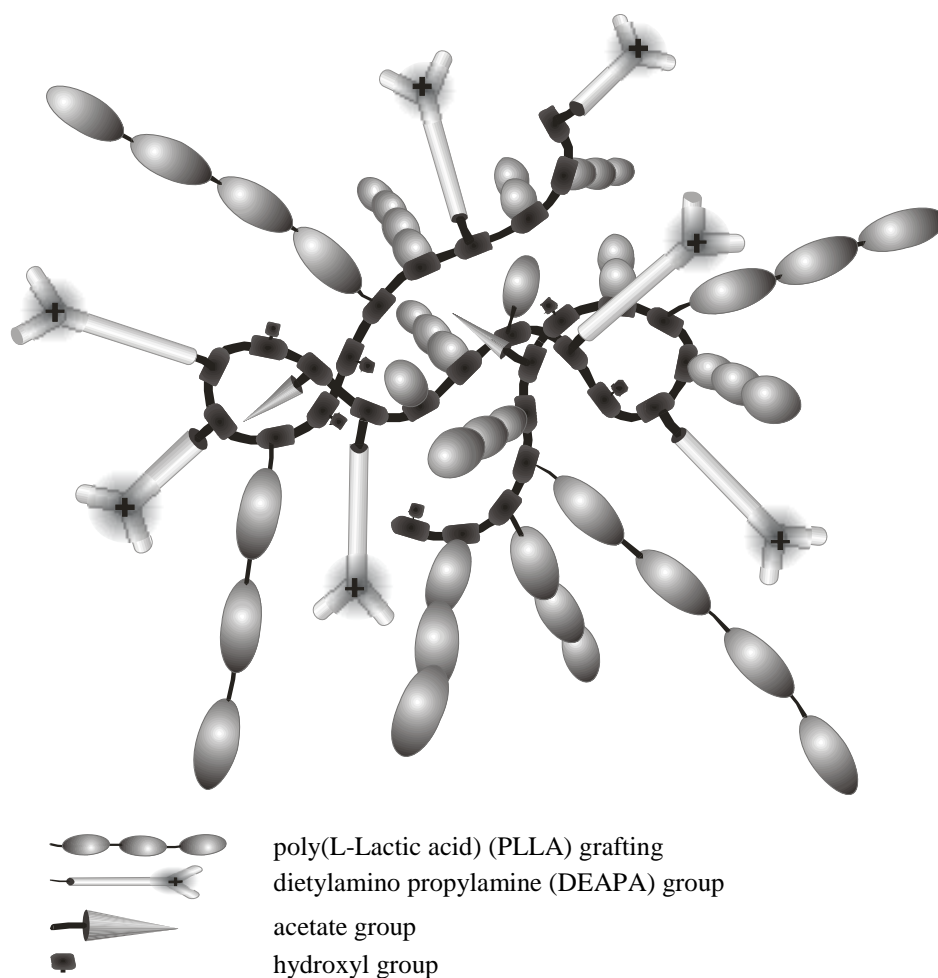


Figure 2: Drawing of a watersoluble DEAPA polymer demonstrating the comb-like structure with multiple interaction sites.

## 1.4. Objectives of this work

In this work, the short-chain comb polyesters are investigated for their suitability as a mucosal drug delivery system for insulin, with respect to:

### **Complexation with insulin (*Chapter 2*)**

- ▶ feasibility of self-assembling with insulin to obtain a stable colloidal solution
- ▶ incorporation of insulin to the highest possible amount
- ▶ controlling particle size in the nanometer range
- ▶ stability in medium
- ▶ binding characteristics of the complex
- ▶ structure function relationships

### **In-vivo-investigations (*Chapter 3*)**

- ▶ feasibility of nasal insulin delivery with NC in a healthy rat model
- ▶ transferability to a diabetic rat model
- ▶ pharmacodynamic and pharmacokinetic parameters
- ▶ relative and absolute bioavailability
- ▶ structure, concentration / effect relationships
- ▶ acute histological effects on the site of absorption

### **In-vitro-characteristics (*Chapter 4*)**

- ▶ protection against enzymatic degradation
- ▶ transport in cell culture model
- ▶ cytotoxicity and reversibility
- ▶ surfactant character of polymers
- ▶ comparison of nanocomplexes with a DEAPA- nanoparticle formulation

Developing safe and effective nasal delivery systems for insulin is an exciting and demanding challenge and there is no doubt that the commercial availability of a nasal insulin formulation would represent a major breakthrough in the treatment of diabetes mellitus and help to improve the lives of millions of diabetics.

## 1.5. References

- (1) P. L. Smith, D. A. Wall, H. Gochoco, and G. Wilson. Routes of delivery: case studies. Oral absorption of peptides and proteins, *Adv Drug Deliv Rev.* **8**: 253-290 (1992)
- (2) X. H. Zhou, and Li Wan Po. Comparison of enzyme activities of tissues lining portals of absorption of drugs: Species differences, *Int J Pharm.* **70**: 271- (1991)
- (3) DCCT, The effect of intensive treatment of diabetes on the development and progression of long-term complications in insulin-dependant diabetes mellitus, *N Engl J Med.* **329**: 977-986 (1993).
- (4) I. B. Hirsch. Insulin analogues, *N Engl J Med.* **352(2)**: 174-83 (2005).
- (5) M. Vazquez-Carrera and J. S. Silvestre. Insulin analogues in the magement of diabetes, *Methods Find Exp Clin Pharmacol.* **26(6)**: 445-461 (2004).
- (6) G. P. Carino and E. Mathiowitz. Oral insulin delivery, *Adv Drug Deliv Rev.* **35(2-3)**: 249-257 (1999).
- (7) A. Fasano. Innovative strategies for the oral delivery of drugs and peptides, *Trends Biotechnol.* **16(4)**: 152-157 (1998).
- (8) D. R. Owens, B. Zinman and G. Bolli. Alternative routes of insulin delivery, *Diabet Med.* **20**: 886-898 (2003).
- (9) G. P. Carino, J. S. Jacobs and E. Mathiowitz. Nanosphere based oral insulin delivery, *J Control Release* **65(1-2)**: 261-269 (2000)
- (10) W. T. Cefalu. Evolving strategies for insulin delivery and therapy, *Drugs* **64(11)**: 1149-1161 (2004).
- (11) J. G. Still. Development of oral insulin: progress and current status, *Diabetes Metab Res Rev.* **18(1)**: 29-37 (2002).
- (12) F. Veuillez, Y. N. Kalia, Y. Jacques, J. Deshusses and P. Buri. Factors and strategies for improving buccal absorption of peptides, *Eur J Pharm Biopharm.* **51**: 93-109 (2001).
- (13) J. A. Hoogestrat and P. W. Wertz. Drug delivery via the buccal mucosa, *Pharm Sci Technol Today.* **1**: 309-316 (1998).
- (14) E.A. Hosny, S. A. Elkheshen and S. I. Saleh. Bucoadhesive tablets for insulin delivery: In-vitro and in-vivo studies, *Boll Chim Farm.* **141(3)**: 210-217 (2002).
- (15) T. Z. Yang, X. T. Wang, X. Y. Yan and Q. Zhang. Phospholipid deformable vesicles for buccal delivery of insulin, *Chem Pharm Bull.* **50**: 749-753 (2002).
- (16) P. Modi, M. Mihic and A. Lewin. The evolving role of oral insulin in the treatment of diabetes using a novel RapidMist™ system, *Diabetes/Metabolism Res Rev* **18(1)**: 38-42 (2002).

- (17) L. Langkjaer, J. Brange, G. M. Grodsky, R.H. Guy. Iontophoresis of monomeric insulin analogues in vitro: effects of insulin charge and skin pre-treatment. *J Contr Release* **51**: 47-56 (1998).
- (18) S. Mitragotri, D. Blankschtein and R. Langer. Ultrasound-mediated transdermal protein delivery, *Science* **269**: 850-853 (1995).
- (19) G. Cevc. Transferosomes, liposomes and other liquid suspensions on the skin: permeation enhancement, vesicle penetration and transdermal drug delivery, *Crit Rev Therapeutic Drug Carrier Systems* **13**: 257-388 (1996).
- (20) J. S. Patton, J. Bukar and S. Nagarajan. Inhaled insulin, *Advanced Drug Delivery Rev.* **35**: 235-247 (1999).
- (21) L. Heinemann, A. Pfutzner and T. Heise. Alternative routes of administration as an approach to improve insulin therapy: update on dermal, oral, nasal and pulmonary insulin delivery, *Curr Pharm Des.* **7**: 1327-1351 (2001).
- (22) M. Simon and T. Kissel. Away with the needle. Noninvasive administration routes for insulin: improved quality of life for diabetics, *Pharm Unserer Zeit* **30(2)**: 136-141 (2001).
- (23) W. T. Cefalu. Concept, strategies, and feasibility of noninvasive insulin delivery, *Diabetes Care* **27(1)**: 239-246 (2004).
- (24) A. C. Moses, G. S. Gordon, M. C. Carey and J. S. Flier. Insulin administered intranasally as an insulin-bile salt aerosol: effectiveness and reproducibility in normal and diabetic subjects, *Diabetes* **32**: 1040-1047.
- (25) A. E. Pontiroli, M. Alberetto, A. Secchi, G. Dossi, I. Bosi and G. Pozza. Insulin given intranasally induces hypoglycemia in normal and diabetic subjects, *Br Med J.* **284**: 303-306 (1982).
- (26) S. Gizurason and E. Bechgaard. Intranasal administration of insulin to humans, *Diabetes Res Clin Pract.* **12**: 71-84 (1991).
- (27) F. W. Merkus, N. G. Schipper, J. C. Verhoef. The influence of absorption enhancers on intranasal insulin absorption in normal and diabetic subjects, *J Controlled Release* **41**: 69-75 (1996).
- (28) D. J. Chetty and Y. W. Chien. Novel methods of insulin delivery. An update, *Crit Rev Therapeutic Drug Carrier System* **15**: 629-670 (1998).
- (29) M. Hinchcliffe and L. Illum. Intranasal insulin delivery and therapy, *Advanced Drug Delivery Rev.* **35**: 199-234 (1999).
- (30) R. R. Hollmann. Intranasal insulin in type 1 diabetes. In M. Berger, F. A. Gries, *Frontiers in insulin pharmacology*, Stuttgart Thieme Verlag 138-143 (1993).
- (31) D. G. Bruce, D. J. Chisom, L. H. Storlien, M. Borkmann and E. W. Kraegen. Meal-time intranasal insulin delivery in type 2 diabetes, *Diabet Med.* **8**: 366-370 (1991).

- (32) A. G. Fraumann, M. E. Cooper, B. J. Parsons, G. Jerums and W. J. Louis. Long-term use of intranasal insulin in insulin-dependant diabetic patients, *Diabetes Care* **10**: 573-578 (1987).
- (33) J. Hilsted, S. Madsbad, A. Hvidberg, M. H. Rasmussen, T. Krarup and H. Ipsen. Intranasal insulin therapy: the clinical realities, *Diabetologia* **38**: 680-684 (1995).
- (34) D. Lelej-Bennis, J. Boillot, C. Bardin, P. Zirinis, A. Coste, E. Escudier et al. Efficacy and tolerance of intranasal insulin administered during 4 months in severely hyperglycaemic type 2 diabetic patients with oral drug failure: a cross over study, *Diabet Med.* **18**: 614-618 (2001).
- (35) D. Lelej-Bennis, J. Boillot, C. Bardin, P. Zirinis, A. Coste, E. Escudier et al. Sixth month administration of gelified intranasal insulin in type 1 diabetic patients under multiple injections: efficacy versus subcutaneous injections and local tolerance, *Diabetes Metab.* **27**: 372-377 (2001).
- (36) S. J. Hersey and R. T. Jackson. Effect of bile salts on nasal permeability in vitro, *J Pharm Sci* **76(12)**: 876-879 (1987).
- (37) D. Duchene, F. Touchard and N. A. Peppas. Pharmaceutical and medical aspects of bioadhesive system for drug administration, *Drug Dev Ind Pharm.* **14**: 283-318.
- (38) D. Quintanar-Guerrero, E. Allemann, H. Fessi and E. Doelker. Preparation Techniques and Mechanisms of Formation of Biodegradable Nanoparticles from Preformed Polymers, *Drug Dev Ind Pharm.* **24(12)**: 1113-1128 (1998).
- (39) C. Tribet. Complexation Between Amphiphilic Polyelectrolytes and Proteins: From Necklaces to Gels. *Physical Chemistry of Polyelectrolytes* (T. Radeva, Ed.): 687-741, Marcel Dekker, New York (2000).
- (40) A. Breitenbach, T. Jung, W. Kamm and T. Kissel. Biodegradable comb polyesters containing polyelectrolyte backbones facilitate the preparation of nanoparticles with defined surface structure and bioadhesive properties, *Polym Adv Technol.* **13**: 938-950 (2002).
- (41) T. Jung, W. Kamm, A. Breitenbach, K. D. Hungerer E. Hundt and T. Kissel. Tetanus toxoid loaded nanoparticles from sulfobutylated poly(vinyl alcohol)-graft-poly(lactide-co-glycolide): evaluation of antibody response after oral and nasal application in mice, *Pharm Res.* **18(3)**: 352-360 (2001).
- (42) M. Wittmar. Charge modified, comb-like graft-polyesters for drug delivery and DNA vaccination: Synthesis and Characterization of Poly(vinyl dialkylaminoalkylcarbamate-co-vinyl acetate-co-vinyl alcohol)-graft-poly(D,L-lactide-co-glycolide)s, Dissertation, Philipps University Marburg, 2004. <http://archiv.ub.uni-marburg.de/diss/z2004/0075/>
- (43) C. G. Oster, M. Wittmar, F. Unger, L. Barbu-Tudoran, A. K. Schaper and T. Kissel. Design of amine-modified graft polyesters for effective gene delivery using DNA-loaded nanoparticles, *Pharm Res.* **21(6)**: 927-931 (2004).

## **Chapter 2**

Self-Assembling Nanocomplexes from Insulin and Water-Soluble Branched Polyesters, Poly[(vinyl-3-(diethylamino)-propylcarbamate-co-(vinyl acetate)-co-(vinyl alcohol)]-graft-poly(L-lactic acid): A Novel Carrier for Transmucosal Delivery of peptides.

Published:

Bioconjugate Chemistry  
Volume 15(4) 841-849, 2004  
American Chemical Society, ACS

## 2.1. Abstract

The design of carriers for protein delivery that provide protection against enzymatic degradation and facilitate protein transport across epithelial surfaces, thus avoiding parenteral administration, remains a challenge. Self-assembling nanoscale protein/polymer complexes might present a promising approach. We synthesized water-soluble, amphiphilic polyesters, poly[(vinyl-3-(diethylamino)-propylcarbamate-*co*-(vinyl acetate)-*co*-(vinyl alcohol)]-graft-poly(L-lactic acid), containing a positively charged backbone, and studied the spontaneous formation of nanocomplexes (NC) with insulin. NC were characterized using dynamic light scattering, zeta-potential measurements, and atomic force microscopy (AFM). Insulin loading was determined with HPLC, and the binding constants were obtained by isothermal titration calorimetry (ITC). The NC formation was followed using nephelometric and light scattering techniques. Water-soluble, positively charged, branched polyesters with amphiphilic properties were obtained in a three-step polymer-analogous reaction. The degree of amine substitution, DS, in the PVAL backbone was varied between 0.04 to 0.5, and grafting this backbone with L-lactide increased the molecular weight from 18 kDa to 81 kDa. The polymer composition was optimized to facilitate NC formation with insulin resulting in a DS of 0.09 and a poly(L-lactide) side chain substitution of 0.5 with an average chain length of two lactic acids. Depending on polymer composition, stable NC of 200-500 nm diameter were formed with insulin, and the binding constants ranged from  $4.7 \times 10^5$  to  $9.5 \times 10^6 \text{ M}^{-1}$ . Positively charged surface charges ranging from +5 to +35mV and an insulin loading up to 98% of 33 I.U./ml were obtained. The NC visualized by AFM revealed spheroidal particles with an entangled internal structure. It was demonstrated that this class of multifunctional polymers is capable of self-assembly with a peptidic substrate. The resulting nanosized complexes offer the potential for mucosal insulin/protein delivery and merit further investigations under in vivo conditions.

## 2.2. Introduction

Diabetes mellitus is the most common of the serious metabolic diseases and prevalence in western societies is estimated to be about 1 %. Long-term complications involving the eyes, kidneys, nerves and blood vessels present a heavy burden for the health care system in western societies. The intensified insulin therapy for diabetic patients requires up to four subcutaneous injections per day to maintain adequate control of serum glucose levels. Compliance with such demanding dosing regimes is difficult for the patient and make the development of an alternative form of insulin administration clearly appealing.

Numerous attempts to deliver insulin by application routes avoiding injections have been reported in the literature. Peroral, pulmonary and nasal insulin administrations fall into this category, but enzymatic lability and inefficient transport across mucosae provide formidable challenges and lead to low and variable bioavailabilities (1). The intranasal route is most attractive for chronic administration of peptides and proteins (2). However, nasal insulin absorption is low without co-administration of absorption enhancers which open the epithelial barrier and/or prolong the residence time in the nasal cavity. Promoters such as bile salts, chelating agents or the surfactant laurth-9 have shown undesirable toxic side effects after chronic administration (3).

Proteins delivery systems relying on complexation and assembly of proteins with amphiphilic polymers could present an alternative to the absorption enhancers described above. These polymers form nanoscale complexes with proteins through electrostatic and van der Waals interactions, protecting them against loss of biological activity and increasing their transmucosal uptake. Several polymers such as chitosan (4), poly(glutamine) (5), poly(ethylenimine-co-polyester) (6), AB block-copolymers, e.g. PEO-poly(L-lysine) (7) or PEO-PLGA (8), polyacrylates (9,10) or poly(L-lysine) derivatives (11) have been proposed for insulin delivery.

Nanoscale delivery systems with strong bioadhesive properties seem to be a promising approach (12) because significant insulin uptake after nasal or oral administration without use of penetration enhancers was observed. Nanoparticles, (NP), of insulin and chitosan were obtained in the size range of ca. 350 nm by ionotropic gelation, leading to blood glucose reduction in rabbits after nasal administration (4). Oral administration of insulin containing NP (~ 700nm) from a fumaric and sebacic acid copolyanhydride resulted in a significant blood glucose reduction and strong adhesive NP/mucus interactions (13). For intranasal drug delivery polymers with positively charged groups like chitosan, poly-L-lysines or protamine has been demonstrated to increase bioadhesion and membran permeability (3) .

Another important concern is the fabrication of NP. Nano-encapsulation techniques often rely on formation of emulsions with subsequent solvent evaporation. Usually a high energy input is necessary to obtain nano-emulsions and hence NP. Under those conditions protein stability is often compromised through temperature-, pH-, and shear stress at interfacial surfaces with organic solvents (14).

Therefore, a self assembling system composed of an “intelligent” polymer designed for spontaneous complexation of a target-protein under gentle aqueous conditions might provide advantages over classic nano-encapsulation strategies. Since the pioneering work of Morawetz and Hugues (15), it is recognized that globular proteins can form stable complexes with polyelectrolytes. The association of proteins with polyelectrolytes can result in soluble complexes, complex coacervation, precipitation or gelation of the resulting system (16,17). The two most important parameters governing polymer/protein association in water are the hydrophobicity and the electrostatic interactions of the partners. Additional phenomena, such as gelation and retardation of precipitation, are thought to result directly from the presence of hydrophobic association in polyelectrolyte complexes (PEC) (18).

Optimal polymer properties for self-assembly with proteins are rarely found in naturally occurring macromolecules. We report here the design and characterization of new synthetic

polymers with amphiphilic properties suitable as self-assembling protein carrier system. By grafting L-lactide onto a hydrophilic, charge-modified poly(vinyl alcohol) backbone with covalently bound diethylamino-propylamine groups, amphiphilic biodegradable comb polyesters with lipophilic side chains were obtained. We hypothesized that insulin, dissolved at a pH above its point of isoelectric charge (PI ~ pH 5.3), carries an overall negative charge (19) and will form PEC with the cationic polymers by electrostatic and hydrophobic interactions. This work is an extension of our experiments using negatively charged branched polyesters, namely SB-PVA-g-PLGA for transmucosal delivery of tetanus toxoid (20,21).

## 2.3. Materials and Methods

### 2.3.1. Materials

Diethylaminopropylamine (*purum*, >98%), poly(vinyl alcohol) (PVA) (15000 g/mol; degree of polymerization 300 (P=300); degree of hydrolysis 86-89%), carbonyl di-imidazole, (CDI), (*purum*, 97%), N-methyl pyrrolidone (NMP) (*purum*, absolute) and 1,3-Dimethyl-3,4,5,6-tetrahydro-2(1H)-pyrimidinone (DMPU) (*puriss.*, absolute, over molecular sieve) were purchased from Fluka GmbH Germany and used as received. L-lactide(S-grade) (Boehringer Ingelheim, Germany) was recrystallized twice from ethyl acetate. Tin(II) 2-ethylhexanoate (Aldrich, Germany) was used as received. Tetrahydrofuran (THF) (BASF, Germany) was dried over sodium and distilled under nitrogen before use. N,N-Dimethylacetamide (for HPLC, 99.8%) was purchased from Fluka and Lithium bromide (extra pure) was ordered from Merck. Human recombinant insulin powder (26.2 I.U./mg) was a gift from Aventis Pharma AG (Germany). All other chemicals were of the highest analytical grade commercially available.

### 2.3.2. Polymer synthesis

The synthesis was described in detail elsewhere (22). Poly[(vinyl-3-(diethylamino)-propylcarbamate-co-(vinyl acetate)-co-(vinyl alcohol)]-graft-poly(L-Lactic acid) were synthesized in a three-step synthesis. Briefly, amino functions were introduced to the PVA backbone using CDI linker chemistry followed by grafting of L-Lactic acid chains using a ring-opening polymerization in bulk. The products were purified by ultrafiltration and lyophilized.

### 2.3.3. Nomenclature

The source-based IUPAC nomenclature for these polymers is Poly(vinyl 3-(diethylamino)propylcarbamate-co-vinyl acetate-co-vinyl alcohol)-graft-poly(L-lactide). As abbreviation we used 'DEAPA' (diethylaminopropylamine) followed by the average number of amine carrying monomer units per 'PVA' (poly(vinyl alcohol)) chain with a polymerization degree of 300. The grafting of PLLA with the average chain length in parentheses follows (e.g. DEAPA(26)-PVA<sub>300</sub>-g-PLLA(2)). One third of the average of amine carrying monomers of the backbone is the same like the degree of amine substitution (DS) of the PVA: e.g. a DS of 0.087 is equivalent to DEAPA(26)-PVA<sub>300</sub>. For simplification, the following code was selected: P for the DEA(P)A substitution, afterwards the number of amine groups per PVA in parentheses, followed by number of the lactide amount from feeding and LL as index, indicating grafting with pure L-Lactide side chains (e.g. P(26)-2<sub>LL</sub>).

### 2.3.4. Polymer Characterization

<sup>1</sup>H and <sup>13</sup>C NMR spectroscopic data were collected using a JEOL Eclipse+ 500 and a Joel GX 400 D at a frequency of 500 or 400 MHz for <sup>1</sup>H NMR and 126 respectively 101 MHz for <sup>13</sup>C NMR at 50 °C in d<sub>6</sub>-DMSO (euriso-top, <0.02% HDO+D<sub>2</sub>O). 40 to 50 mg samples were used for each measurement. <sup>1</sup>H NMR was performed with 64 and <sup>13</sup>C NMR with 4096 scans.

Gel permeation chromatography (GPC) was performed using a SDV linearM column (8 x 300 mm, 5 $\mu$ m, with pre-column 8 x 50mm) from Polymer Standard Services (Mainz). The eluent was dimethylacetamide with an addition of 2.50g LiBr/L and a flow rate of 0.5 ml /min at 60°C. The GPC consisted of a Merck-Hitachi AS-2000A autosampler, an L-6000 pump, a Merck T-6300 Column Thermostat and Differential Refractometer Optilab DSP, a Wyatt DAWN Eos multi-angle-light-scattering detector (The dn/dc was calculated with total mass recovery, Dawn EOS calibrated against PMMA 200k) and a Duratec DDG-75 degasser. The molecular weights of the samples were determined (third order fit) with the Wyatt Astra V4.73 Software.

### **2.3.5. Nanocomplex Preparation and Characterization**

Preparation of Insulin Nanocomplexes: An insulin stock solution (2.50 mg/ml) was prepared in two steps. 1. The insulin powder was dissolved in 87% (V/V) 1.15x10<sup>-2</sup> N-HCl in 10,0 ml-Pyrex® tubes. 2. 13% (V/V) of 0.1 N-Tris(hydroxymethyl)aminomethane solution was added resulting in a clear Tris-buffer with low ionic strength (I=0.01) and pH 7.40. Polymer stock solutions in concentrations (table 2) from 0.64 mg/ml for P(150) up to 7.0 mg/ml for P(26)-3<sub>LL</sub> were prepared in Tris-buffer. An equal volume of the stock solutions of insulin and polymer were mixed resulting in defined mass ratios (table 2) of insulin/polymer 1: 0,26-2,8 (m/m) in the final NC-solution. The colloidal polymer-insulin complexes formed immediately after mixing by spontaneous self-assembly.

Particle Size and  $\zeta$ - potential characterization: Average size and the size distribution of the NCs was investigated using photon correlation spectroscopy (21) with a Zetasizer 4 equipped with an AZ110 cell (Malvern Instruments UK), a 4-mV laser source, a 64-channel correlator, and a multi-angle photomultiplier. Each buffer solution was filtered through 0.2  $\mu$ m-Acrodisc® filters (Gelman Laboratory) and measurements were performed in serial mode. The photon correlation spectroscopy (V.1.26 Software) was used to calculate particle mean

diameter and width of the fitted Gaussian distribution. The  $\zeta$ -potential of the NC suspension was determined by laser-Doppler-anemometry in distilled water (conductance 0.055  $\mu\text{s}/\text{cm}$ ) using the AZ 104 cell. The  $\zeta$ -potential was derived from electrophoretic mobility of the NC. Each measurement was performed in triplicate.

**Insulin Loading of Nanocomplexes:** After centrifugation of the complex dispersions in 2.0 ml Eppendorf-Cups for 30 min at 14.000 U/min, the supernatant was filtered through 0.1  $\mu\text{m}$  Millex® (Millipore) and the insulin content was determined by high performance liquid chromatography (HPLC). HPLC was based on a LiChrosphere®100 RP18 (5 $\mu\text{m}$ ), 250-4-column (Merck) with isocratic elution (65% H<sub>2</sub>O + 0.1% TFA / 35% Acetonitrile 90/ H<sub>2</sub>O 10 + 0.1%TFA (flow rate 1.0ml/min) and detection of insulin by a fluorescence spectrophotometer (Ex 276nm/Em 600nm). The HPLC system consisted of a T6300 column thermostat, a 6200A pump, a F1050 fluorescence spectrophotometer, an AS 2000A autosampler (Merck, Germany) and a vacuum degasser (Duratec). Data processing was performed with the Millennium<sup>32</sup> software Version 3.05. (Waters).

### **2.3.6. Isothermal Titration Calorimetry**

Microtitration calorimetry was performed using the MSC-ITC equipment from Microcal Inc. (Northampton, USA). The cell volume was 1351  $\mu\text{l}$  containing insulin and the syringe volume 250  $\mu\text{l}$  with the respective polymer solution. All Tris buffer solutions were filtered with 0.2  $\mu\text{m}$ -Acrodisc® and the pH values in the final solutions were controlled to be 7.40 to avoid pH compensation signals. The injection scheme was 14 x 15  $\mu\text{l}$  every 190 sec at 400 rpm at 25 °C and data processing was performed with the software Microcal Origin 3.5. The measurements were carried out in triplicate.

### **2.3.7. NC stoichiometry by colloid titration**

Turbidimetric measurements were carried out according to the method of Kokufuta et al. (23,24). A constant volume of 0.30 ml insulin stock solution (2.50 mg/ml) was mixed with an appropriate volume of polymer solution and filled up with Tris buffer to a constant volume of 3.30 ml to avoid dilution effects. Transmission data were recorded on a Shimadzu UV-160 spectrophotometer at 630 nm using Suprasil® cuvettes with 10 mm path length. Scattering data were obtained in the same way as PCS at an angle of 90°. The extrema were read directly from curves after plotting the data points with B-spline connection using Microcal Origin 6.0 software. Determinations were carried out in triplicate.

### **2.3.8. Atomic force microscopy**

The polymer/insulin NC were prepared as described above. After 20 minutes, the complexes were directly transferred onto a silicon chip by dipping into the NC solution. Atomic force microscopy was performed on a Digital Nanoscope IV Bioscope (Veeco Instruments, Santa Barbara, CA) as described elsewhere (25). The microscope was vibration-damped. Commercial pyramidal Si<sub>3</sub>N<sub>4</sub> tips (NCH-W, Veeco Instruments, Santa Barbara, CA) on a cantilever with a length of 125 μm, a resonance frequency of about 220 kHz and a nominal force constant of 36N/m were used. All measurements were performed in tapping mode to avoid damage of the sample surface. The scan speed was proportional to the scan size and the scan frequency was between 0.5 and 1.5 Hz. Images were obtained by displaying the amplitude signal of the cantilever in the trace direction, the height signal in the retrace direction, and the phase signal in retrace direction, both signals being simultaneously recorded. The results were visualized either in height, amplitude or/and in phase modulus. The phase mode permits assessment of material properties (viscoelastic properties). These are expressed as “brightness” of the AFM image.

## 2.4. Results and Discussion

### 2.4.1. Synthesis and Structural Characterization of the Copolymers

Nanoscience is a rapidly developing area of research with considerable potential for drug delivery because cellular interaction and transport of nanoscale objects may offer new opportunities not available to larger devices. Especially NP based on hydrophilic/biodegradable polymers can be designed to provide particle characteristics, protease inhibition and permeation enhancement for peptidic drugs.

To explore the potential of the NP approach, novel materials are necessary which allow formation of NP under mild conditions, such as self-assembly leading to nanocomplexes. We have designed amphiphilic charge-containing biodegradable copolyesters composed of a hydrophilic PVA backbone grafted with short hydrophobic lactic acid groups to complex proteins and peptides. Cationic carriers such as DEAE-dextran, chitosan and poly(L-lysine) are suitable for complexation of a large number of negatively charged pharmacologically active agents, e.g. insulin, oligonucleotides, and DNA (26-28). The use of CDI chemistry allows the modification of amine-substitution in a broad range. We coupled amino-groups to the PVA backbone and investigated the effect of different degrees of DEAPA substitution on complex formation with insulin. PVA is known as a non-toxic and biocompatible polymer which exhibits mucoadhesive properties and is therefore used in drug delivery (29). The degree of amino-substitution was varied from moderate 13 (DS=0.04), up to a highly substituted backbone with 150 (DS=0.5) of the ca. 300 hydroxyl-groups of PVA substituted (c.f. Table 1). To introduce amphiphilicity in the PVA backbone, hydrophobic L-lactic acid side chains were grafted to the backbone in a second step to yield a brush-like and biodegradable copolyester structure. For a P(26) backbone (DS=0.09), the highest possible lactic acid substitution while remaining water soluble was 1:3 (w/w). By combining hydrophilic

backbones with hydrophobic domains, numerous benefits were reported in literature such as increased drug loading, self-association or complex stability (18,30,31).

The polyesters were characterized using  $^1\text{H-NMR}$  spectroscopy and gel permeation chromatography. A typical  $^1\text{H-NMR}$  spectrum (Figure 1) of these graft polymers show signals of both polymers, PVA and poly(L-lactide). The ratio between end group and central group integrals depends on the side chain length and could be used to calculate the average chain length and the molecular weight (MW) of the sample. The reproducibility of the synthesis is demonstrated for two different batches of polymer P(26)-2<sub>LL</sub> (Table 1, footnote f) with similar degrees of substitution. It could be shown that the MW of the polyesters is increasing as expected. The polymer with the highest calculated side chain length, P(26)-3<sub>LL</sub>, shows the highest molecular weight and the polymer with the lowest lactic acid grafting, P(26)-1<sub>LL</sub>, yields the smallest molecular weight of all polyesters. The molecular weights calculated from NMR spectra of all tested polymers are in good agreement with the number average molecular weights,  $M_n$ , obtained by GPC/MALLS. The only exception was P(26)-2<sub>LL</sub>, which exhibited an apparent higher molecular weight measured by light scattering caused by a fraction of polymer aggregates. Otherwise, the elution time of P(26)-2<sub>LL</sub> measured by a refractive index detector is in the range of the other polyesters (Figure 2), indicating a MW of the same order of magnitude.

**Table 1. Physicochemical Properties of the Polymers**

Polymer	Length of side chain <sup>a</sup>	MW, g/mol <sup>b</sup>	M <sub>n</sub> /M <sub>w</sub> (by LS) <sup>c</sup> g/mol	Substitution (amine) <sup>d</sup> /%	Substitution (lactide) <sup>d</sup> /%	Yield (w/w) <sup>f</sup> /%
DEAPA(13)	-	16200	14640 / 16640	4.4	-	78
DEAPA(26)	-	17800	15410 / 19590	8.1	-	74
DEAPA(68)	-	23900	33590 / 67790	22.7	-	42
DEAPA(150)	-	38700	-	50.0	-	22
DEAPA(26)-(1)	2.1	34500	42940 / 81680	8.1	32.1	84
DEAPA(26)-(2)	3.1	51700	221900 / 3855000 <sup>e</sup>	8.1	48.7	67
DEAPA(26)-(2)	2.8	48300	-	8.5	46.8	-
DEAPA(26)-(3)	4.3	74600	71550 / 124500	8.1	60.9	70

<sup>a</sup> Average lactic acid units per chain calculated by <sup>1</sup>H NMR data. <sup>b</sup>Molecular weight calculated from <sup>1</sup>H NMR data. <sup>c</sup>Molecular weights measured by GPC-MALLS (dawn Eos + optilab). <sup>d</sup>Percent of hydroxyl groups carrying amine or lactid calculated on *P* (PVAL) = 300 (*P*: degree of polymerization). <sup>e</sup>Heavy polymer aggregation. <sup>f</sup>Yield calculated on used educt masses and resulting product mass.

**Table 2. Characterization of NC**

Polymer	Mass ratio: insulin/polymer <sup>a</sup>	PCS: NC sizes/nm	AFM: NC sizes/nm <sup>b</sup>	AFM: diameter/height	ζ- Potential, mV	Drug loading <sup>c</sup>	Charge ratio +/- <sup>d</sup>	Stoichiometry: turb./ITC <sup>e</sup>
DEAPA(13)	1 : 0.45	450 ± 89	-	-	3.0 ± 0.4	20.4 ± 0.6	1.15	-
DEAPA(26)	1 : 0.50	394 ± 61	274 ± 68	1.04	17.7 ± 2.7	78.9 ± 1.2	0.97	12.4 / 22.0
DEAPA(68)	1 : 0.23	195 ± 30	-	-	24.6 ± 3.2	94.0 ± 2.9	0.75	25.6 / 83.2
DEAPA(150)	1 : 0.26	430 ± 98	434 ± 43	1.27	34.6 ± 4.7	97.1 ± 2.5	0.61	45.4 / 164
DEAPA(26)-(1)	1 : 1.60	370 ± 48	418 ± 51	1.15	15.0 ± 2.4	72.4 ± 2.6	0.56	7.1 / 16.0
DEAPA(26)-(2)	1 : 1.70	250 ± 39	285 ± 65	1.07	18.8 ± 3.3	76.4 ± 13.4	0.75	9.5 / 16.0
DEAPA(26)-(3)	1 : 2.80	290 ± 120	340 ± 86	1.35	32.7 ± 2.5	98.7 ± 0.1	0.50	-

<sup>a</sup> Optimized mixing ratios, standard insulin concentration 1.25 mg/mL in NC solution. <sup>b</sup>Measured from 25 x 25 μm scale AFM images. <sup>c</sup> Determined by HPLC after filtration of NC with 0,22 μm. <sup>d</sup>Ratios at the turbidimetric/scattering extrema. <sup>e</sup>Molar insulin/polymer ratio: first value at extrema turbidimetry, second value at turning point ITC.

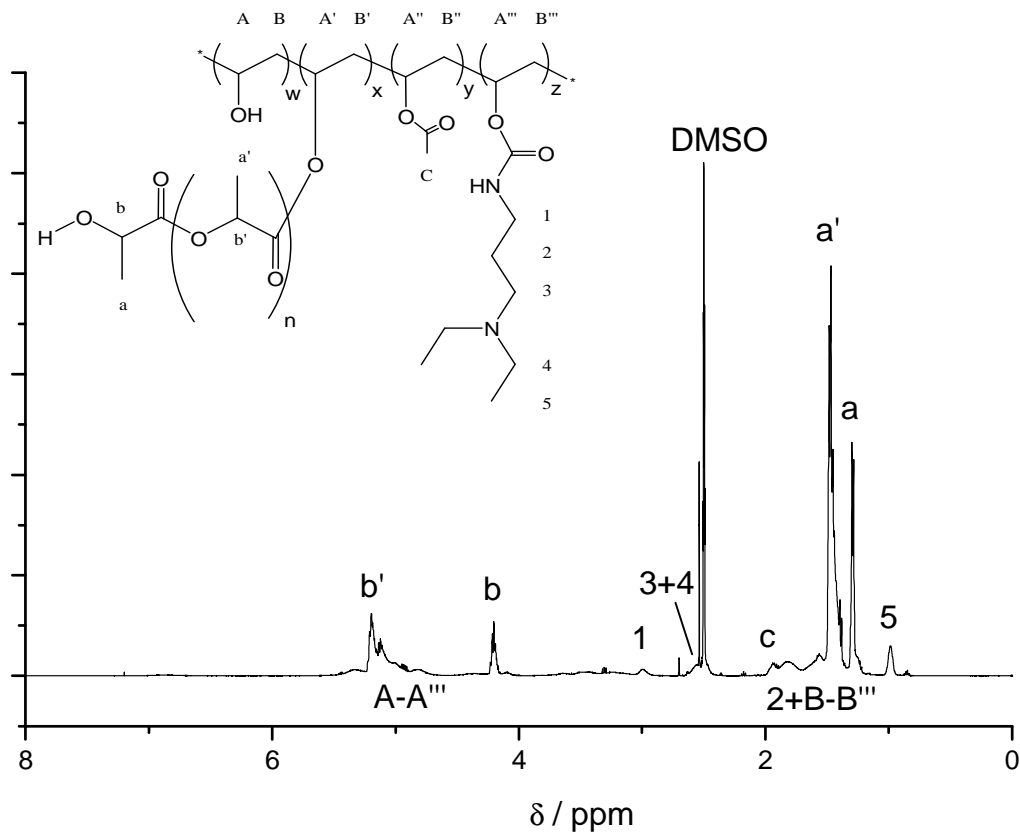


**Figure 1.**  $^1\text{H-NMR}$  spectra of DEAPA (26)-(3) and the correlation of structure and signal. The lactide chains have four different signals. These are the multiplet of the methine central groups between 5.24 and 5.03 ppm, the multiplet of the methine end group between 4.25 and 4.15 ppm, the multiplet of the methyl central groups between 1.51 and 1.40 and the multiplet of the methyl end groups between 1.32 and 1.27.

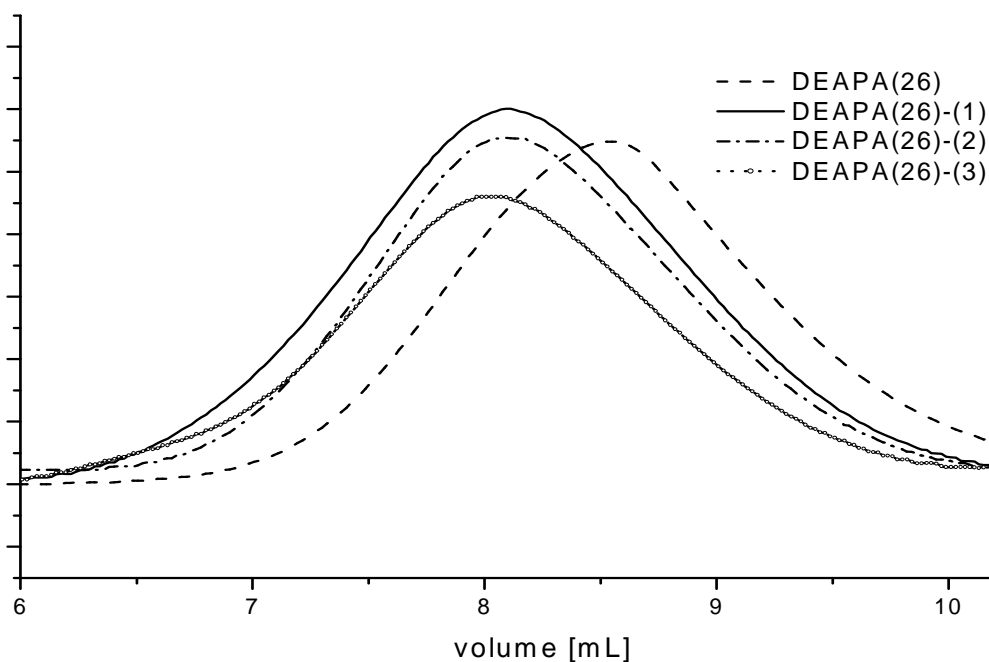


**Figure 2.** GPC signals of the refractive index detector of the polymers DEAPA-(26), -(26)-(1), -(26)-(2) and -(26)-(3). There is only a small difference between the three polyesters. The modified PVA shows a higher elution volume.

#### 2.4.2. Formation of NC with insulin

Complex formation between proteins and polymers is influenced by a large number of parameters. Apart from mixing conditions (polymer concentration, rate of mixing, stirring), medium parameters (pH value, ionic strength, type of salt, polarity of solvent) and particularly the characteristics of the polyelectrolyte (molecular weight, polydispersity, branching, charge density) are known to play an important role. We investigate the complexation process in a systematic manner using turbidity as a simple and non-invasive measurement of NC formation (32). The formation of supramolecular structures leads to a corresponding increase in particle mass, which can be sensitively monitored by light scattering. In turbidimetric studies, the transmission of a light beam passing through a cuvette with a dispersion is given by  $T = I/I_0 = \exp(-\tau \cdot l)$  where  $I_0$  is the intensity of the light beam,  $I$  is the intensity after the cuvette of the length  $l$ , and  $\tau$  is the turbidity. In non-absorbing systems (630nm), the transmittance is determined by the scattering of light. According to the Rayleigh theory, the scattered intensity is proportional to the square of the particles mass (33,34). Turbidimetry monitors structural changes caused by the onset of association respectively particle formation. The characteristics of a turbidimetric curve for different mixing ratios of a  $3.2 \times 10^{-5}$  mol insulin solution with increasing concentrations of polymer are shown in Figure 3.

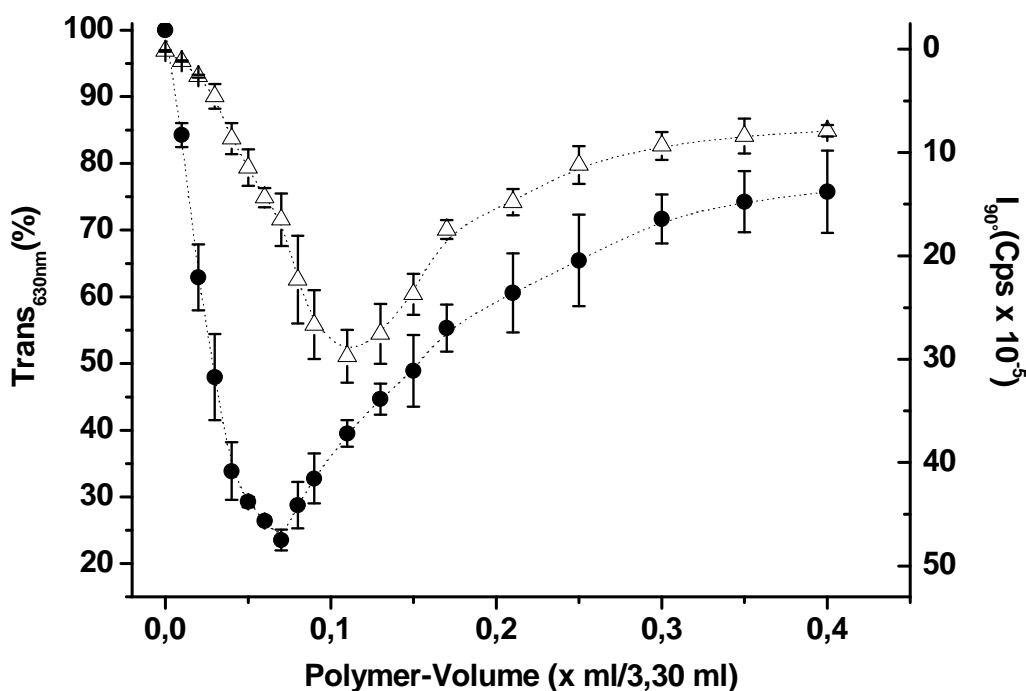


**Figure 3.** Turbidimetry (●) and scattering (Δ) of DEAPA(26) and insulin.

The graph does not represent a classic colloid titration because every data point was generated from a separate experiment with a constant volume of 3.30 ml to eliminate dilution effects. All polymers exhibited the same turbidimetric profile characterized by a sharp decrease of transmission and a sharp increase of scattered light at increasing polymer concentrations resulting in distinct minima and maxima. The turbidimetric profile suggests that at initially low polymer concentration, large and incoherent complexes are formed with an excess of insulin. These complexes condense to a more defined and compact structure at increasing polymer concentration, corresponding to mixing ratios at the extrema and the ascending part of the turbidimetric curve. Furthermore, addition of the same type of polymer to NC dispersion leads to a redistribution of the insulin to the new binding partner resulting in a decrease of scattering intensity and absorption. The NC size measurements as a function of

the mixing ratios confirm this assumption (Figure 4). A transition to small sized NC was achieved upon exceeding the described minima/maxima.

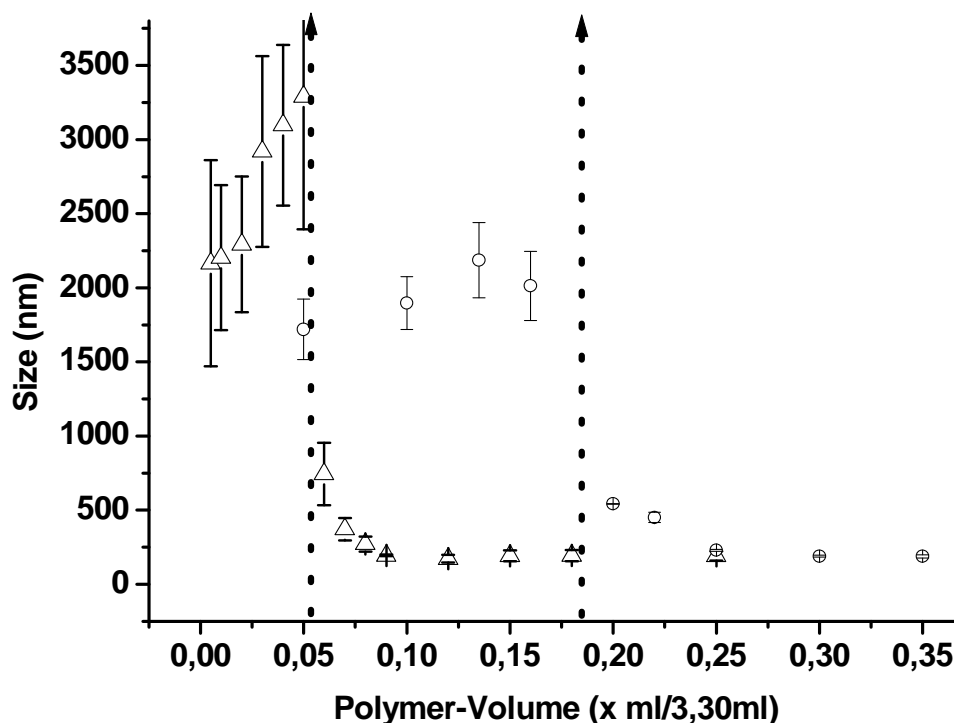


**Figure 4.** Size measurements for DEAPA(68) ( $\Delta$ ) and DEAPA(26)-(3) (O). Dashed lines represent turbidimetric/scattering extrema: Abrupt size decrease to defined NC after exceeding critical mixing ratios.

At a physiological pH human insulin carries two negative charges per molecule (19). The terminal tertiary amino groups of DEAPA are predominantly protonated at neutral pH, allowing calculation of charge ratios at the extreme values of the turbidity curves. The calculations are based on the total concentrations. In Figure 5, a linear relationship between the number of DEAPA groups in the backbone and the molecular ratio of insulin/polymer is shown.

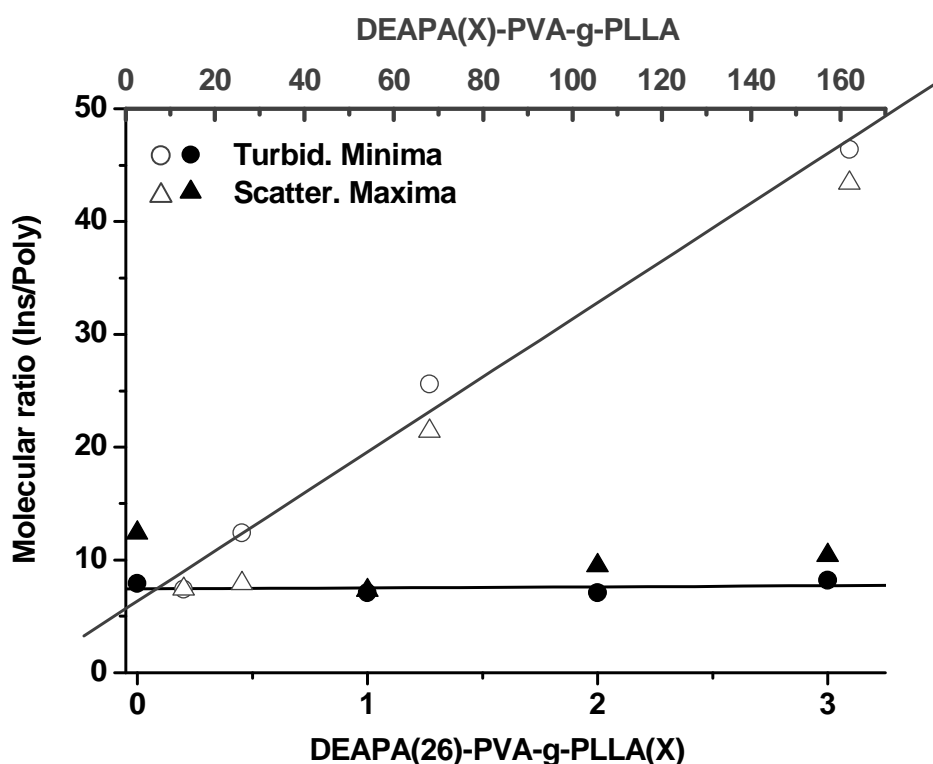


**Figure 5.** Turbidimetric and scattering extrema: correlation of molecular ratio and substitution degree of DEAPA ( $\circ, \Delta$ ) respective amount grafted lactide ( $\bullet, \blacktriangle$ ).

With higher degrees of amino substitution, increasing from 13 to 150, higher molar ratios between DEAPA and insulin with 1:7 up to 1:45 are observed. These data suggest that at the extreme values approximately 1:1 charge ratios are observed (Table 2) and highlight the importance of electrostatic interactions. On the other hand, with increasing amounts of lactic acid grafting is no change in the molar ratio of insulin/polymer is observed. This suggests that the stoichiometry of the complexes is primarily determined by coulombic interactions and that hydrophobic forces play a minor role.

Under our experimental conditions, the NC demonstrated no tendencies of precipitation or macroscopic flocculation. The only exception is P(26)-3<sub>LL</sub>-NC which tended to precipitate after ~1-2 hours, possibly due to the high lactic acid grafting. It is very important to mention

that turbidimetry does not provide information on the affinity between insulin and the different polymers. Therefore, isothermal microtitration calorimetry was performed.

### 2.4.3. Nanocomplex Characterization

Ideal nanocomplex containing insulin should meet the following requirements: (i) particle sizes < 500nm to facilitate epithelial uptake (35); (ii) high positive  $\zeta$ -potential to increase interaction with negatively charged cell surfaces (36); and (iii) high insulin loading. These parameters were determined at different points of the turbidimetric profile (figure 4). It was found that the optimal range is located at the ascending part of the profile. This observation was made with all polymers and thus permitted a calculation and even a prediction of the optimal ratios of both binding partners (Table 2).

Using a simple mixing procedure and short incubation times, it was possible to obtain NC with an average diameter of ~200 to 500 nm. Within a homologous series of backbone composition, an increasing amount of lactic acid grafting ( $0 < 1_{LL} < 2_{LL}$ ) led to more compact and smaller NC, pointing to the influence of hydrophobic interactions for the complex structure. The degrees of amino-substitution allowed variation of the positive surface charge of the NC. The observed  $\zeta$ -potentials ranged from +3 mV at a low ('13') to + 35 mV with a higher degree of substitution ('150'). Furthermore, when the number of amino groups was kept constant at 26 and the lactic acid ratio was increased from  $1_{LL}$  to  $3_{LL}$  the  $\zeta$ -potential increased from +15 mV to +33 mV. This could be explained by increased internal hydrophobic interactions leading to a displacement of positive charges from the inner parts of the complex to the outer layer.

The high loading of insulin (Table 2) in NC was obtained either with high degrees of amine-substitution or by a combination of medium charge density ('26') and a higher lactic acid grafting ( $2_{LL}$ ,  $3_{LL}$ ). At the standard concentration of 1.25 mg/ml insulin (26.2 I.U./mg) ca.

98% were bound in NC. A degree of amino-substitution of 0.04 was insufficient for sufficient insulin complexation.

The hydrophobic B-chain, C-terminal end plays an important role in the complexation behavior of insulin (e.g. self-association or fibrillation). The increased complexation capacity of the higher grafted polyesters possibly results from more pronounced hydrophobic interactions with these nonpolar residues of insulin. In the literature, the formation of complexes was even observed with partners of the same charge, namely serum albumin and hydrophobically modified anionic polyacrylic acid (37), pointing to the importance of hydrophobic interactions.

#### **2.4.4. Microcalorimetry**

Interactions between proteins and polymers and their assembly to NC, are the result of cooperative interactions of many weak inter- and intra-molecular forces. Isothermal titration calorimetry (ITC) provides a tool to determine equilibrium constants and enthalpies under identical experimental conditions. From these data, entropy values and standard free energies can be derived, giving insight into the complexation reactions. The binding constant,  $K_{bin}$ , allows an assessment of the influence of polymer modifications on the affinity to a target-protein. The so called “final plot” in Figure 6a displays the titration of insulin solution with P(26)-1<sub>LL</sub> polymer. The peaks in the upper window represent the heat flow of the ongoing complexation reaction. This continues until only dilution effects of excessive polymer addition are detected within the last 3-4 peaks. The lower window represents the fit of the integrals according to the least squares method. The binding constants ranged from  $4.68 \times 10^5$  with P(26)-1<sub>LL</sub> to  $9.53 \times 10^6 \text{ M}^{-1}$  with P(150) (Figure 6b).

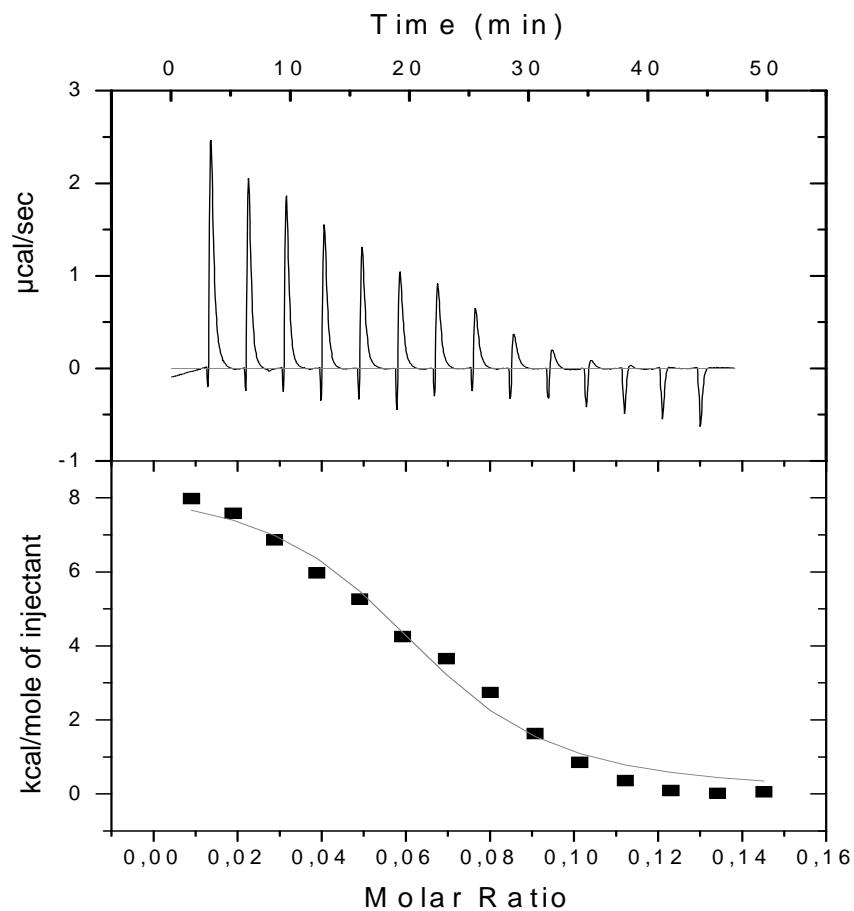


**Figure 6a.** MTC final plot of DEAPA(26)-(1)/insulin.

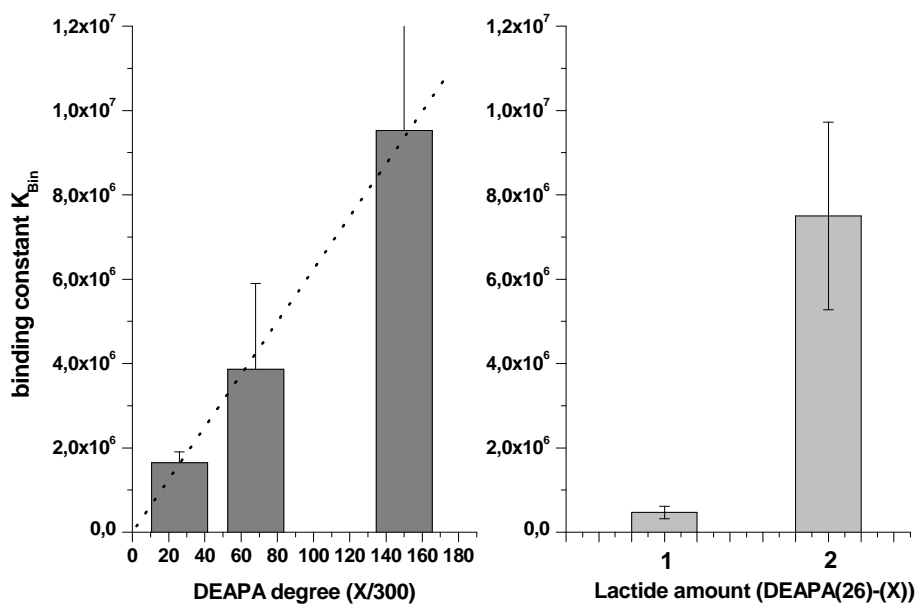


**Figure 6b.** Correlation of binding constants for different amine substitutions (26, 68, 150) of PVAL and comparison of polyesters DEAPA(26)-(1) and -(2).

An increase in the binding constant can be attained by two ways: First with a higher degree of amine substitution, leading to a higher charge density. The binding constant increased almost linearly (correlation coefficient  $\sim 0,998$ ) for P(26), -(68) and -(150). Second is by the introduction of hydrophobic lactic acid side chains, which have to exceed a critical length to influence the complexation of insulin significantly. A strong increase of  $K_{bin}$  to  $7.54 \times 10^6 M^{-1}$  was seen when lactic acid grafting increased from (1<sub>LL</sub>) to (2<sub>LL</sub>), due to additional hydrophobic binding forces. It was not possible to investigate P(13) because of its weak complexation properties and P(26)-3<sub>LL</sub> due to its precipitation tendency.

For comparison, the binding constant for soluble insulin to crystals of cationic protamine/insulin (0.27mg/100 I.U.) at pH 7.5 is (buffer dependent)  $15.5 - 37.7 \times 10^5 M^{-1}$  (38) and the strong binding of the two first hexacoordinated zinc atoms per insulin hexamer is in the magnitude of  $1.9 - 4.7 \times 10^6 M^{-1}$  (39), documenting a substantial affinity of insulin to the DEAPA polymers.

The calorimetric enthalpy change ( $\Delta H$ ) measured in an ITC experiment is the total change in enthalpy for the whole system. That means exothermic or endothermic events can be associated with conformational change of the reactants, ionization of polar groups and interactions with the solvent. The determination of the true (intrinsic) enthalpy requires additional experiments in different solvents and should in this context not be discussed in detail. The driving force of complex formation is mainly the gain in entropy due to the liberation of the low molecular counterions. The derived entropy values for the complexation reactions ranged from 45 for P(26) to 255 kcal/mol for P(150). From a thermodynamic point of view, polyelectrolytes with stronger ionic groups and/or higher molecular masses are generally favored in complex formation (33).

Another parameter directly obtained by ITC is the stoichiometry of the binding partners at the turning point of the isotherm. This stoichiometry cannot be directly compared with turbidimetry due to different physicochemical principles. The thermodynamic stoichiometry

of insulin/polymer was about two to three times higher than the molar ratios derived from turbidimetry (Table 2).

#### **2.4.5. Visualization of NC**

Atomic force microscopy (AFM) is a microscopic technique which allows the imaging of NC formulations independent of their composition under wet (physiological) conditions. Using AFM, in contrast to the electron microscopy, samples can be measured without preparation or fixation. AFM is an excellent method for imaging soft and flexible objects with high resolutions, allowing determination of particles sizes and surface morphology on a nanometer scale resolution. For size determination, all NC within a representative scan area ( $25 \times 25 \mu\text{m}$ ) were evaluated individually (Table 2). These data can deviate from the results of PCS measurements for several reasons. First, interaction of soft and flexible polymer NC with the surface of the silicon support can cause artifacts. The individual particle analysis allows exclusion of such artifacts.

In addition, the visualization and evaluation of NC enables us to investigate the stability of these particles. The morphology of spreaded surface films of the pure polymer solution exhibited a uniform appearance for all polymers. The polymers form globular structures with a high tendency to generate fractal structures. The size for the globuli ranged between 25nm for P(26) (Figure 10/B) and 38 nm for P(26)-2<sub>LL</sub>. The investigated polymer/insulin nanocomplexes showed average particle sizes between 274 nm (P(26)) and 434 nm (P(150)). These values are in excellent accordance with the results determined by PCS. A general overview of a NC distribution is seen in Figure 7 for P(26)/insulin. All particles were of round shape and stable; no tendency for agglomeration could be observed. Only the formulation of P(26)-3<sub>LL</sub> NC showed a very inhomogeneous particle distribution and the tendency of stack formation. In the case of P(26), two major sub-populations were observed.

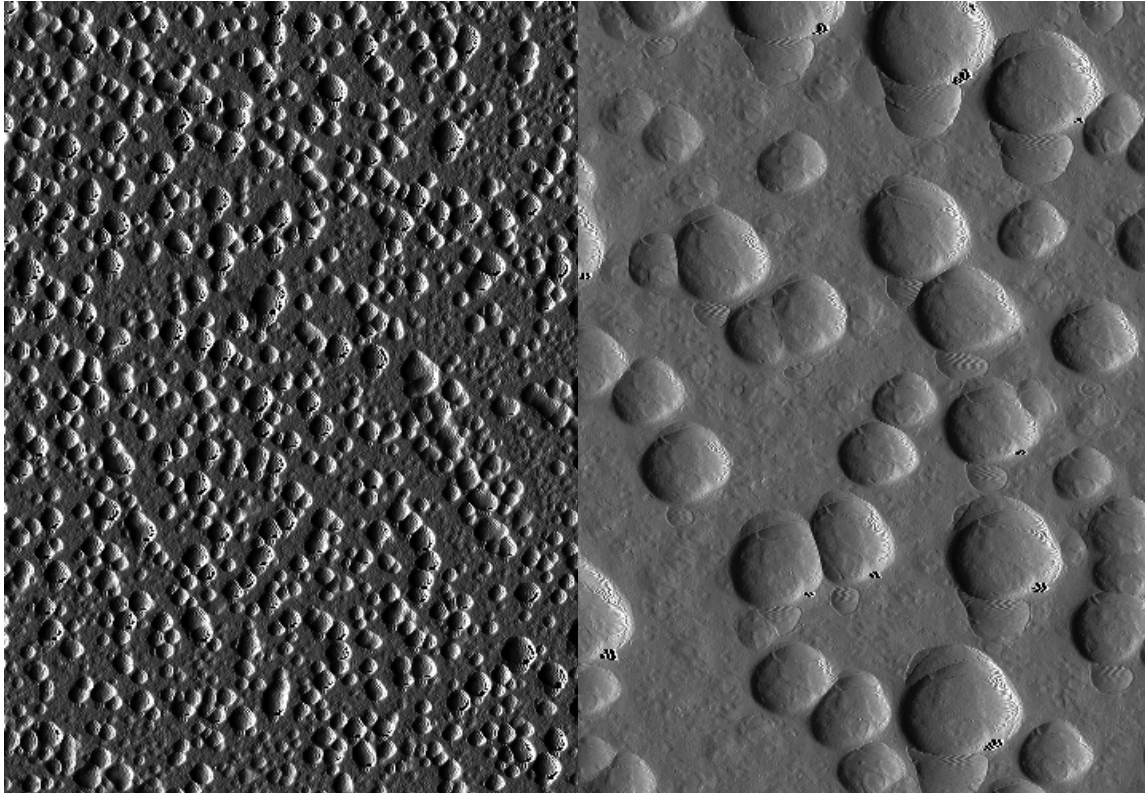


**Figure 7.** Tapping mode AFM images: Overview of DEAPA(26)/insulin complexes: (left) 10.0  $\mu\text{m}$  and (right) 2.0  $\mu\text{m}$  scale.

The smaller fraction had an average diameter of approx. 204 nm, and the larger fraction showed sizes between 300 nm and 400 nm. This feature also explains the differences in the size measurements between the used methods. The surface of the particle is very smooth, no breaks or cracks could be seen.

A general problem with soft objectives like NC, even in the non-contact mode, is to obtain accurate height information. Often nanoparticles show a tendency to coalesce at the surface leading to significant height differences and very flat structures (40). Under our experimental conditions the NC exhibited a good aspect ratio between height and diameter (figure 8) which was confirmed by a cross-section of 2  $\mu\text{m}$  and additional height measurements (figure 9).

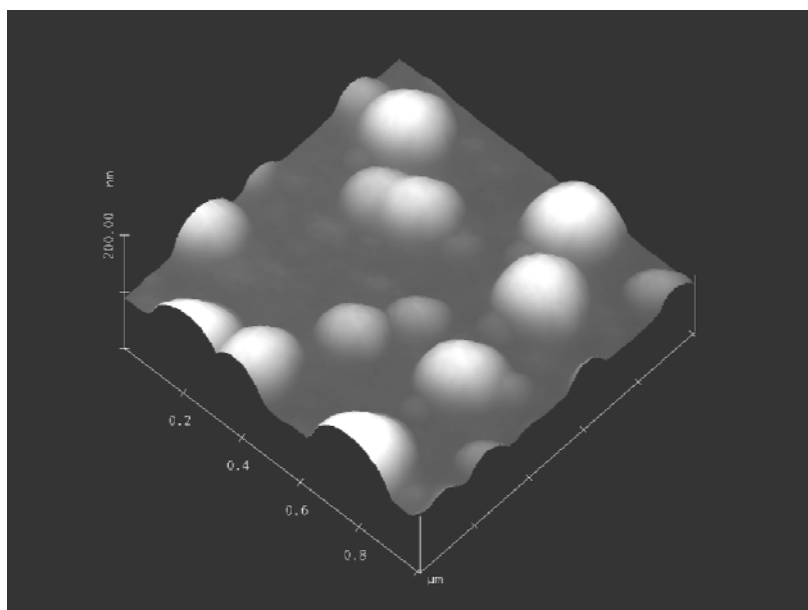


**Figure 8.** Three-dimensional structure of nanocomplexes.

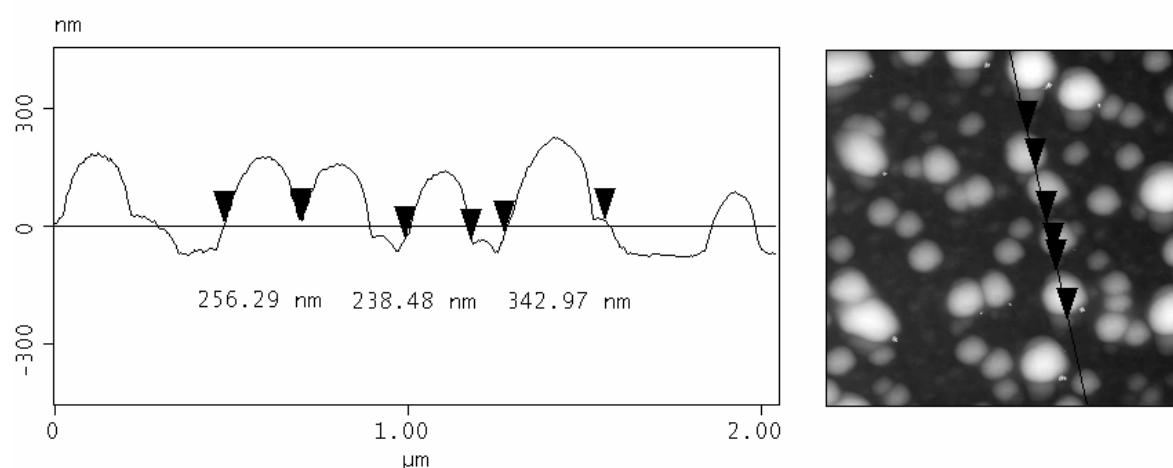


**Figure 9.** Cross-section for nanocomplexes from AFM line analysis.

A special technique of AFM is the so-called phase imaging mode measuring the material contrasts depending on the stiffness or elasticity of the object (41). Differing material properties are presented in different color intensities in images of insulin (a) and DEAPA polymers (b) as shown in Figure 10. More rigid materials show a brighter image than softer materials. In the case of P(26), different bright areas within the particles could be observed (Figure 10/c). The areas were very small with a size between 5 and 20 nm and can be discussed as a distribution of polymer/insulin nanostructures with different compositions.

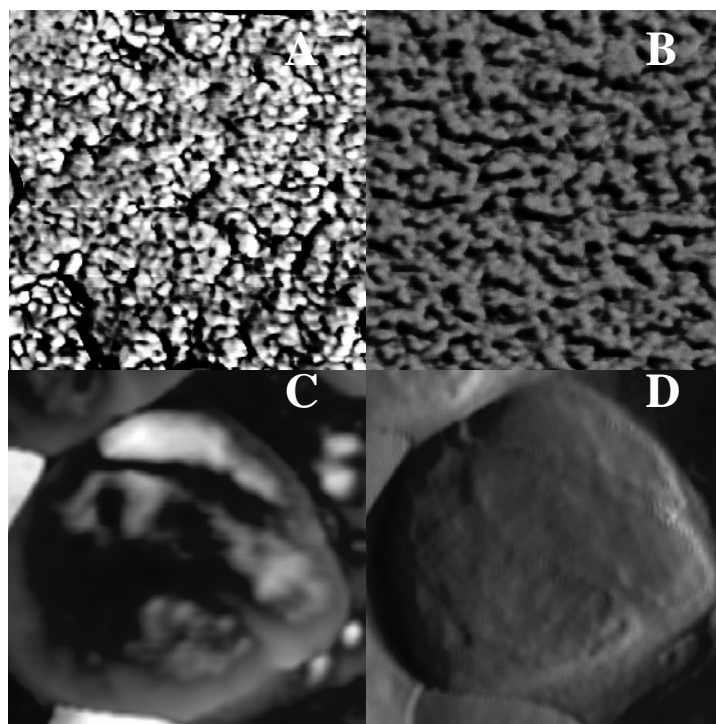


**Figure 10.** AFM phase mode: (A) Insulin, (B) DEAPA(26) polymer, (C) NC of A/B. AFM Tapping mode: (D) surface structure of C.

Brighter areas consist of domains with a higher content of insulin and were more rigid, while darker areas consist of regions with higher polymer content. The results of the AFM investigation are compatible with a spheroidal shape for the nanocomplexes and an entangled internal structure for insulin and DEAPA polymers.

## 2.5. Conclusion

A series of polymers was synthesized and characterized exhibiting a comb-like structure. The variation of hydrophobicity by lactic acid side chain grafting and charged groups, at physiological pH, resulted in branched polyesters with a positively charged backbone offering multiple binding sites for the preparation of colloidal nano-carrier systems. It was possible to manipulate the hydrophilic-hydrophobic balance of these polyesters by factors such as molecular weight, PLLA chain lengths and degree of amine-substitution. Water solubility of these polymers allowed the self-assembling of small NC with narrow size distribution without any mechanic emulsification procedures and without the use of surfactants.

Insulin was complexed to a high extent resulting in uniform particles with an entangled structure. The increase in binding affinity, drug loading, zeta potential and the decrease in size could be correlated with a higher substitution degree of DEAPA groups and a higher lactic acid grafting of the backbone. The possibility of designing the polymer structure in a rational manner may provide significant advantage for generating nanocarriers for mucosal drug delivery. The potential of these NC for nasal delivery of insulin with in-vivo models is currently under investigation in our laboratory.

## 2.6. References

- (1) Pillai, O., and Panchagnula, R. (2001) Insulin therapies - past, present and future. *Drug Discov. Today* 6(20), 1056-1061.
- (2) Behl, C. R., Pimplaskar, H. K., Sileno A. P., Xia, W. J., Gries, J. C., and Romeo, V.D. (1998) Optimization of systemic nasal drug delivery with pharmaceutical excipients. *Adv. Drug Del. Rev.* 29, 117-133.
- (3) Hinchcliffe, M., and Illum, L. (1999) Intranasal insulin delivery and therapy. *Adv. Drug Del. Rev.* 35, 199-234.
- (4) Fernandez-Urrusuno, R., Calvo, P., Remunan-Lopez, C., Vila-Jato, J. L., and Alonso, M. J. (1999) Enhancement of Nasal Absorption of Insulin Using Chitosan Nanoparticles. *Pharm. Res.* 16(10), 1576-1581.
- (5) Iuchi, S., Hoffner, G., Verbeke, P., Djian, P., and Green, H. (2003) Oligomeric and polymeric aggregates formed by proteins containing expanded polyglutamine. *Proc. Natl. Acad. Sci. U.S.A.* 100(5), 2409-2414.
- (6) Nam, Y. S., Kang, H. S., Han, S. H., and Chang, I. S. (2003) Amphiphilic biodegradable block copolymers and self-assembled polymer aggregates formed from the same in aqueous milieu. *U.S. Pat. Appl. Publ. US2003009004*, 1-16.
- (7) Xiong, X., Li, Z., Du, F., and Li, F. (2001) Synthesis of new block copolymer containing glycopolymer segment PEO-b-P(lys-ML) and their aggregation behavior in water. *Gaofenzi Xuebao* (6), 787-792.
- (8) Morlock, M., Kissel, T., Li, Y. X., Koll, H., and Winter, G. (1998) Erythropoietin loaded microspheres prepared from biodegradable LPLG-PEO-LPLG triblock copolymers: protein stabilization and in-vitro release properties. *J. Control. Release* 56(1-3), 105-115.
- (9) Nath, S., Patrickios, C. S., and Hatton, T. A. (1995) Turbidimetric Titration Study of the Interaction of Proteins with Acrylic Polyampholytes. *Biotechnol. Prog.* 11(1), 99-103.
- (10) Patrickios, C. S., Hertler, W. R., and Hatton, T. A. (1994) Protein complexation with acrylic polyampholytes. *Biotechnol. and Bioeng.* 44(9), 1031-1039.
- (11) Maruyama, A., Ishihara, T., Kim, J. S., Kim, S. W., and Akaike, T. (1997) Nanoparticle DNA carrier with poly(L-lysine) grafted polysaccharide copolymer and poly(D,L-lactic acid). *Bioconjug. Chem.* 8(5), 735-742.
- (12) Takeuchi, H., Yamamoto, H., and Kawashima, Y. (2001) Mucoadhesive nanoparticulate systems for peptide drug delivery. *Adv. Drug Del. Rev.* 47, 39-54.
- (13) Mathiowitz, E., Jacob J. S., Jong Y. S., Carino, G. P., Chickering, D. E., Chaturvedi, P., Santos, C. A., Vijayaraghavan, K., Montgomery, S., Bassett, M., and Morell, C. (1997) Biologically erodable microspheres as potential oral drug delivery systems. *Nature* 386(27), 410-414.

- (14) Schwendemann, S. P., Cardamone, M., Klibanov, A., and Langer, R. (1996) Stability of proteins and their delivery from biodegradable polymer microspheres. *Microparticulate Systems for the Delivery of Proteins and Vaccines* (S. Cohen, H. Bernstein, Ed.) pp 1-49, Marcel Dekker, New York.
- (15) Morawetz, H., and Hugues, W. L. (1951) The interaction of proteins with synthetic polyelectrolytes. I. Complexing of bovine serum albumine. *J. Phys. Chem.* 56, 64-69.
- (16) Tribet, C., Audebert, R., and Popot, J. L. (1996) Amphipols: polymers that keep membrane proteins soluble in aqueous solutions. *Proc. Natl. Acad. Sci. U.S.A.* 93, 15047-15050.
- (17) Ahmed, L. S., Xia, J., and Dubin, P. L. (1994) Stoichiometry and the mechanism of complex formation in protein-polyelectrolyte coacervation. *J. M. S. Pure Appl. Chem.* A31(1), 17-29.
- (18) Tribet, C. (2000) Complexation Between Amphiphilic Polyelectrolytes and Proteins: From Necklaces to Gels. *Physical Chemistry of Polyelectrolytes* (T. Radeva, Ed.) pp 687-741, Marcel Dekker, New York.
- (19) Brange, J. (1987) *Galenics of Insulin: The Physio-chemical and Pharmaceutical Aspects of Insulin and Insulin Preparations* pp 1-103, Springer-Verlag, Berlin
- (20) Jung, T., Kamm, W., Breitenbach, A., Kaiserling, E., Xiao, J. X., and Kissel, T. (2000) Polymeric carriers for the oral delivery of polypeptides and peptides based on biodegradable nanoparticles from charge containing brush-like branched polyesters. *Eur. J. Pharm. Biopharm.* 50, 147-160.
- (21) Jung, T., Kamm, W., Breitenbach, A., Klebe, G., and Kissel, T. (2002) Loading of Tetanus Toxoid to Biodegradable Nanoparticles from Branched Poly(Sulfobutyl-Polyvinylalcohol)-g-(Lactide-Co-Glycolide) Nanoparticles by Protein Adsorption: A Mechanistic Study. *Pharm. Res.* 19(8), 1105-1113.
- (22) Wittmar, M. (2004) Charge modified, comb-like graft-polyesters for drug delivery and DNA vaccination: Synthesis and Characterization of Poly(vinyl dialkylamino-alkylcarbamate-co-vinyl acetate-co-vinyl alcohol) –graft-poly (D,L-lactide-co-glycolide), Dissertation, Department of Pharmaceutical Technology and Biopharmacy, Philipps University of Marburg
- (23) Tsuboi, A., Izumi, T., Hirata, M., Xia, J., Dubin, P. L., and Kokufuta, E. (1996) Complexation of proteins with a strong polyanion in an aqueous salt-free system. *Langmuir* 12(26), 6295-6303.
- (24) Kokufuta, E., Shimizu, H., and Nakamura, I. (1982) Stoichiometric complexation of human serum albumin with strongly acidic and basic polyelectrolytes. *Macromolecules* 15, 1618-1621
- (25) Oberle, V., Bakowsky, U., Zuhorn, I., and Hoekstra, D. (2000) Lipoplex formation under equilibrium conditions reveals a three step mechanism. *Biophys. J.* 79(3), 1447-1454.

- (26) Manosroi, A., and Bauer, K. H., (1990) Interaction of human insulin with DEAE-dextran. *Drug Dev. Ind. Pharm.* 16(5), 807-819.
- (27) Liu, G., Molas, M., Grossmann, G. A., Gregory, A., Pasumarthy, M., Perales, J. C., Cooper, M. J., and Hanson, R. W. (2001) Biological properties of poly-L-lysine-DNA complexes generated by cooperative binding of the polycation. *J. Biol. Chem.* 276(37), 34379-34387.
- (28) Zimmer, A., Zobel, H. P., Werner, D., Noe, C. R., and Kreuter, J. (1997) Cationic nanoparticles as enhancers for cellular uptake of antisense oligonucleotides. *Proc. Int. Symp. Control. Release Bioact. Mater.* 24<sup>th</sup>, 679-680.
- (29) Breitenbach, A., Jung, T., Kamm, W., and Kissel, T. (2002) Biodegradable Comb Polyesters Containing Polyelectrolyte Backbones Facilitate the Preparation of Nanoparticles with Defined Surface Structure and Bioadhesive Properties. *Polym. Adv. Technol.* 13, 938-950.
- (30) Ouchi, T., Hirano, T., Maruhashi, S., Nishizawa, H., Shizuno, K., and Ohya, Y. (2000) Synthesis of biomedical graft-copolymers using polysaccharides as backbone polymers. *Abstr. Pap. Am. Chem. Soc.* 220<sup>th</sup>, Poly-222.
- (31) Kang, H., Jong-Duk, K., Sang-Hoon, H., Ich-Seop, C. (2002) Self-aggregates of poly(2-hydroxyethyl aspartamide) copolymers loaded with methotrexate by physical and chemical entrapments. *J. Controlled. Release* 81, 135-144.
- (32) Park, J. M., Muhoberae B. B., Dubin, P. L., and Xia, J. (1992) Effects of protein charge heterogeneity in protein-polyelectrolyte complexation. *Macromolecules* 25, 290-295.
- (33) Dautzenberg, H. (2000) Polyelectrolyte Complex Formation in Highly Aggregating Systems: Methodical Aspects and General Tendencies. *Physical Chemistry of Polyelectrolytes* (T. Radeva, Ed.) pp 743-792, Marcel Dekker, New York.
- (34) Burgess, D. J. (1994) Complex Coacervation: Microcapsule Formation. *Macromolecular Complexes in Chemistry and Biology* (P. Dubin, J. Bock, R. M. Davies, D. N. Schulz, C. Thies, Ed.) pp 285-300, Springer-Verlag, Berlin
- (35) Jani, P., Halbert, G. W., Langridge, J., and Florence, A. T. (1990) Nanoparticle Uptake by the Rat Gastrointestinal Mucosa: Quantitation and Particle Size Dependency. *J. Pharm. Pharmacol.* 42, 821-826
- (36) Soane, R. J., Frier, M., Perkins, C., Jones, N. S., Davis, S. S., and Illum, L. (1999) Evaluation of the clearance characteristics of bioadhesive systems in human. *Int. J. Pharm.* 178, 55-65.
- (37) Tribet, C., Porcar, I., Bonnefont, P. A., and Audebert, R. (1998) Association between hydrophobically modified polyanions and negatively charged bovine serum albumin. *J. Phys. Chem.* 102, 1327-1333.

- (38) Dodd, S. W., Havel, H. A., Kovach, P. M., Lakshminarayan, C., Redmon, M. P., Sargeant, C. M., Sullivan, G. R., and Beals, J. M. (1995) Reversible Adsorption of Soluble Hexameric Insulin onto the Surface of Insulin Crystals Cocrystallized with Protamine: An Electrostatic Interaction. *Pharm. Res.* 12(1), 60-68.
- (39) McGraw, S. E., Lindenbaum, S. (1990) The Use of Microcalorimetry to Measure Thermodynamic Parameters of the Binding of Ligands to Insulin. *Pharm. Res.* 7(6), 606-611.
- (40) Montasser, I., Fessi, H., and Coleman, A. W. (2002) Atomic force microscopy imaging of novel type of polymeric colloidal nanostructures. *Eur. J. Pharm. Biopharm.* 54, 281-284.
- (41) Yip, C. M., Brader, M. L., Frank, B. H., DeFelippis, M. R., and Ward, M. D. (2000) Structural Studies of a Crystalline Insulin Analog Complex with Protamine by Atomic Force Microscopy. *Biophys. J.* 78, 466-473.

## **Chapter 3**

Insulin containing nanocomplexes formed by self-assembly from biodegradable amine-modified poly(vinyl alcohol)-graft-poly(L-lactide): Bioavailability and nasal tolerability in rats.

Published:

Pharmaceutical Research  
Volume 22(11) 1879-86, 2005  
American Association of Pharmaceutical Scientists  
Springer Science

### 3.1. Abstract

**Purpose:** Bioavailability and local tolerability of insulin containing nano-complexes from amine-modified poly(vinyl alcohol)-graft-poly(L-lactide) were studied in rats after nasal application. Histology of the nasal epithelium was investigated to verify the integrity of the nasal mucosa. **Methods:** Nano-complexes (NC) were prepared by spontaneous self-assembly of insulin and the water-soluble amphiphilic polymer. Changes in blood glucose and insulin blood concentration were monitored in anaesthetized rats using a glucose meter and ELISA respectively. Histological sections of the nasal cavity were examined after H&E staining by light microscopy. **Results:** NC reduced blood glucose level in fasted healthy rats by 20% after 50-80 min and in streptozotocin induced diabetic rats by 30% within 75-95 min compared to basal levels. In both animal models significant concentrations of human insulin were detected, with relative bioavailabilities  $F_{rel}$  of 2.8 up to 8.3 %. The more hydrophobic, lactic acid grafted polyester were more effective at a threefold higher polymer concentration, increasing the relative bioavailability  $F_{rel}$  of a 5 I.U./kg dose from 2.8 to 5.7 %. Histological examination of the nasal mucosa after 4h showed no signs of toxicity at the site of nasal administration. **Conclusions:** These results demonstrate that the NC significantly enhanced insulin absorption, suggesting that amphiphilic biodegradable comb-structured polymers could be a promising approach for nasal peptide delivery.

## 3.2. Introduction

Recent progress in biotechnology led to an enormous growth in the number of peptide and protein drugs which usually require parenteral administration to become therapeutically useful (1,2). Non-parenteral administration across mucosal surfaces, e.g. rectal, buccal, vaginal, nasal and pulmonary epithelia have been considered as alternative routes of application to replace parenteral injections (3,4). Among them, nasal delivery of peptides attracted strong interest due to its favorable biopharmaceutical properties. The structure of the nasal epithelium, its high blood perfusion and lower detrimental enzyme concentrations may result in higher bioavailabilities as compared to oral administration (5). Nasal drug administration facilitates self-medication thus improving patient compliance. Protein and peptide drugs show, however, frequently low and variable bioavailabilities after nasal administration e.g. for insulin <1% (6). Therefore, nasal insulin therapy necessitates co-administration of absorption enhancers such as surfactants, bile salts, fusidic acid derivatives, medium-chain fatty acids, chelators or enzyme inhibitors to increase absorption and hence bioavailability (7,8). Although these absorption enhancers significantly increase transmucosal peptide transport, local tolerability and safety concerns, related to membrane damage, ciliary toxicity, mucus discharge and epithelial disruption need to be overcome (9).

Consequently, the design of appropriate peptide carrier systems avoiding harmful additives has become a topic of intensive research. Nanoscale colloidal carriers from hydrophilic and biocompatible polymers, such as chitosan (10), were found to be useful for nasal vaccine (11) and insulin delivery (12) without employing additional penetration enhancers. Not only size and surface properties but also the polymer composition and architecture affected functional properties of nano-carriers such as transport of macromolecules across biological surfaces. In general nanoscale dimensions favor transport of particles across mucosal epithelia (13,14).

Moreover, nano-carriers with bioadhesive properties, e.g. NP coated with Carbopol, prevented rapid nasal clearance (15). Increasing residence time in the nasal cavity, was thought to improve drug absorption (16,17). Through design of polymer properties, nanoparticle characteristics can be manipulated such as hydrophilicity and surface charge. Especially polycations like poly(L-lysine), protamine, poly(ethylene imine), chitosan and dextran derivatives seem to increase mucosal permeability (18-20). The combination of enhancing properties, mediated through cationic surfaces charges, with the formation of nanoparticulate carriers was realized by encapsulating insulin into chitosan NP by ionotropic gelation, which yielded a significant blood glucose reduction in rabbits after nasal administration (21).

In an attempt to combine different enhancer principles, namely amphiphilicity, cationic charges and bioadhesion into one macromolecule, we studied water-soluble amine-modified polyesters, namely poly(vinyl 3-(diethyl)propylcarbamate-co-vinyl acetate-co-vinyl alcohol)- as cationic backbone and the corresponding graft-polyesters with short (L-lactic acid) side chains for their potential to form insulin-nano-complexes by spontaneous self-assembly (22). The objective of the present work was to evaluate two formulations of NC, composed of the polymers P(26) and P(26)-2<sub>LL</sub>, as a novel nasal delivery system for insulin in a rat model and to explore the influence of the different polymeric structures on absorption enhancement.

### **3.3. Materials and Methods**

#### **3.3.1. Materials**

Polymers were synthesized and characterized as previously described (20). As abbreviation for the polymers we use: P(X)-YLL. P(26) carried 26 amino-groups per PVA molecule (DP=300). P(26)-2<sub>LL</sub> had additional 48 short lactide chains per backbone with an average

chain length of about three lactic acid units. Human recombinant insulin (26.2 I.U./mg) was a gift from Aventis Pharma AG (Germany).

### **3.3.2. Nanocomplexes Preparation**

Insulin stock solutions with concentrations of 4.3, 5.7 and 11.4 mg/ml for 4.0, 5.0 and 10 I.U./kg doses respectively were prepared in two steps: 1. The insulin powder was dissolved in 87% (V/V)  $1.15 \times 10^{-2}$  N-HCl in 10 ml-Pyrex® tubes. 2. 13% (V/V) of 0.1 N-Tris(hydroxymethyl)amino methane solution was added resulting in a clear Tris-buffer solution with low ionic strength ( $I=0.01$ ) and pH 7.4. Polymer stock solutions in concentrations from 2.15 mg/ml for P(26) and 7.30, 9.70 respectively 29.70 mg/ml for P(26)-2<sub>LL</sub> were prepared in Tris-buffer. An equal volume of the filtered stock solutions of insulin and polymer were mixed resulting in defined ratios (Table 1) of insulin/polymer in the final NC-solution as previously described (22). The colloidal polymer-insulin complexes were formed after mixing of the aqueous buffer solutions containing insulin and polymer by spontaneous self-assembly.

### **3.3.3. Animal Preparation and Dosing**

Male Wistar rats of about 250g (Charles-River Wiga, Germany) were fasted overnight with free access to water. Diabetic rats were obtained after streptozotocin treatment (55 mg/kg) and included into the experiment when blood glucose levels exceeded 250 mg/dl. Rats were anesthetized by ether inhalation for ~ 2 min in a sealed glass container followed by intraperitoneal injection of avertin. Preparation of avertin: Stock solution was prepared with 25.0g 2,2,2-tribromoethanol in 15.5 ml tert-amyl-alcohol (Sigma-Aldrich, Germany) mixed for 12h in a dark bottle at room temperature. Working solution was made fresh before use of 0.5 ml Avertin stock added with 39.5 ml 0,9% NaCl (Braun Melsungen, Germany) and filtered through a 0.2µm filter. The animals were dosed with 10 µl/g body weight by

intraperitoneal injection and remained anesthetized for 60-90 min (healthy) and 30-40 min (diabetic) in a supine position, ensuring that the administered dose was not swallowed or sniffed during the resorption period. Nasal delivery took place 15-20 min after injection of Avertin. NC suspensions (~ 20µl) were carefully delivered to the right nostril only, using a Hamilton syringe with an attached polyethylene tube, which was inserted about 0.5 cm into the nostril. The animal study was conducted according to the principles outlined in the “Guide for the Care and Use of Laboratory Animal Resources” (National Academy Press, Washington) and had received approval by the Animal Review Committee at the local authorities.

#### **3.3.4. Glucose and Insulin Measurements**

Blood glucose levels were directly measured in blood collected from the tip of the rat tail using a glucose meter (Glucometer Elite, Bayer Corp., Germany). Blood samples (~ 200µl) for insulin determination were collected in Microvettes® CB300 (Sarstedt, Germany) at the same time points of -10 and -5 min before formulation application and at various time intervals up to 4h post administration. The glucose content was calculated as a percentage of the mean value of the first three measurements for each animal. The values of the blood glucose baselines were in the range of 75-105 mg/dl for healthy rats and 350-500 mg/dl for diabetic rats. The quantitative determination of human insulin in serum was carried out using an enzyme immunoassay ELISA (Cat. EIA-2935, DRG Instruments GmbH, Germany), which exhibited no cross-reactivity to rat insulin.

#### **3.3.5. Analysis of Data**

The areas under the curve (AUC) for the insulin concentration against time respective the glucose percent against time were calculated for the various groups using the trapezoidal method. Statistical analysis was performed by one-way analysis of variances (ANOVA) using

the Origin 6.0 software (OriginLab, USA). Throughout the level of significance was chosen as  $p < 0.05$ .

### **3.3.6. Histological studies**

From the healthy rats three animals per group were randomly selected. The animals were decapitated, the mandible, brain and excess soft tissue removed and the residuals were fixated in formalin solution and decalcified in 10% Titriplex® III solution adjusted to pH 7.2 (Merck KG, Germany) for three weeks. All regions were processed through to Paraplast® embedding (Carl Roth GmbH, Germany) using routine histological methods. Sections were cut serially at 7µm thickness with a Reichert-Jung Biocut 2030, mounted and stained with haematoxylin and eosin. According to the method by Thomas N.W. (24) the cross-sections of the nasal cavity were examined with the light microscope (Olympus BHZ).

## **3.4. Results and discussion**

### **3.4.1 Non Diabetic Rats**

Previously we described nanocomplex (NC) formation between insulin and amphiphilic cationic charge-containing biodegradable copolyesters composed of a hydrophilic PVA backbone grafted with short hydrophobic lactic acid groups (22). From a range of compounds we selected two polymers, the charge modified backbone P(26) and a corresponding graft-polyester P(26)-2<sub>LL</sub> to evaluate the influence of PLA grafting. Insulin NC revealed interesting properties for a nasal peptide delivery system: positive zeta potential  $\sim +20$  mV, small particle sizes in the range of 200-450 nm, high insulin loading efficiency and bioadhesive attributes as demonstrated for NP of DEAPA-PVA-g-PLGA (25). The dose for insulin was selected based on the expected pharmacological effect and the respective route of

administration. Polymer concentrations ranged from 0.076 to 0.973 mg/kg body weight and reflected optimal polymer/insulin ratios from systematic investigations of the complexation process (Table 1).

Formulation	Insulin single dose (IU) <sup>a</sup>	Insulin conc. (IU/kg)	Polymer conc. (mg/kg)	Particle size (mean ± SD) (nm)	Zeta potential (mV)	Mass ratio (Ins/Poly)
<b>Group of healthy rats</b>						
INS Sol s.c.	0.125	0.5	-	-	-	-
INS Sol i.n.	1.0	4.0	-	-	-	-
INS/P(26) NC	1.0	4.0	0.076	394 ± 61	17.7 ± 2.7	2.0 : 1.0
INS/P(26)-2 <sub>LL</sub> NC	1.0	4.0	0.260	250 ± 39	18.8 ± 3.3	1.0 : 1.7
<b>Group of diabetic rats</b>						
INS Sol s.c.	0.1875	0.75	-	-	-	-
INS/P(26)-2 <sub>LL</sub> NC	1.25	5.0	0.324	275 ± 52	18.4 ± 3.4	1.0 : 1.7
INS/P(26)-2 <sub>LL</sub> NC	1.25	5.0	0.973	448 ± 25	5.0 ± 1.1	1.0 : 5.1
INS/P(26)-2 <sub>LL</sub> NC	2.50	10	0.649	290 ± 62	22.9 ± 2.5	1.0 : 1.7

<sup>a</sup> based on an average of 250 g body weight per animal

**Table 1.** Characterization of administered solutions/nanocomplexes

Evaluation of these NC in an animal model is one prerequisite for studying these nasal delivery system in human clinical trials. Therefore, Wistar rats were used as well established animal model for nasal absorption studies. First we studied the absorption enhancing properties of both formulations after nasal application in a non-diabetic, fasted rat model. Figure 1 shows the blood glucose time profiles, figure 2 the insulin time curves and table 2 the corresponding pharmacokinetic and pharmacodynamic parameters:  $c_{\max/\min}$ ,  $T_{\max/\min}$ , AUC and  $F_{\text{rel/dyn}}$ .

The pharmacodynamic effect of insulin NC versus a subcutaneous reference is shown in fig. 1. In the control group receiving a buffered solution with 4.0 IU/kg insulin intranasally only a slight decrease in blood glucose concentration was observed in accordance with the literature (9).

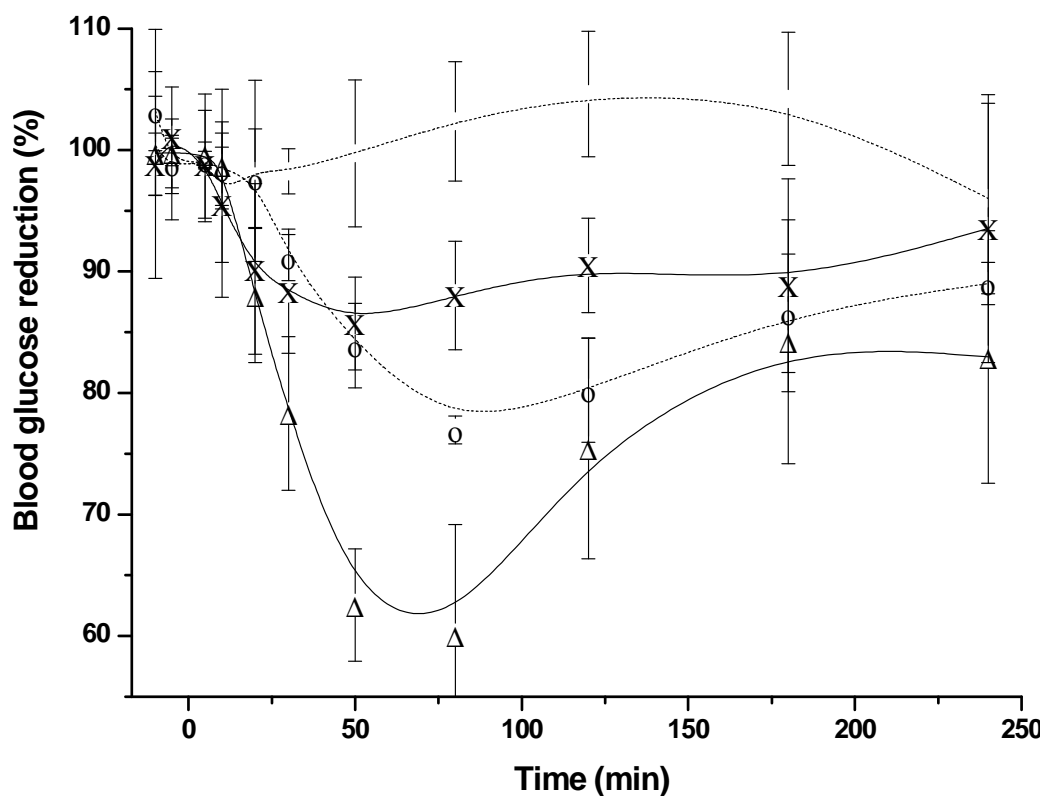


**Figure 1.** Blood glucose reduction in healthy rats: — $\Delta$ — Insulin s.c. with 0,5 IU/kg, — $\circ$ — NC composed of P(26)-2<sub>LL</sub> with 4,0 IU/kg insulin, — $\times$ — NC composed of P(26) with 4,0 IU/kg insulin, — — control solution with 4,0 IU/kg insulin in buffer.

Stable glucose concentration (95-105%) in this group over the experimental period of 240 min indicated that the animals were not stressed by anesthesia and blood sampling procedures. Stress could provoke an increase of blood glucose levels due to hormonal effects. The subcutaneous reference of 0.5 IU/kg insulin yielded a  $C_{\min}$  56% of the basal glucose concentration after 72 min. Corresponding insulin data in figure 2 showed values of  $C_{\max}$  and  $T_{\max}$  of about 79  $\mu$ IU/ml and 18 min respectively. The glucose profiles, which reflected insulin action, followed the plasma insulin levels with a slight delay. The AUC values resulting from s.c. application were used as benchmark to calculate the relative bioavailability  $F_{\text{dyn/rel}}$ .

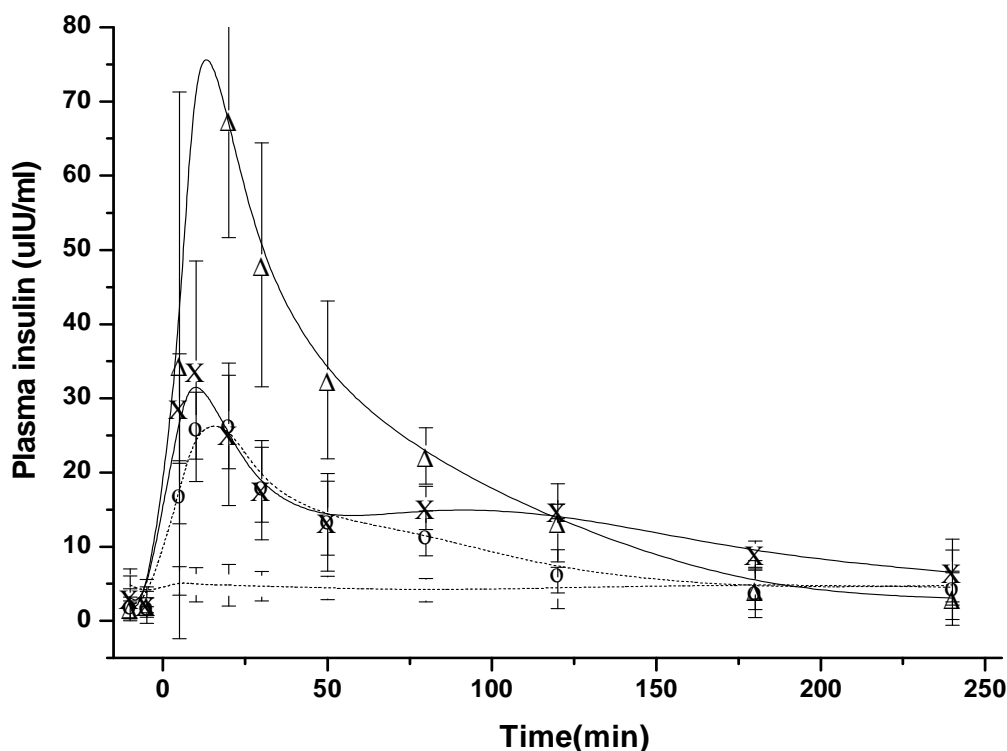


**Figure 2.** Plasma insulin from healthy rats: —△— Insulin s.c. with 0,5 IU/kg, —○— NC composed of P(26)-2<sub>LL</sub> with 4,0 IU/kg insulin, —X— NC composed of P(26) with 4,0 IU/kg insulin, — — control solution with 4,0 IU/kg insulin in buffer.

Both the NC of insulin/P(26)-2<sub>LL</sub> and - P(26) increased the insulin plasma level up to  $29.1 \pm 5.1 \mu\text{IU/ml}$  or  $35.7 \pm 13.8 \mu\text{IU/ml}$  respectively about 10-15 minutes after nasal instillation.

The administration of insulin solution without polymer (control group) resulted in a low plasma level of  $5.9 \pm 2.4 \mu\text{IU/ml}$ . The partially elevated insulin absorption in the control group could be due to an effect of the anesthetic agent as suggested by Illum and Mayor (26).

It was not possible to dose fully conscious rats as control in order to investigate the effects of avertin, because non-anaesthetized rats, as obligatory nose breathers, sneeze vigorously and nasally administered solutions are discharged from the nasal cavity. Therefore, relative bioavailabilities between the different treatment groups were assessed, with all animals anesthetized in the same way. Those treated with insulin NC exhibited elevated insulin levels with  $F_{\text{rel}} 5.84 \pm 0.9\%$  for insulin/P(26)-2<sub>LL</sub> and  $8.32 \pm 1.2\%$  for insulin/P(26), in comparison

to the insulin control group with  $F_{rel} 2.82 \pm 1.0\%$ . These findings suggest that the changes in blood glucose concentrations are a direct consequence of elevated insulin blood levels and not a decrease e.g. due to other hormonal counter regulatory effects. The AUC values for both types of NC were significantly different compared to the control group ( $P < 0.05$ ). The observation that the insulin control group exhibited no glucose change despite slightly elevated human insulin levels could be due to an auto regulation effect observed in healthy rats: small amounts of absorbed exogenous insulin depresses the endogenous secretion of insulin by  $\beta$ -cells, and consequently the amount of exogenous insulin is not sufficient to affect glycaemia (27). Otherwise the exogenous insulin concentration in the NC treated groups was too high for compensation by regulatory mechanism. A correlation between applied insulin dose and insulin plasma level requires additional experiments and is beyond the scope of this investigation.

Improved insulin absorption after nasal administration of NC formulations was supported by the corresponding glucose data: The decrease in plasma glucose levels in both groups treated with nasally applied NC was significantly different ( $P < 0.05$ ) from that induced by the insulin control solution. Insulin NC with P(26) lowered the basal glucose concentration about 17% within 52 min and the NC with insulin/P(26)-2<sub>LL</sub> about 22% after 82 min respectively. The decrease lasted up to 180 min since values close to basal levels were recorded at the last measuring time point at 240 min.

The relative bioavailability  $F_{dyn}$  for insulin/P(26)-2<sub>LL</sub> was in the range of 7.7 % and for insulin/P(26) about 6.38 % in contrast to 0.96% for the control group. This reflects a significant and distinctive metabolic response as consequence of insulin NC application. While the pharmacological difference between both NC groups is not significant ( $P < 0.05$ ), the glucose-time curve exhibited a differential course: The glucose minimum for P(26)-2<sub>LL</sub> NC is more clearly pronounced and lasted for longer time than the NC composed of insulin/P(26) indicating improved properties for the more hydrophobic polymers.

Analysis of Pharmacodynamics					
Formulation	n	T <sub>min</sub> (min)	C <sub>min</sub> (% basal glucose)	AUC <sub>0-240min</sub> (% x min)	F <sub>dyn</sub> (%) <sup>f</sup>
INS Sol s.c. <sup>a</sup>	4	72.5 ± 15.0	56.3 ± 4.2	4488 ± 795	100.0 ± 17.7
INS Sol i.n. <sup>b</sup>	4	107.5 ± 56.2	96.6 ± 2.0	348 ± 72	0.96 ± 0.2
INS-DEAPA26 <sup>c</sup>	4	52.5 ± 20.6 <sup>*/-</sup>	83.5 ± 2.1 <sup>*/-</sup>	2292 ± 470	6.38 ± 1.3 <sup>*/-</sup>
INS-DEAPA26/2 <sup>d</sup>	4	82.5 ± 28.7 <sup>*/-</sup>	78.2 ± 4.1 <sup>*/-</sup>	2770 ± 324	7.72 ± 0.9 <sup>*/-</sup>
<i>one-way ANOVA<sup>e</sup></i>		<i>P &gt; 0.05</i>		<i>P &gt; 0.05</i>	
Analysis of Pharmacokinetics					
Formulation	n	T <sub>max</sub> (min)	C <sub>max</sub> (μIU/ml)	AUC <sub>0-240min</sub> (μIU/ml x min)	F <sub>rel</sub> (%) <sup>f</sup>
INS Sol s.c. <sup>a</sup>	4	17.5 ± 9.6	78.7 ± 37.1	4861 ± 669	100.0 ± 13.7
INS Sol i.n. <sup>b</sup>	4	37.5 ± 55.5	5.9 ± 2.4	1098 ± 393	2.82 ± 1.0
INS-DEAPA26 <sup>c</sup>	4	8.8 ± 2.5 <sup>*/-</sup>	35.7 ± 13.8 <sup>*/-</sup>	3237 ± 464	8.32 ± 1.2 <sup>*/**</sup>
INS-DEAPA26/2 <sup>d</sup>	4	15.0 ± 5.8 <sup>*/-</sup>	29.1 ± 5.1 <sup>*/-</sup>	2270 ± 360	5.84 ± 0.9 <sup>*/**</sup>
<i>one-way ANOVA<sup>e</sup></i>		<i>P &gt; 0.05</i>		<i>P &gt; 0.05</i>	

**Table II.** The Pharmacokinetics and Pharmacodynamics of insulin in a healthy rat model

<sup>a</sup> Insulin solution, administered by subcutaneous injection

<sup>b</sup> Insulin solution administered intranasally

<sup>c</sup> Insulin/P(26)-Polymer nanocomplexes administered intranasally

<sup>d</sup> Insulin/P(26)-2<sub>LL</sub>-Polymer nanocomplexes administered intranasally

<sup>e</sup> Significance level of comparisons made between treated and control groups(\*<sup>/</sup>), respective between nasally treated groups (\*<sup>\*\*</sup>), denoted when significant different otherwise (-)

<sup>f</sup> Calculation according to formula:  $F = \frac{AUC_{Test} \times Dosis_{s.c.}}{AUC_{s.c.} \times Dosis_{Test}} \times 100$

### 3.4.2. Diabetic Rats

In diabetic rats insulin deficiency causes severe changes in metabolism amongst others, a reduction in liver protein synthesis, decreased activity of the sympathetic nervous system, dehydration, glycosuria and osmotic diuresis (28,29). Thus, streptozotocin-diabetic rats showed a different response profile to environmental stress factors (30). For instance, duration of anesthesia is significantly reduced and variability of blood glucose levels is increased. As this was observed for different control groups especially after 120 min, the pharmacological data were evaluated only for a timeframe up to 120 min.

After establishing the penetration enhancement of P(26)-2<sub>LL</sub>-insulin NC we investigated in more detail formulation aspects, varying polymer and insulin concentration in the diabetic rat model. Figure 3 shows the glucose time courses, figure 4 the insulin time curves and table 3 the corresponding pharmacokinetic and pharmacodynamic parameters:  $c_{\max/\min}$ ,  $T_{\max/\min}$ , AUC and  $F_{\text{rel/dyn}}$ .

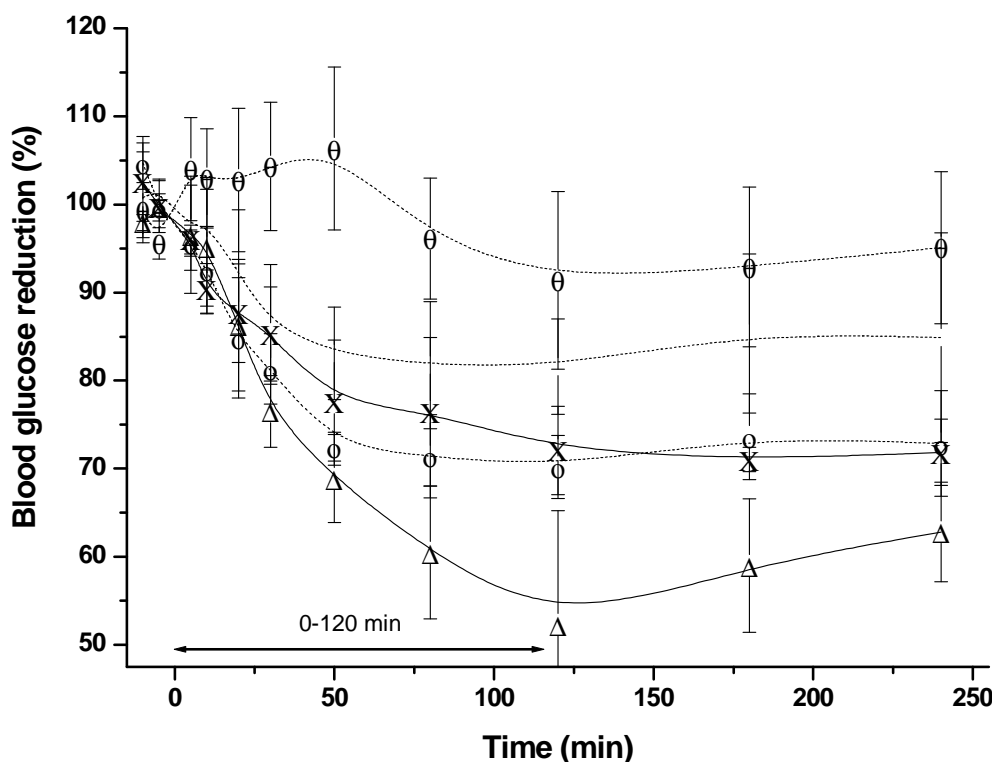


**Figure 3.** Blood glucose reduction in diabetic rats. — $\Delta$ — Insulin s.c. with 0,75 IU/kg, Option 1: — — NC composed of P(26)-2<sub>LL</sub> (1.7 : 1.0 m/m polymer/insulin) with 5,0 IU/kg insulin, Option 2: — $\circ$ — NC composed of P(26)-2<sub>LL</sub> (5.1 : 1.0 m/m) with 5,0 IU/kg insulin, Option 3: — $\times$ — NC composed of P(26)-2<sub>LL</sub> (1.7 : 1.0 m/m) with 10,0 IU/kg insulin, — $\theta$ — control solution with 5,0 IU/kg insulin in buffer.

We administered an insulin dose of 5.0 IU/kg keeping the polymer concentration constant at a mass ratio of 1:1.7 insulin/polymer (Option 1). At a constant insulin dose we increased the polymer concentration threefold to a 1:5.1 mass ratio, to probe if an increase in insulin bioavailability could be related to the amount of instilled polymer (Option 2). Finally, we

increased concentration of NC in the suspension reaching a dose of 10.0 IU/kg at a constant 1:1.7 mass ratio (Option 3). After subcutaneous administration of insulin solution (0.75 IU/kg) an immediate and distinctive decrease of glycemia was observed (figure 3).

The  $AUC_{0-120min}$  values for glucose/time and the  $AUC_{0-240min}$  for insulin/time resulting from s.c. application were used as reference to calculate the bioavailabilities  $F_{dyn/rel}$ . The NC of P(26)-2<sub>LL</sub>-insulin according to option 1 caused a clear blood glucose reduction as expected. The minimum was achieved after 93 min with 20% decrease of the blood glucose basal levels and a relative bioavailability  $F_{dyn}$  of 8.5 %.

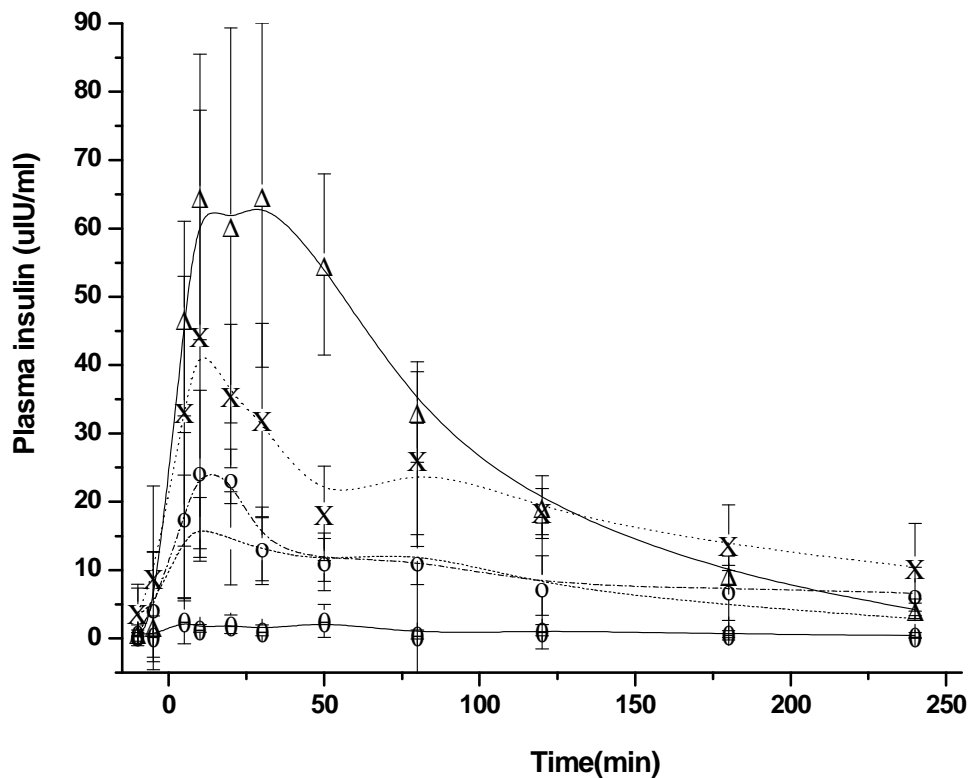


**Figure 4.** Plasma insulin from diabetic rats: — $\Delta$ — Insulin s.c. with 0,75 IU/kg, ...X... NC composed of P(26)-2<sub>LL</sub> with 10,0 IU/kg insulin (1.7:1.0), ---o--- NC composed of P(26)-2<sub>LL</sub> with 5,0 IU/kg insulin (5.1:1.0), — — NC composed of P(26)-2<sub>LL</sub> with 5,0 IU/kg insulin (1.7:1.0), — $\theta$ — control solution with 10,0 IU/kg insulin in buffer.

Figure 4 depicts the corresponding rapid increase in human insulin levels for option 1 up to 18  $\mu$ IU/ml within 14 min, corresponding to a bioavailability  $F_{rel}$  about 2.8 %. The strongest

decrease in blood glucose was achieved with option 2, containing a threefold higher polymer concentration. The formulation according to option 2 exhibited a fast onset of insulin action in the first 50 min, which is comparable to the s.c. application (figure 3). The blood glucose decrease reached a maximum of 30% of the basal values after 75 min. That correlates with the fast increasing blood insulin concentration to 30  $\mu$ IU/ml after 14 min (figure 4).

Analysis of Pharmacodynamics					
Formulation	n	T <sub>min</sub> (min)	C <sub>min</sub> (% basal glucose)	AUC <sub>0-120min</sub> (% x min)	F <sub>dyn</sub> (%) <sup>f</sup>
INS Sol s.c. <sup>a</sup>	4	140.0 ± 34.6	50.7 ± 10.2	3576 ± 581	100.0 ± 16.3
INS Sol i.n.	4	110.0 ± 663	87.7 ± 5.8	487 ± 93	2.04 ± 0.4
5.0 I.U. with 1.7 <sup>b</sup>	4	93.3 ± 23.1 <sup>-/-</sup>	80.3 ± 6.1 <sup>*/-</sup>	2038 ± 261	8.54 ± 1.1 <sup>*/**</sup>
5.0 I.U. with 5.1 <sup>c</sup>	4	75.0 ± 33.2 <sup>-/-</sup>	70.2 ± 4.2 <sup>*/-</sup>	2803 ± 213	11.76 ± 0.9 <sup>*/**</sup>
10.0 I.U. with 1.7 <sup>d</sup>	4	160.0 ± 34.6 <sup>-/**</sup>	68.8 ± 3.1 <sup>*/-</sup>	2703 ± 401	5.67 ± 0.1 <sup>*/**</sup>
<i>one-way ANOVA<sup>e</sup></i>		<i>P &gt; 0.05</i>			<i>P &gt; 0.05</i>
Analysis of Pharmacokinetics					
Formulation	n	T <sub>max</sub> (min)	C <sub>max</sub> ( $\mu$ IU/ml)	AUC <sub>0-240min</sub> ( $\mu$ IU/ml x min)	F <sub>rel</sub> (%) <sup>f</sup>
INS Sol s.c. <sup>a</sup>	3	16.7 ± 11.5	67.5 ± 23.9	6456 ± 1063	100.0 ± 16.5
INS Sol i.n.	4	21.3 ± 20.1	3.8 ± 2.9	261 ± 178	0.30 ± 0.2
5.0 I.U. with 1.7 <sup>b</sup>	4	13.8 ± 7.5 <sup>*/-</sup>	17.9 ± 6.9 <sup>*/-</sup>	1194 ± 521	2.77 ± 1.2 <sup>*/**</sup>
5.0 I.U. with 5.1 <sup>c</sup>	4	13.8 ± 7.5 <sup>*/-</sup>	30.0 ± 10.6 <sup>*/-</sup>	2438 ± 476	5.67 ± 1.1 <sup>*/-</sup>
10.0 I.U. with 1.7 <sup>d</sup>	4	16.7 ± 5.8 <sup>*/**</sup>	47.0 ± 29.9 <sup>*/**</sup>	4533 ± 2201	5.27 ± 2.6 <sup>*/-</sup>
<i>one-way ANOVA<sup>e</sup></i>		<i>P &gt; 0.05</i>			<i>P &gt; 0.05</i>

**Table III.** The Pharmacokinetics and Pharmacodynamics of insulin in a diabetic rat model

<sup>a</sup> Insulin solution administered by subcutaneous injection

<sup>b-d</sup> Insulin/P(26)-2<sub>LL</sub>-Polymer nanocomplexes administered intranasally  
(Option 1<sup>b</sup>, Option 2<sup>c</sup>, Option 3<sup>d</sup>)

<sup>e</sup> Significance level of comparisons made between treated and control groups(\*<sup>/</sup>), respective between nasally treated groups (<sup>/</sup>\*\*), denoted when significant different otherwise (-)

<sup>f</sup> Calculation according to formula:  $F = \frac{AUC_{Test} \times Dosis_{s.c.}}{AUC_{s.c.} \times Dosis_{Test}} \times 100$

The resulting bioavailabilities with F<sub>dyn</sub> 11.8 % and F<sub>rel</sub> 5.67 % were significantly higher than for option 1 (p <0.05). Then we evaluated the effect of increasing the dose to 10.0 IU/kg at a higher concentration not increasing the volume. After nasal administration the blood insulin

concentrations rise to 47  $\mu\text{IU/ml}$  after 17 min. The bioavailability  $F_{\text{rel}}$  with 5.3 % was significantly increased compared to option 1. This increase could be explained due to a higher local NC concentration, leading to a higher concentration gradient at the site of absorption. Furthermore the absolute polymer concentration was two-fold higher compared to option 1. Systematic investigations of the complex assembly demonstrated that a defined ratio of both binding partners is necessary for optimal NC formation (22). For insulin/P(26)-2<sub>LL</sub> NC the optimal ratio is 1.0 insulin to 1.7 polymer (m/m) (see table 1). A threefold increase of the ratio for P(26)-2<sub>LL</sub> NC from 1.7 to 5.1 increases the average complex size from 275 to 448 nm and decreases the zeta potential from about +18.4 to +5.0 mV to (table 1). Increasing the ratio obviously reduces specific advantages of nanocarriers, however, the bioavailability of 5.0 I.U. insulin as a single dose increases. We assume the spontaneous occurrence of complex rearrangement processes and an overall increase in free polymer concentration especially for higher polymer ratios (22). Increased bioavailability could therefore be likely related to a higher polymer concentration, resulting in more direct interaction of polymer and epithelium, rather than the nanoparticle character of the carrier. Similar observations were published by Dyer and Illum et al. (31). They reported insulin-chitosan solution to be significantly more effective than the NP formulation, and they also observed an influence of chitosan concentration (20). Other researchers demonstrate the superiority of chitosan-insulin NP against solutions (12), but also discuss whether the effect of the nanoparticulate system is more likely due to an interaction of chitosan to epithelial membranes, in terms of bioadhesion and transient opening of the tight junctions (32).

It is generally accepted that two major pathways are available for transport of drugs across the epithelial membrane, namely the paracellular and transcellular route. The tight junctions can be influenced by interaction of the epithelia with polymeric materials and actually we are investigating on the caco-2 cell line if the cationic poly(vinyl 3-(diethyl amino) propylcarbamate-co-vinyl acetate-co-vinyl alcohol)-graft-poly(L-lactide) can interact with the

junctional complex, temporarily opening the paracellular transport pathway as reported for chitosan (32).

### **3.4.3. Histological Studies**

Increased absorption of peptides after nasal application has been reported in a number of studies after co-administration with absorption enhancers such as: surfactants, including bile salts and their derivatives, chelators and enzyme inhibitors. Many absorption enhancers are irritating to mucous membranes and the histological effects of some agents on nasal mucosa have been reported. Even after a single application of formulations containing enhancer like laurth-9 (1% w/v) cellular erosion, cell-cell separation, dense mucous coating and subsequent reduction of epithelial height from rat nasal epithelium were observed within five minutes after nasal application (9). Therefore, it is desirable to evaluate histopathological effects. The anatomical division of the rat nasal cavity by the midline septum enables the assessment of histopathological effects by direct comparison of the treated and untreated side. Errors due to inter-animal variability and tissue sampling are thus minimized. The major structural features in each region of the rat nasal cavity, including the septum and the turbinates, could be identified in the overview micrographs (figure 5a). Especially the area of the nasal septum, which consists of respiratory epithelium, is of interest, because it is the projected deposition site for the administered dose.

The magnification in figure 5a shows the typical anatomy of the septum: cartilage, covered by ciliated pseudo stratified columnar epithelium, populated with goblet cells. A basic requirement, for comparability and reproducibility of the histological and pharmacological results is that the administered dose is deposited on a restricted area. For small volumes of 20-30  $\mu$ l per dose no leakage via the septal window in more posterior regions was reported. Volumes in this range are known to be retained exclusively at the site of application (9). It was necessary to insert the tubing in the rat nostril 5 min prior to the application of the

solutions. This procedure allowed the rats to acclimate on hampered breathing and prevented loss of the administered dose through sniff or exhale from the nasal cavity.

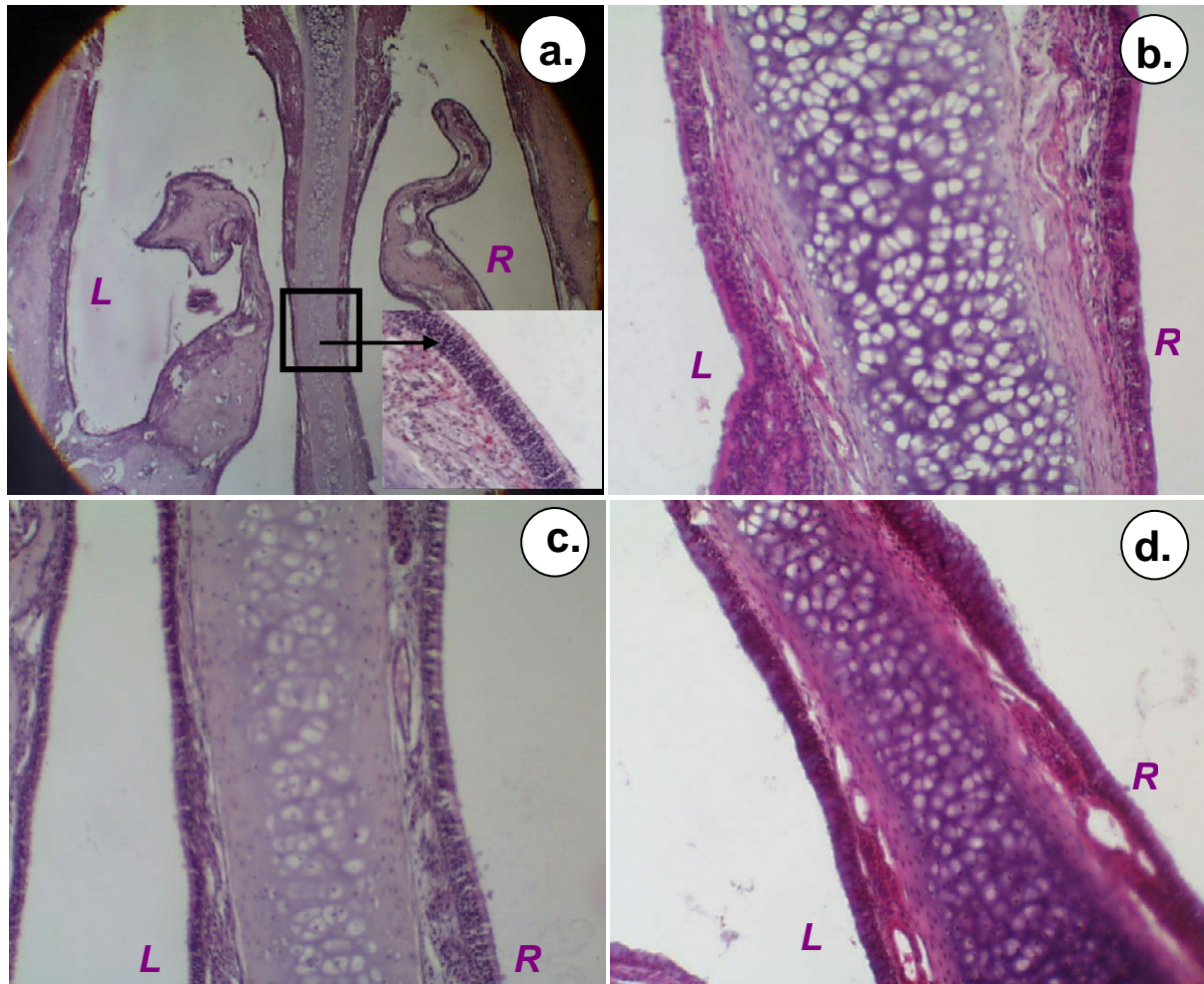


**Figure 5.** Photomicrographs of vertical sections through the anterior rat nasal cavity showing two sides of the nasal septum 4h after application of 20-25 microliter of insulin solution into the right side (R). Normal respiratory epithelium populated with goblet cells covers the undosed left side (L) in each case. Treated tissue on the right side can be compared with untreated tissue on the left of the septum; epithelium thickness on the right side was  $134 \pm 14$  micrometer and on the left side  $137 \pm 15$  micrometer (n.s.). a.) a section overview from control group (insulin s.c.), magnification x 20. b-d.) represents the septum region from (a) indicated by the black rectangle, magnification x 100 b.) nasal insulin application without polymer (non-polymeric control) c.) NC composed of insulin and P(26)-2<sub>LL</sub> d.) NC composed of insulin and P(26) b-d.) show no clear difference of the epithelial lining between dosed side and untreated side.

The rat experiments were performed without surgical procedures like tracheotomy or esophagus ligation to simulate, as far as possible, realistic conditions. This animal model

saves certainly the potential danger of aspiration of a part of the dose volume. However, the supine position of the animal, as well as the small volume, would contribute to a restricted distribution and a reproducible disposition at the site of absorption.

The histological tissue preparation was performed at the end of the blood measurements after 4h, so that toxicological effects of longer lasting adhesion of polymer residues were taken in account. In each animal treated with NC or insulin control solution, all regions of the dosed side of the cavity were covered by an intact, undamaged epithelium layer, comparable to that observed in the sections of the non dosed side. On the dosed side none epithelial disruption has occurred on septal and nasoturbinatate surfaces neither for insulin/P(26)-2<sub>LL</sub> NC (figure 5c) nor for insulin/P(26) NC (figure 5d). Moreover, the treated and untreated side of the nasal cavity in each cross-section matched each other with respect to the height of the respiratory epithelia. Repeated dosing and recovery studies are necessary to establish the full toxicological implications for a chronic administration. However, none acute adverse effects were registered in our single dose experiment for both NC preparations.

### 3.5. Conclusion

As an alternative application route for insulin, the intra-nasal administration along with pulmonary delivery represents one of the most promising options for diabetic patients. The commercial exploitation of nasal insulin delivery depends on the development of new and safe enhancers, increasing the absorption and hence bioavailability. Here we report on the feasibility for two types of Insulin NC from a novel class of amphiphilic comb-like polyesters demonstrating enhanced insulin absorption across rat nasal mucosa. These data indicated that amphiphilic NC with grafted lactic acid side chains were superior to more hydrophilic backbones. The relative effect availabilities (glucose) and bioavailability (insulin) suggest that significant enhancement factors can be attained using NC. Both nanocomplex preparations were shown to be non-toxic after a single nasal administration. The effect of lowering blood glucose levels observed in healthy rats could be reproduced in diabetic rats. Therefore, NC on the basis of insulin/P(26)-2<sub>LL</sub> NC may present a promising delivery system for peptides enhancing mucosal absorption. Further work is warranted to elucidate the enhancer mechanism.

### 3.6. References

- (1) L. Andersson, L. Blomberg, M. Flegel, L. Lepsa, B. Nilsson, and M. Verlander. Large-Scale synthesis of Peptides, *Biopolymers* **55**: 227-250 (2000).
- (2) A. E. Pontiroli. Peptide hormones: Review of current and emerging uses by nasal delivery, *Adv Drug Deliv Rev.* **29**: 81-87 (1998).
- (3) D. J. Chetty, and Y. W. Chien. Novel methods of insulin delivery: an update, *Crit Rev Ther Drug Carrier Syst.* **15(6)**: 629-670 (1998).
- (4) M. Simon, and T. Kissel. Away with the needle. Noninvasive administration routes for insulin: improved quality of life for diabetics, *Pharm Unserer Zeit* **30(2)**: 136-141 (2001).
- (5) S. Gizurarson, E. Bechgaard. Study of nasal enzyme activity towards insulin. In vitro, *Chem Pharm Bull.* **39(8)**: 2155-2157 (1991).
- (6) M. J. Deurloo, W. A. Hermens, S. G. Romeyn, J. C. Verhoef, and F. W. Merkus. Absorption enhancement of intranasally administered insulin by sodium taurodihydrofusidate (STDHF) in rabbits and rats, *Pharm Res.* **6(10)**: 853-856 (1989).
- (7) M. Hinchcliffe, and L. Illum. Intranasal insulin delivery and therapy, *Adv Drug Deliv Rev.* **35**:199-234 (1999).
- (8) A. Sanchez, P. Ygartua, and D. Fos. Role of surfactants in the bioavailability of intranasal insulin, *Eur J Drug Metab Pharmacokinet.* **3**: 120-124 (1991).
- (9) S. G. Chandler, L. Illum, and N. W. Thomas. Nasal absorption in the rats. II. Effect of enhancers on insulin absorption and nasal histology, *Int J Pharm.* **76**: 61-70 (1991).
- (10) C. Prego, M. Garcia, D. Torres, and M. J. Alonso. Transmucosal macromolecular drug delivery, *J Control Release* **101(1-3)**: 151-162 (2005).
- (11) M. Koping-Hoggard, A. Sanchez, and M. J. Alonso. Nanoparticles as carriers for nasal vaccine delivery, *Expert Rev Vaccines* **4(2)**: 185-196 (2005).
- (12) R. Fernandez-Urrusuno, P. Calvo, C. Remunan-Lopez, J. L. Vila-Jato, and M. J. Alonso. Enhancement of nasal absorption of insulin using chitosan nanoparticles, *Pharm Res.* **16(10)**: 1576-1581 (1999).
- (13) J. Brooking, S. S. Davis, and L. Illum. Transport of nanoparticles across the rat nasal mucosa, *J Drug Target.* **9(4)**: 267-279 (2001).
- (14) A. Vila, A. Sanchez, C. Evora, I. Soriano, O. McCallion, and M. J. Alonso. PLA-PEG particles as nasal protein carriers: the influence of the particle size, *Int J Pharm.* **292(1-2)**: 43-52 (2005).
- (15) H. Takeuchi, H. Yamamoto, and Y. Kawashima. Mucoadhesive nanoparticulate systems for peptide drug delivery, *Adv Drug Deliv Rev.* **47(1)**: 39-54 (2001).

- (16) P. Dondeti, H. Zia, and T. Needham. Bioadhesive and formulation parameters affecting nasal absorption, *Int J Pharm.* **127**: 115-133 (1996).
- (17) M. R. Jimenez-Castellanos, H. Zia, and C. T. Rhodes. Mucoadhesive drug delivery systems, *Drug Dev Ind Pharm.* **19**: 143-194 (1993).
- (18) D. N. Granger, P. R. Kvielys, M. A. Perry, and A. E. Taylor. Charge selectivity of rat intestinal capillaries – influence of polycations, *Gastroenterology* **91**: 1443-1446 (1986).
- (19) Y. Maitani, Y. Machida, and T. Nagai. Influence of molecular weight and charge on nasal absorption of dextran and DEAE-dextran in rabbits, *Int J Pharm.* **76**: 43-49 (1992).
- (20) L. Illum, N. F. Farraj, and S. S. Davis. Chitosan as novel nasal delivery system for peptide drugs, *Pharm Res.* **11**: 1186-1189 (1994).
- (21) R. Fernandez-Urrusuno, P. Calvo, C. Remunan-Lopez C., J. L. Vila-Jato, and M. J. Alonso. Enhancement of nasal absorption of insulin using chitosan nanoparticles, *Pharm Res.* **16(10)**: 1576-1581 (1999).
- (22) M. Simon, M. Wittmar, U. Bakowsky, and T. Kissel. Self-assembling nanocomplexes of insulin and water-soluble branched poly[(vinyl-3-(diethyl amino)propylcarbamate-co-(vinyl acetate)-co-(vinyl alcohol)]-graft-poly(L-Lactid): A novel carrier for transmucosal delivery of peptides, *Bioconjugate Chem.* **15(4)**: 841-849 (2004)
- (23) M. Wittmar. *Charge modified, comb-like graft-polyesters for drug delivery and DNA vaccination: Synthesis and Characterization of Poly(vinyl dialkylaminoalkylcarbamate-co-vinyl acetate-co-vinyl alcohol)-graft-poly(D,L-lactide-co-glycolide)s*, Dissertation, Philipps University Marburg, 2004. <http://archiv.ub.uni-marburg.de/diss/z2004/0075/> (accessed 01/13/04).
- (24) S. G. Chandler, L. Illum, and N. W. Thomas. Nasal absorption in the rats. I: A method to demonstrate the histological effects of nasal formulations, *Int J Pharm.* **70**: 19-27 (1991).
- (25) L. A. Dailey, E. Kleemann, M. Wittmar, T. Gessler, T. Schmehl, C. Roberts, W. Seeger, and T. Kissel. Surfactant-free, biodegradable nanoparticles for aerosol therapy based on the branched polyesters, DEAPA-PVAL-g-PLGA, *Pharm Res.* **20(12)**: 2011-2020 (2003).
- (26) S. H. Mayor, and L. Illum. Investigation of the effect of anesthesia on nasal absorption of insulin in rats, *Int J Pharm.* **149**: 123-29 (1997).
- (27) C. Damge, C. Michel, M. Aprahamian, and P. Couvreur. New Approach for Oral Administration of Insulin With Polyalkylcyanoacrylate Nanocapsules as Drug Carrier, *Diabetes* **37(2)**: 246-251 (1988).
- (28) A. B. Anwana , and H. O. Garland. Intracellular dehydration in the rat made diabetic with streptozotocin: effects of infusion, *J Endocrinol.* **128(3)**: 333-337 (1991).
- (29) T. Yoshida, H. Nishioka, Y. Nakamura, and M. Kondo. Reduced noradrenalin turnover in streptozotocin-induced diabetic rats, *Diabetologia* **28(9)**: 692-696 (1985).

- (30) L. L. Bellush and W. N. Henley. Altered responses to environmental stress in streptozotocin-diabetic rats. *Physiol Behav.* **47(2)**: 231-238 (1990).
- (31) A. M. Dyer, M. Hinchcliffe, P. Watts, J. Castille, I. Jabbal-Gill, R. Nankervis, A. Smith, and L. Illum. Nasal Delivery of Insulin Using Novel Chitosan Based Formulations: A Comparative Study in Two Animal Models between Simple Chitosan Formulations and Chitosan Nanoparticles, *Pharm Res.***19(7)**: 998-1008 (2002).
- (32) N. G. Schipper, S. Olsson, J. A. Hoogstraate, A. G. deBoer, K. M. Varum, and P. Artursson. Chitosans as absorption enhancers for poorly absorbable drugs 2: mechanism of absorption enhancement, *Pharm Res.***14(7)**: 923-929 (1997).

## **Chapter 4**

Nanosized insulin-carrier based on amine-modified graft polyesters:  
Protection from enzymatic degradation, interaction with Caco-2 cell  
monolayers, peptide transport and cytotoxicity.

Publication in preparation  
(for European Journal of Pharmaceutics and Biopharmaceutics)

## 4.1. Abstract

**PURPOSE:** Non parenteral insulin delivery via the gastrointestinal tract faces serious hurdles in form of epithelial barriers and enzymatic degradation. Here we investigated novel insulin containing nano-complexes (NC) and –particles (NP) based on amine modified comb-like polyesters to overcome these barriers. **METHODS:** Trypsinic insulin degradation on NC and surface tension measurements on polymer solutions were performed. The interaction with enterocyte-like Caco-2 cells in terms of cytotoxicity, transport through and uptake in the cell layers was evaluated by measuring transepithelial electrical resistance (TEER), release of lactate dehydrogenase (LDH), confocal laser scanning microscopy (CLSM) and transport studies. **RESULTS:** The protection capacity of nanocomplexes and their interaction with Caco-2 cells varied strongly as a function of lactide-grafting. With increasing lactide grafting ( $P(26) < P(26)-1_{LL} < P(26)-2_{LL}$ ) NC protected more than 95% of a 1,0 mg/ml insulin NC dispersion against trypsinic degradation. Insulin transport and layer uptake increased with higher L-lactid grafting. About 25% of a 1,25 mg/ml TRITC insulin NC dispersion with  $P(26)-2_{LL}$  was recovered in the layer after 90 min, also visualized by CLSM. Accompanied by a concentration dependent cytotoxicity profile with elevated LDH release and decreased TEER values. The cytotoxicity correlates with the surfactant like character of the polymers, decreasing the surface tension to 45 mN/m for the amphiphilic  $P(26)-2_{LL}$ . Nevertheless, the observed TEER decrease was reversible after 20 hours. **CONCLUSIONS:** These results demonstrate that the NC protect insulin and enhanced its absorption, suggesting that amphiphilic biodegradable comb-polymers offer a promising approach to overcome intestinal barriers.

## 4.2. Introduction

Non-parenteral administration of peptide drugs, like insulin for the treatment of diabetes mellitus, remains a great challenge to pharmaceutical research. To circumvent the tedious injection regime of insulin therapy, several attempts have been made to exploit mucosal surfaces, especially the nasal, pulmonary and oral mucosa, for the delivery of macromolecules (1,2). Of these routes peroral administration would be the most desirable on a long term basis. However, enzymatic degradation by proteolytic enzymes and a low absorption rate (< 1.0%) over the gastrointestinal mucosa limits its relative bioavailability (3). Numerous strategies have been devised to enhance insulin absorption (4,5). Most often these strategies have focused at addressing one of the barriers to intestinal absorption, either the epithelial cell layer or the digestive enzymes. These include the co-administration of insulin with penetration enhancers and/or protease inhibitors, enteric coatings, colloidal drug carriers, such as nanoparticles and liposomes and chemically modification of insulin by covalent attachment of amphiphilic oligomers to increase its lipophilicity (6). Especially particles in the nanosize range, based on biodegradable and mucoadhesive polymers, are of particular interest, as they provide protection of sensitive proteins against enzymatic degradation and prolong intestinal residence time (7). Their transport however, across the intestinal barrier is controversially discussed. Uptake can occur not only via micro-fold (M)-cells, highly specialized epithelial cells in the Peyer's patches, and isolated follicles of the gut associated lymphoid tissue (GALT), but also across the apical membrane of enterocytes (8). Non-covalent complexes formed between hydrophilic carrier molecules and insulin can induce partial and reversible unfolding of the insulin molecule, facilitating permeability by passive transcellular diffusion across cell membranes due to the increased flexibility and lipophilicity, before dissociation of the complex beyond the epithelial cell (9). As a new approach to non-parenteral insulin delivery, biodegradable nanocomplexes composed of insulin and poly[(vinyl-3-

(diethylamino)-propylcarbamate-*co*-(vinyl acetate)-*co*-(vinyl alcohol)]-graft-poly(L-lactic acid) polymers were investigated. The preparation and characterization of the NC were previously described, emphasizing the gentle preparation technique of NC by spontaneous self-assembling of polymer and insulin (10). The subsequent trials with NC at healthy and diabetic rats demonstrated significant insulin uptake after nasal administration (11). The results motivated us to further investigate the enhancing effect of insulin absorption in a model biological environment for better understanding the performance of DEAPA-PVA-*g*-PLLA nanocomplexes *in vivo*. As it is difficult to grow confluent layers of nasal epithelial cell layers (12), we utilize the well established human intestinal cell line Caco-2 as a model for epithelial cell layers. We compared the nanocomplexes against a nanoparticle preparation of P(26)-10<sub>LG</sub> polymer, which belongs in principle to the same polymer class of amine modified branched polyesters. In comparison to the watersoluble polymers P(26)-/1,2,3<sub>LL</sub> with short L-lactide side chains, the P(26)-10<sub>LG</sub> variant exhibited longer hydrophobic lactide-*co*-glycolide chains. Particles therefrom were prepared with a solvent displacement technique and afterwards loaded with insulin through adsorption on the positive particle surface. This concept was already successful utilized for the preparation of cationic particles for aerosol therapy (13), respectively adsorptive loading of tetanus toxoid on sulfobutylated (SB) SB-PVA-*g*-PLGA particles and immunisation experiments on mice (14).

In the present study, the effect of DEAPA-PVA-*g*-PLLA NC and DEAPA-PVA-*g*-PLGA NP on the cellular response involving peptide absorption behavior was thus evaluated using the Caco-2 cell line. Viability and integrity of the cell monolayers, which affect the permeability of cell monolayers for peptide molecules and transport behaviour through the cell monolayer was examined. Furthermore we investigated the protection capabilities of the NC against the harsh attack of trypsinic enzymes, contributing essentially to luminal insulin degradation.

### **4.3. Materials and Methods**

#### **4.3.1. Materials**

Polymers: Poly[(vinyl-3-(diethylamino)-propylcarbamate-*co*-(vinyl acetate)-*co*-(vinyl alcohol)]-graft-poly(L-lactic acid), respective -poly(D,L-lactic-*co*-glycolic acid) polymers were synthesized and characterized as previously described (15). As abbreviation for the polymers we use: P(X)-Y<sub>LL</sub>. P(26) carried 26 amino-groups per PVA molecule (DP=300). P(26)-1<sub>LL</sub>/P(26)-2<sub>LL</sub> had additional 32/ 48 short lactide chains (L-lactide) per backbone with an average chain length of about two/ three lactic acid units. P(26)-10<sub>LG</sub> contains about 180 chains of lactide *co*- glycolide (PLGA) per PVA backbone with an average chain length of 12 units lactide/glycolide.

Human recombinant insulin (26.2 I.U./mg) was a gift from Aventis Pharma AG (Germany). Trypsin (TPCK treated, from bovine pancreas, 10.000 units/mg) and alpha-chymotrypsin (TLCK treated, Type VII, from bovine pancreas, 55 units/mg), lactate dehydrogenase assay and FITC-WGA were obtained from Sigma (Taufkirchen, Germany). Tissue culture reagents and fetal calf serum (FCS) were obtained from Gibco (Eggstein, Germany), and tissue culture articles from Nunc (Wiesbaden, Germany). All other chemicals were obtained from Merck (Darmstadt, Germany) in analytical quality.

#### **4.3.2. Nanocomplexes Preparation**

The colloidal polymer-insulin complexes were prepared and characterized as previously described (10). Stock solutions of insulin (2.50 mg/mL) and polymers (2.50 – 12.50 mg/mL) were prepared in Tris (hydroxymethyl)-aminomethane (TRIS) buffer supplemented with 18 mM glucose, 49  $\mu$ M MgCl<sub>2</sub>, and 170  $\mu$ M CaCl<sub>2</sub> at a pH of 7.70 (0.01 M). The nanocomplexes (NC) were obtained by spontaneous self-assembly after mixing of an equivalent volume of insulin and polymer stock solution.

### **4.3.3. Nanoparticle Preparation**

The particles of P(26)-10<sub>LL</sub> were prepared according to the solvent displacement technique (13). About 30,0 mg of polymer were dissolved in 4,0 ml acetone. The solution was slowly diluted via a syringe in 20,0 ml 0,01 % Pluronic F-68 solution containing 90,0 µg sodium carboxymethyl cellulose. The reaction mixture was stirred with a magnetic stirring bar at 400 U·min<sup>-1</sup> for 16 hours until total evaporation of the acetone. The nanoparticle dispersion was mixed with an equal volume of insulin stock solution (2.50 mg/ml). The resulting insulin-loaded nanoparticles were stable for 24 h, afterwards flocculation occurred. Insulin binding efficiency, size and zeta potential were determined as previously described for the nanocomplexes (10).

### **4.3.4. Enzymatic degradation**

Stock solutions of insulin with 1.0 mg/ml and the respective enzyme were prepared in Tris buffer pH 8.0 supplemented with 1.0 mM CaCl<sub>2</sub>. Both solutions were incubated for 15 min at 37°C. Afterwards 5,0 ml insulin solution was mixed with ~ 50 µl enzyme solution resulting in a molar enzyme/insulin ratio of 1 : 173, according to the method of Schilling and Mitra (16). Probes were incubated at 37°C and 100 µl samples withdrawn at preset time intervals and transferred to ice-cold Tris-buffer containing 1% trifluoroacetic acid (TFA) to abort enzyme activity. The experiments were performed in triplicate. Samples were analyzed with HPLC.

### **4.3.5. Labeling of insulin with tetra-methyl-rhodamine isothiocyanate (TRITC)**

Insulin was dissolved at a concentration of 4.50 mg/mL in Na<sub>2</sub>CO<sub>3</sub> buffer pH 9.30. A solution of TRITC (1.0 mg/mL) in dimethyl sulfoxide (DMSO) was quickly added (molar ratio of insulin/TRITC, 1:2.9) and the mixture stirred for 18 h at 4°C under light exclusion. The reaction was quenched with an excess of ammonium chloride and stirred for another 4 h. Separation was performed on a PD-10 column Sephadex G-25 (Amersham Bioscience,

Germany) with PBS pH 7.40. For the CLSM and uptake experiments the insulin stock-solution for NC/NP preparation was mixed of labeled and non-labeled insulin solution according to a 1 : 10 (V/V) ratio.

#### **4.3.6. Cell culture**

Mycoplasma-free Caco-2 cells were used at passage numbers 42-50 (HD, DKFZ, German Cancer Research Institute, Heidelberg, Germany) under conditions described earlier (17). Cells were seeded at a density of  $6 \cdot 10^4$  cells/cm<sup>2</sup> either on cell culture dishes or on uncoated polycarbonate Transwell™ filter inserts (Costar, Bodenheim, Germany, 0.40 μm pore size, area: 4.71 cm<sup>2</sup>) and cultivated over 21 days. Medium was changed every second day.

#### **4.3.7. Release of lactate dehydrogenase (LDH)**

Caco-2 monolayers, grown on 12 well dishes (polystyrene) for 21 days, were incubated with one of the NC dispersions (1.0 mL), 0.1 % Triton X-100 in PBS (positive control) or pure PBS (negative control). After 60 and 120 min of exposure, 100 μL samples were taken and processed as described in (18). Each experiment was performed in triplicate.

#### **4.3.8. Transepithelial electrical resistance (TEER)**

The integrity of the monolayer was checked at 21 day post seeding by measuring TEER before and after the experiment (19). The resistance of the monolayers in the present study was approximately 400 ohms × cm<sup>-2</sup>. To study TEER reversibility, monolayers were rinsed with fresh transport buffer directly after the transport experiment and allowed to regenerate in fresh culture medium under conditions mentioned above. After preset time intervals of up to 27 h monolayer integrities were checked in buffer and then buffer was replaced with fresh culture medium. Each experiment was run in triplicate.

#### 4.3.9. Confocal laser scanning microscopy (CLSM)

Cells grown on filter inserts for 21 days were treated with NC-suspensions consisting of TRITC-labeled insulin and the polymers as described above. After 15, 60 and 120 min, cells were washed rigorously three times with ice-cold PBS, fixed with 3% (v/v) formalin in PBS at room temperature for 30 min and counterstained with FITC-labeled wheat germ agglutinin (WGA) (0.01 $\mu$ g/ $\mu$ L) for 30 min and DAPI (4',6-Diamidino-2-phenylindole) (1  $\mu$ g/mL) for 20 min, both under light exclusion. Filters were embedded in PBS/glycerol (2:1) and imaged by CLSM (Axiovert™, Zeiss CLSM 501, Jena, Germany) equipped with a Zeiss Neofluor 40\*/1.3 objective. Excitation wavelengths were 364 nm (long pass filter (LP) 385 nm) for DAPI, 488 nm (LP 505 nm) for FITC and 543 nm (LP 560 nm) for TRITC. A gallery of 80 optical sections (0.4  $\mu$ m) was imaged and xz and yz composites were processed using Zeiss LSM 510 software. Sensitivity was kept constant during different experiments.

#### 4.3.10. Transport studies

*Layer passage:* Transport studies were performed 21 days post seeding. Filter inserts (Costar Transwells, 6 well) were rinsed with PBS supplemented with 15mM glucose pH 7.40 and allowed to equilibrate at 37°C for 15 min. Experiments were started by replacing the apical buffer with the test solution (1.5 mL) and the basolateral buffer with fresh PBS (2.50 mL). Before replacing the buffer with NC dispersions, monolayers were washed once with Tris buffer. After 2.5 h a sample (1.5 mL) was drawn from the basolateral chamber and analyzed by reversed-phase HPLC as previously described (10). Permeability in % was calculated from the concentration profiles using the following equation: (cumulative amount transported / initial amount)\* 100.

*Layer uptake:* After incubation of polystyrene 12 wells with transport buffer for 15 min at 37°C and intermediate washing with supplemented Tris buffer, the test solutions (1.0 ml) were applied and incubated for 90 min. After removal of the NC solutions and a threefold

washing with PBS, the cells were dried up for 24 h under light exclusion. Each layer was afterwards dissolved in 300  $\mu$ l 2.0 % Triton-X solution and the insulin-TRITC concentration measured with a Luminescence Spectrometer LS50B (Perkin Elmer).

Results were expressed as mean value  $\pm$  S.D. of three experiments. Significance between mean values was calculated using ANOVA one way analysis (GraphPad InStat version 3.00 for Windows 95, GraphPad Software, San Diego, USA). Probability values  $p < 0.05$  were considered significant.

#### **4.3.11. Surface Tension**

The Noüy Ring method (diameter 2,0 cm) was used to measure the surface tension. All measurements were performed in triplicate at 20°C. Maximum pull exerted on the ring by the surface is measured in  $\text{mN}\cdot\text{m}^{-1}$  with a spring dynamometer against purified water as control. The concentrations of the polymer solutions were 1.0 mg/ml.

### **4.4. Results and Discussion**

#### **4.4.1. Preparation of nanocomplexes and nanoparticles**

Branched polyesters consisting of poly (vinyl alcohol) (PVA) grafted with chains of poly (lactic-co-glycolic acid) (PLGA), respectively poly (L-lactic acid) (PLLA) represent a new class of biodegradable polymers showing significant potential for the development of a variety of drug delivery vehicles (20). The modification of the PVA backbone by introduction of diethylamino-propylamine (DEAPA)-groups creates a polymer with positively charged functions and increases its hydrophilicity. The resulting amphiphilic DEAPA-PVA-g-PLLA polymer is characterized by a three-dimensional comb-like architecture with hydrophobic and hydrophilic moieties. By reduction of the PLLA units ( $\leq 3$ ) for a PVA backbone with 8,5 %

amine substitution, corresponding to 26 DEAPA-groups, water-soluble polymers could be synthesized (15). We recently demonstrated the spontaneous formation of complexes by self-assembly from these polymers with insulin (10). The resulting complexes were in the size range of 200-400 nm, exhibiting a positive zeta potential between +15-20 mV and an insulin association efficiency of about 75 % for a 1,25 mg/ml insulin solution. We compared the NC with a NP preparation based on the same backbone P(26), but with an increased grafting amount of PLGA, corresponding to about 180 chains per PVA with an average length of 12 lactide-/glycolide-units. Dissolving of the hydrophobic P(26)-10<sub>LL</sub> polymer requires therefore an organic solvent and the blank particles were prepared by a solvent displacement technique. After complete removal of acetone by evaporation, nanoparticles were obtained in the narrow size range of  $212 \pm 29$  nm, with a positive zeta potential of  $+41 \pm 5$  mV. The preformulated NP were loaded afterwards, by mixing with insulin solution. Peptide adsorption was confirmed by the inversion of the zeta potential to negative values of  $-18 \pm 3$  mV, accompanied by a size increase to  $424 \pm 281$  nm, indicating adsorption of negatively charged insulin on the positive particle surface. Insulin association efficiency, for a 1,25 mg/ml insulin solution, was found to be  $89,8 \pm 2,5$  %. A comparable core-corona structure was described for the tetanus-toxoid adsorption on NP made of SB-PVA-g-PLGA (21). The driving force of adsorption, electrostatic and coulombic interactions, are the same as for the assembly of the NC. We compared the NP preparation against the NC in view of transport and cytotoxicity in the cell experiments.

#### **4.4.2. Protection from enzymatic degradation of insulin in NC**

In addition to promote its epithelial absorption, insulin must also be protected from digestive enzymes to provide the greatest amount of intact, biologically active insulin to be available for absorption. The utilized Caco-2 cells exhibit a high degree of differentiation resulting in a distinctive brush border enzyme pattern, like peptidases and hydrolases (22). Nevertheless,

the enzymatic degradation during epithelial transit is still moderate in comparison to the enzymatic environment during gastrointestinal passage. Especially the enzymes  $\alpha$ -chymotrypsin and trypsin, the major proteolytic enzymes secreted by the pancreas into the intestinal lumen, account for the degradation of orally administered insulin (16). Therefore we utilized the both proteases to investigate the protection of insulin by NC from enzymatic degradation.

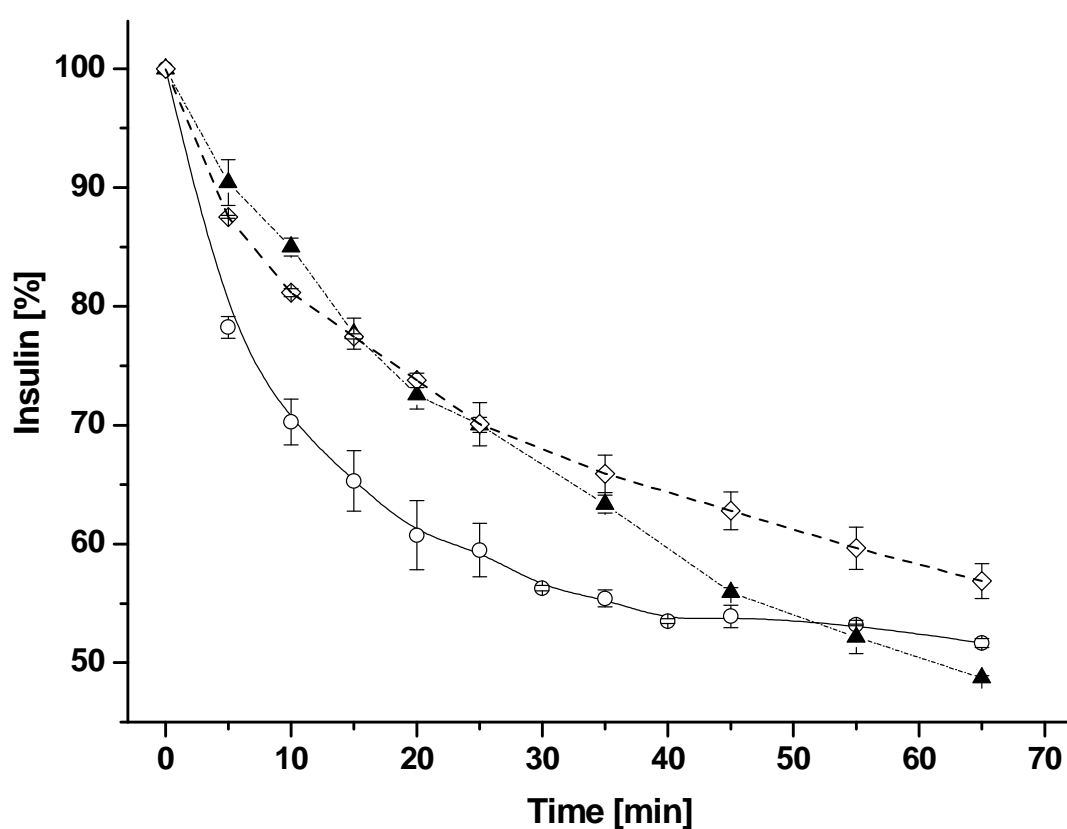


**Figure 1.** Enzymatic degradation of insulin (1,0 mg/ml) by alpha-chymotrypsin. The insulin control solution (—○—) exhibited a fast degradation, which was alleviated when insulin was incorporated in complexes with P(26)-1<sub>LL</sub> (---▲---) respective P(26)-2<sub>LL</sub> – polymer (---◇---).

As presented in Figure 1, in the presence of  $\alpha$ -chymotrypsin, free insulin was found to be markedly degraded. Indeed, under the experimental conditions only about  $51.7 \pm 0.4$  % of the

initial concentration of insulin (1,0 mg/ml) remained undegraded within 60 min. By contrast, nanocomplexes of P(26)-1<sub>LL</sub> and -2<sub>LL</sub> decelerated the degradation for 30 min with an average 10% higher insulin concentration recovered in this timeframe in comparison to the control. Beyond 30 min the effect continued only for the P(26)-2<sub>LL</sub> NC. The data for P(26)-NC are not shown as there was no significant difference in comparison to the control group.

In general, the insulin molecule consist of two chains, the A-chain with 21 amino acids and the B-chain with 30 amino acids, linked by two disulfide bonds. Protection from  $\alpha$ -chymotrypsin is difficult because of the numerous initial cleavage sides distributed all over the insulin molecule (B26-Tyr, A19-Tyr, B16-Tyr, B25-Phe and A14-Tyr). The shielding of the susceptible bonds would require an adequate embedding of the insulin molecule within the particle structure. As recently discussed (10), the complexes represent a state of equilibrium between polymer and insulin, characterized by exchange processes of binding partners. The uncomplexed insulin in solution is degraded very fast due to the high intrinsic acivity of  $\alpha$ -chymotrypsin, Schilling found apparent  $V_{\max}$  of  $6.48 \times 10^{-6}$  (M/min) in comparison to trypsin with  $0.75 \times 10^{-6}$  (M/min) (16), whereby the equilibrium of the complexes is constantly shifted towards released insulin and dismantling of complexes. The longer lasting protection of P(26)-2<sub>LL</sub> NC is in accordance with its higher binding constant in comparison to P(26)-1<sub>LL</sub> NC (10). However, the insulin concentration profile in the presence of trypsin exhibited an excellent and long-lasting protection effect (Figure 2).

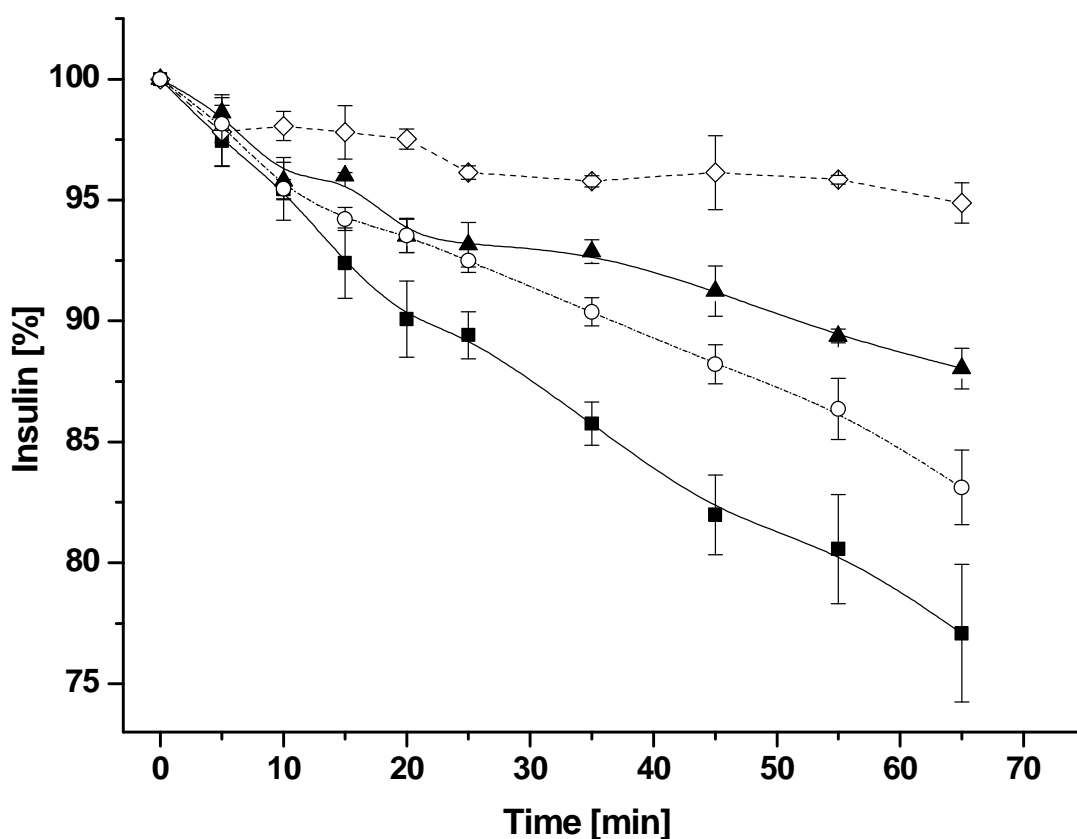


**Figure 2.** Enzymatic degradation of insulin (1,0mg/ml) by trypsin. The nanocomplexes of insulin and P(26)- (---○---), P(26)-1<sub>LL</sub>- (—▲—), respective P(26)-2<sub>LL</sub> – polymer (---◇---) exhibited a significant protection against enzymatic attack in comparison to the unprotected insulin control solution (—■—).

After one hour about  $23.0 \pm 2.8$  % of the free insulin control solution with 1,0 mg/ml is degraded. In comparison, the NC decreased the degradation of insulin dependent on lactide-grafting of the polymers. The complexes made of P(26) polymer reduced the degraded amount to  $16,9 \pm 1.5$  %, P(26)-1<sub>LL</sub> NC to  $12.0 \pm 0.8$  % and the best protection was realized with P(26)-2<sub>LL</sub> NC, with a reduction to only  $5.1 \pm 0.8$  % degraded insulin of the initial 1,0 mg/ml.

Trypsin itself cleaves insulin at only two sites, on the carboxyl side of residues B29-Lys and B22-Arg (23). Since the bonds susceptible to tryptic cleavage are located at the carboxyl

terminus of the B-chain, which is known as hydrophobic domain of insulin, it is obvious that the longer hydrophobic PLLA chains of P(26)-2<sub>LL</sub> could better interact and shield this segment.

#### 4.4.3 In vitro cytotoxicity studies

A colloidal drug carrier designated for routine application should display as little cytotoxicity as possible and polycationic molecules have often been linked to cytotoxic reactions (24,25). Therefore we investigated the in vitro cytotoxicity of NC using various techniques. Membrane damaging effects were evaluated by the release of the cytosolic enzyme lactate dehydrogenase (LDH). The enzyme is found in almost all body tissues and released upon damaging of cells.

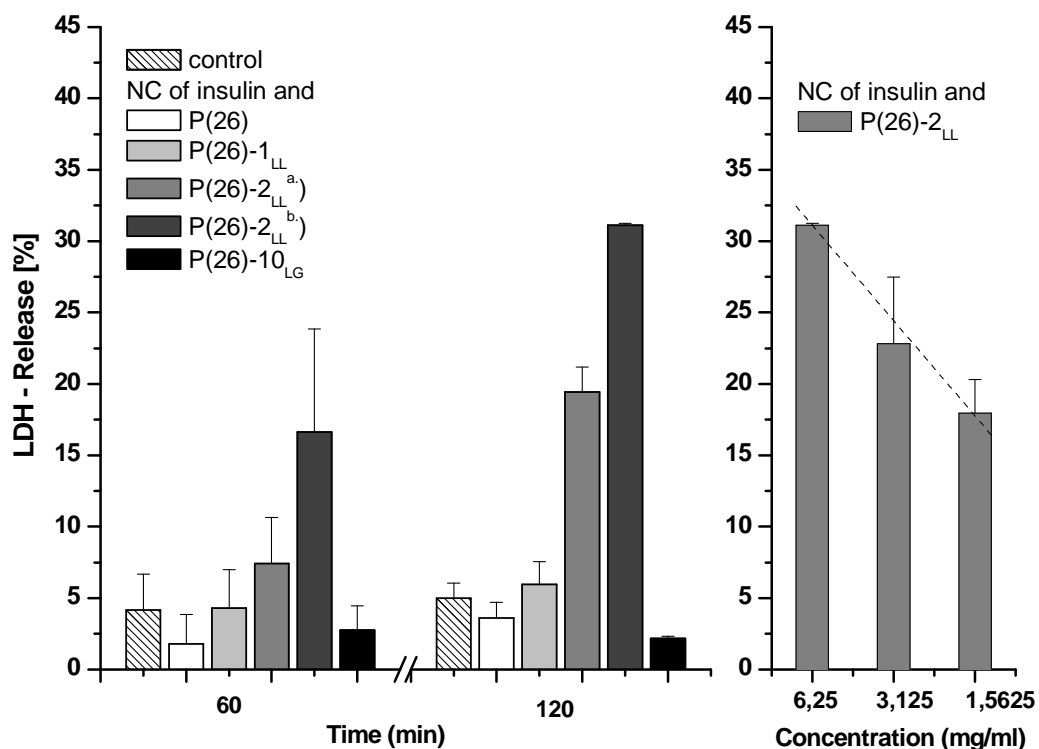


**Figure 3.** Left plot: LDH release after 60 and 120 min of buffer control and NC/NP composed of insulin and the respective polymers. NC's of P(26)-2<sub>LL</sub> with a.) 2,125 mg/ml and b.) 6,25 mg/ml exhibited a concentration dependent increase of LDH release. Right plot: In the investigated dilution series with 100, 50 and 25% of 6,25 mg/ml the dependence of LDH release is nearly linear to polymer concentration (---- linear fit with R = 0,9982).

As shown in Figure 3 left, only a negligible release of LDH was observed after 60 and 120 min for P(26), P(26)-1<sub>LL</sub> NC and P(26)-10<sub>LG</sub> NP, in comparison to the buffer control. However, P(26)-2<sub>LL</sub> NC showed a significant increase of LDH-release, reaching  $16.6 \pm 7.2\%$  after 60 min and  $28.5 \pm 4.1\%$  after 120 min. This effect was concentration dependent and decreased linearly with decreasing concentration (Fig. 3 right).

Since all DEAPA-polymers have the same degree of amine-substitution with about 26 amine groups per PVA, the cytotoxic effects of P(26)-2<sub>LL</sub> NC must be due to other properties. A large number of amphiphilic, surfactant-like molecules used for absorption enhancing have been shown to have cytotoxic effects (26). We investigated the polymers in terms of surface activity with the Noüy Ring method (Figure 4). Each of the polymer solutions, with a concentration of 1.0 mg/ml, exhibited a decrease of the surface tension from 55 mN/m for P(26) polymer to 46 mN/m for P(26)-2<sub>LL</sub> polymer in comparison to the pure Tris-buffer control with 69 mN/m.

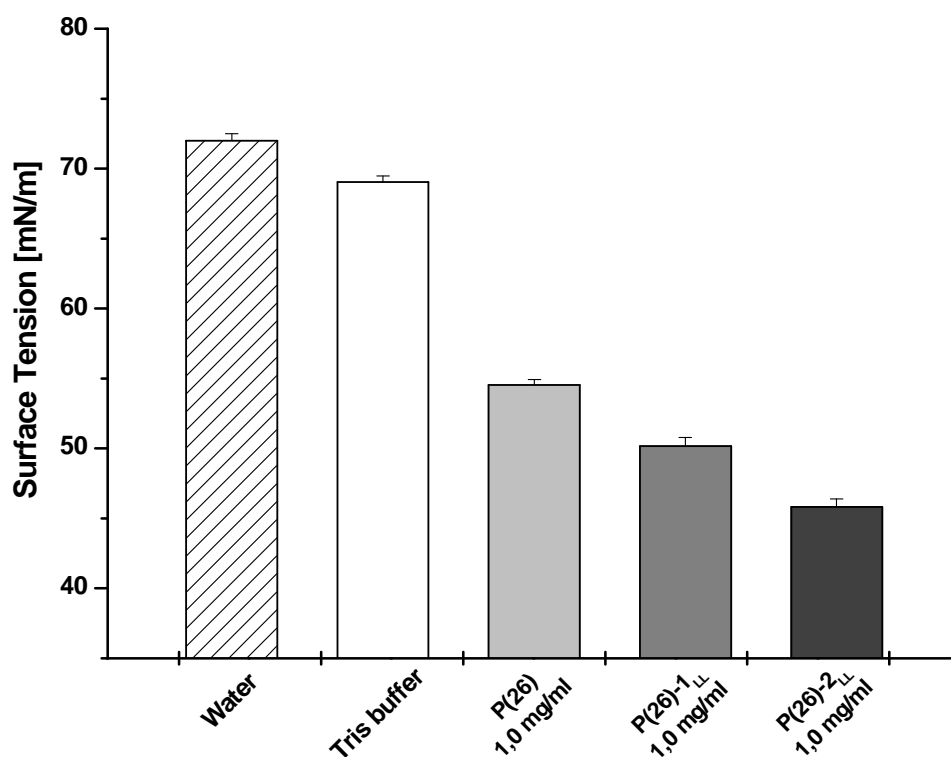


**Figure 4.** Surface tension of polymer solutions.

The basic structure of the DEAPA-PVA-g-PLLA polymers is a polyvinyl alcohol, whose properties are mainly governed by the degree of polymerisation and the degree of hydrolysis. For the polymer synthesis we utilized a PVA with a hydrolysis degree of 86-89%. Aqueous solutions of such partially hydrolysed PVA grades decrease the surface tension of water and are therefore utilized as protective colloids (27). Even the very hydrophilic amine-modified P(26) backbone kept this basic characteristic. The hydrophobically modification by grafting with lactide side chains, leads to a more amphiphilic, surfactant-like character of the polymer. A similar increase in surface activity, dependent on the chain length of the introduced hydrophobic groups to partially hydrolysed PVA, was reported for PVA modifications with alkyl groups (28) or fatty acids (29). The negligible LDH release for NP of P(26)-10<sub>LG</sub> correlates with its non-surfactant properties in aqueous solutions (30), as it is a hydrophobic organic-soluble polymer. Furthermore the positive charges at the particle corona are shielded by adsorbed insulin.

The integrity of cell monolayers upon contact with the NC and NP was assessed by measuring the transepithelial electrical resistance (TEER). While P(26) – NC with 34 % and P(26)-10<sub>LG</sub> – NP with 38 % decrease of initial values, exhibited a moderate influence on TEER in comparison to the buffer control with 10 % after 2,5 hours, resistance was significantly decreased with an increasing amount of lactide-grafting, being highest for P(26)-2<sub>LL</sub> – NC (Figure 5). As observed for the release of lactate dehydrogenase this effect was concentration dependent. The P(26)-2<sub>LL</sub> - NC formulation with 2,125 mg/ml polymer concentration decreased the resistance to about 62 %, while a formulation with a threefold higher concentration decreased it to about 88 %. Again, this ranking is more likely related to the higher amphiphilic character of the grafted DEAPA-polymers with increasing number of lactic side chains, than to the cationic character caused by amine modification.

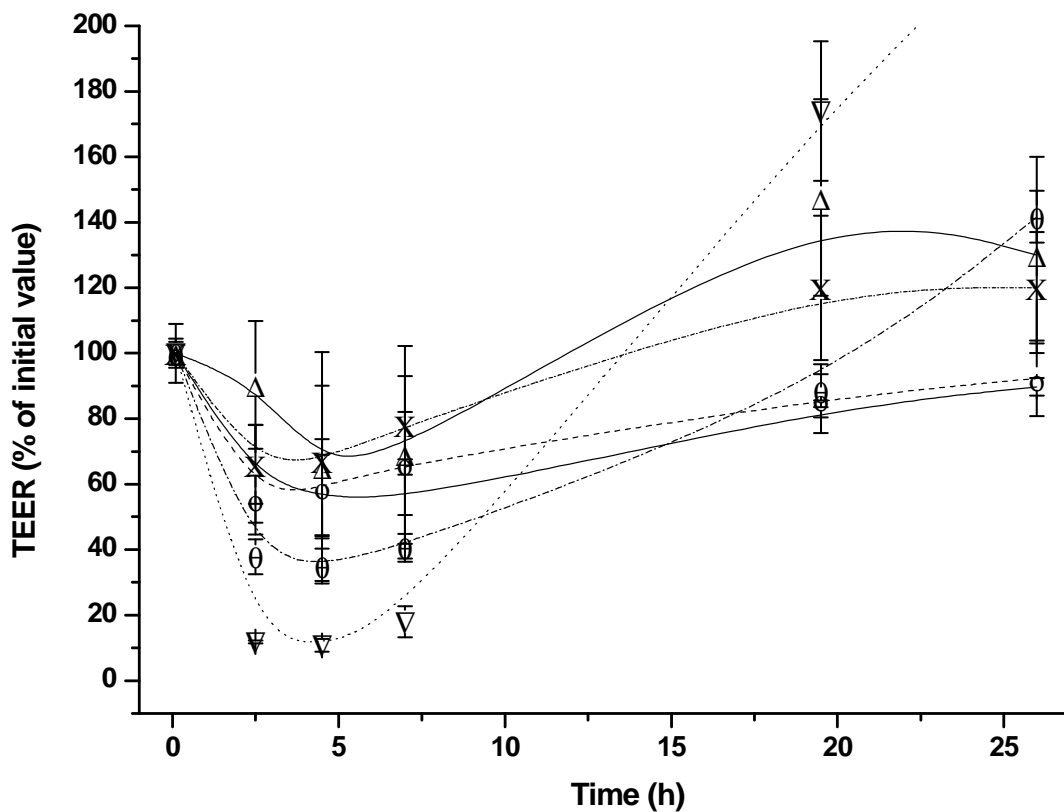


**Figure 5.** Reversibility of TEER decrease over 26 hours. Layer were incubated with nanocomplexes for 150 min followed by removal of NC, washing three times and further incubation with culture medium. Applied were a control solution (—Δ—) and NC composed of insulin and /P(26) polymer (···X···), /P(26)-1<sub>LL</sub> polymer (---o---), /P(26)-2<sub>LL</sub> polymer a.) with 2,125 mg/ml (—·θ—·), b.) with 6,25 mg/ml (···▽···), /P(26)-10<sub>LG</sub> polymer (— —).

Both, the influence of positive charge and surface activity are reported to decrease epithelial resistance: For instance, a comparable reduction in transepithelial resistance was found for NP made of chitosan (31), a biodegradable polymer with positive charges, respective for its solutions in a concentration dependent manner (32). For chitosan an influence of its positive charges on epithelial cells, resulting in structural reorganisations of tight junction associated proteins is discussed (33). Nevertheless the observed decrease in TEER upon contact with chitosan NP was reversible after removal (31). Furthermore, the effects of several absorption enhancing agents exhibiting surface activity on epithelial integrity were studied on caco-2

cells (26,34). All of the wetting agents induced a concentration dependent decrease of resistance, whereas at intermediate concentrations, the effects were reversible. It was concluded that apical membrane wounds occurred, which were repaired when the enhancing agent were removed.

In order to test the reversibility of NC and NP modulation on cellular permeability, the recovery of the initial monolayer electrical resistance was monitored over 27 h following washing with buffer and the incubation of cells with culture medium (Figure 5.). The curve progression of TEER observed for the control and P(26) - NC was not significantly different and resulted from the influence of TRIS-buffer used. The increase of TEER for the control after 20 and 27 h is probably connected to the differing conditions during measurement. While initial TEER measurements were performed after pre-incubation with transport buffer for 15 min, following measurements were performed directly after the replacement of medium with buffer. In general, all NC and NP made of grafted polymers exhibited a progressive reversibility of the epithelial resistance. The P(26)-2<sub>LL</sub> - NC, having shown the most dramatic decrease after 150 min, displayed a progressive and complete recovery after 17 h. TEER-levels even increased to  $234 \pm 32\%$  after 27 h. This final increase might be due to a reorganization of junctional-complexes after they have been damaged by the exposure to NC.

#### **4.4.4. Confocal laser scanning microscopy**

Confocal scanning microscopy was utilized to visualize a possible internalization of insulin NC into Caco-2 cell monolayers. Cells were incubated with NC prepared from different polymers and TRITC-labeled insulin over different time periods. To distinguish between the different cellular structures, cells were double-stained with FITC-WGA (membrane, green) and DAPI (nuclei, blue) (Figure 7a). The lectin WGA strongly binds to the tetra-saccharide N-acetylglucosamine, which is located abundantly at the apical membrane of Caco-2 cells. DAPI intercalates DNA and, therefore, was used as a marker for cell nuclei. As judged from

the xz and the yz sections in Figure 7, a significantly higher internalization of cell-associated insulin was found for all investigated NC compared to the control. When comparing nanocomplexes of DEAPA-polymers, it was shown that the internalized TRITC fluorescence varied strongly as a function of lactide-grafting. After 120 min, the following rank order was observed: P(26)-NC < P(26)-1<sub>LL</sub>-NC < P(26)-2<sub>LL</sub>-NC (Figure 7b-d) after 120 min. This can be explained by the smaller size of the NC made of higher grafted versions, since it has been previously reported that smaller colloidal carriers achieve a higher internalization in adsorptive cells in comparison to larger ones (35). Another explanation might be cytotoxic

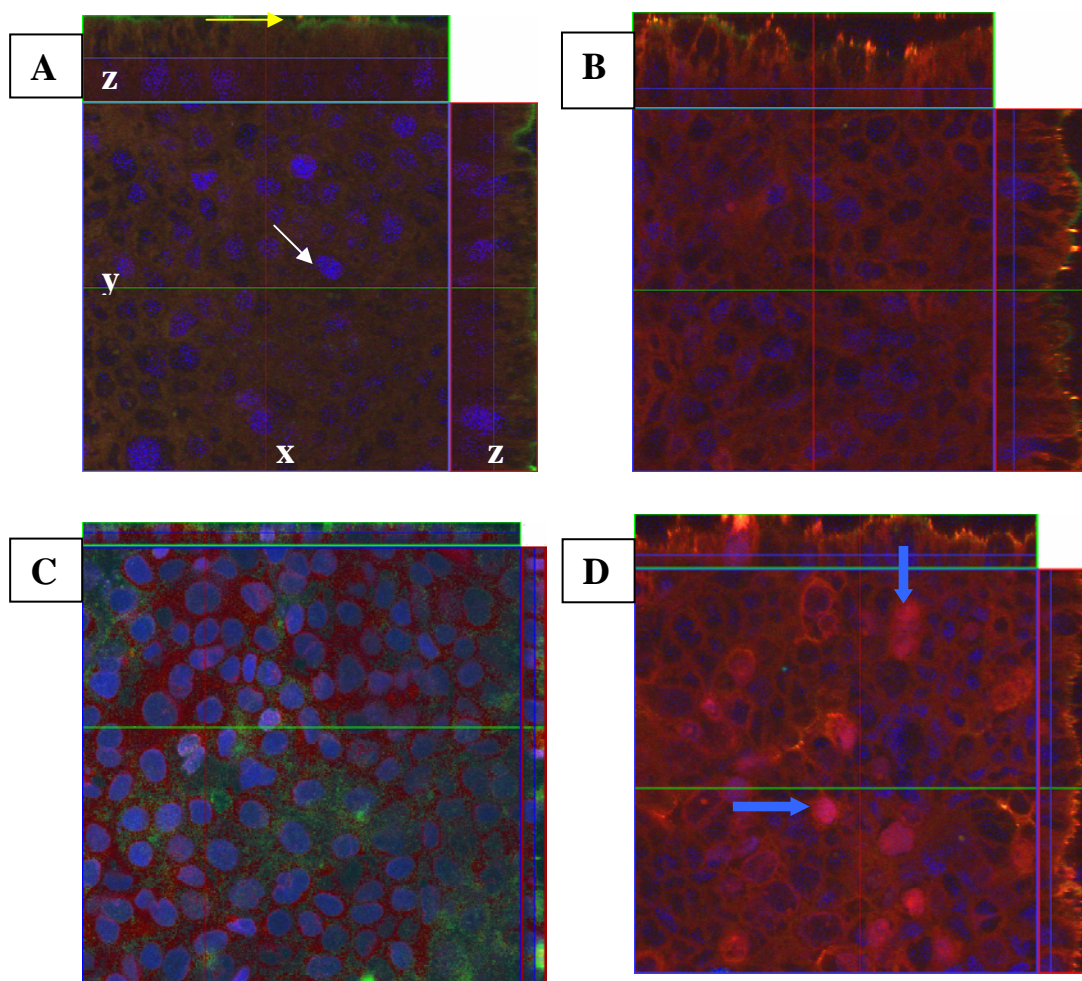


**Figure 7.** CLSM micrographs of Caco-2 monolayers treated over 120 min with nanocomplexes consisting of TRITC-labeled insulin (red fluorescence) and polymer: (a) insulin control, (b) P(26) - NC, (c) P(26)-1<sub>LL</sub>, (d) P(26)-2<sub>LL</sub>. Cells were counterstained with DAPI (nuclei, blue) (white arrow) and FITC-WGA (membrane, green/yellowish) (yellow arrow). The blue arrows indicate dead cells. Data are presented as xy, xz and yz projections.

side effects described above. The damaging effects of P(26)-2<sub>LL</sub>-NC can even be seen from the micrographs. Cells, displaying a strong red color, are dead (Figure 7 d, blue arrow).

In general, FITC-WGA staining was weaker after exposure to DEAPA-NC, indicating alterations in N-acetylglucosamine distribution in the apical membrane and, thereby, damaging effects. Comparable observations were reported for chitosan, with alterations of cytoskeletal organization, shortening of microvilli and weakening of actin staining after treatment of Caco-2 cells with different chitosan formulations (36).

Following the time course of TRITC fluorescence internalization for e.g. P(26) – NC, the first fluorescence appeared 30 min just below apical membrane. It progressively moved to the basolateral sections, where it begins to appear after 60 min and intensified until 120 min. These observations suggest a transcytotic mechanism of uptake for all NC. The slight perturbation of the plasma membrane, as indicated by the rise in extracellular LDH release, implicates an increased intracellular uptake suggesting an action of NC on the intracellular pathway as well. However, since fluorescence was distributed diffusely in the cytoplasm and was not found in discrete cytosolic vesicles, the lysosomal compartment seemed to be avoided and a different mechanism of uptake as described in (37) is presumable.

#### **4.4.5. Transport studies**

After having shown that insulin-NC were able to overcome the membrane and enter Caco-2 cells, we wanted to quantify the internalization in and the transport through the monolayers using transport studies (Figure 8). Caco-2 monolayers were incubated with NC or pure insulin as a control. After 2.5 hours, the permeated amount of insulin in the acceptor part was quantified by HPLC (Figure 8, upper plot). The layer uptake was determined after removal of the NC solutions and rigorous washing of the apical side followed by layer dissolution and TRITC fluorescence measurements of the cell lysis (Figure 8, lower plot).

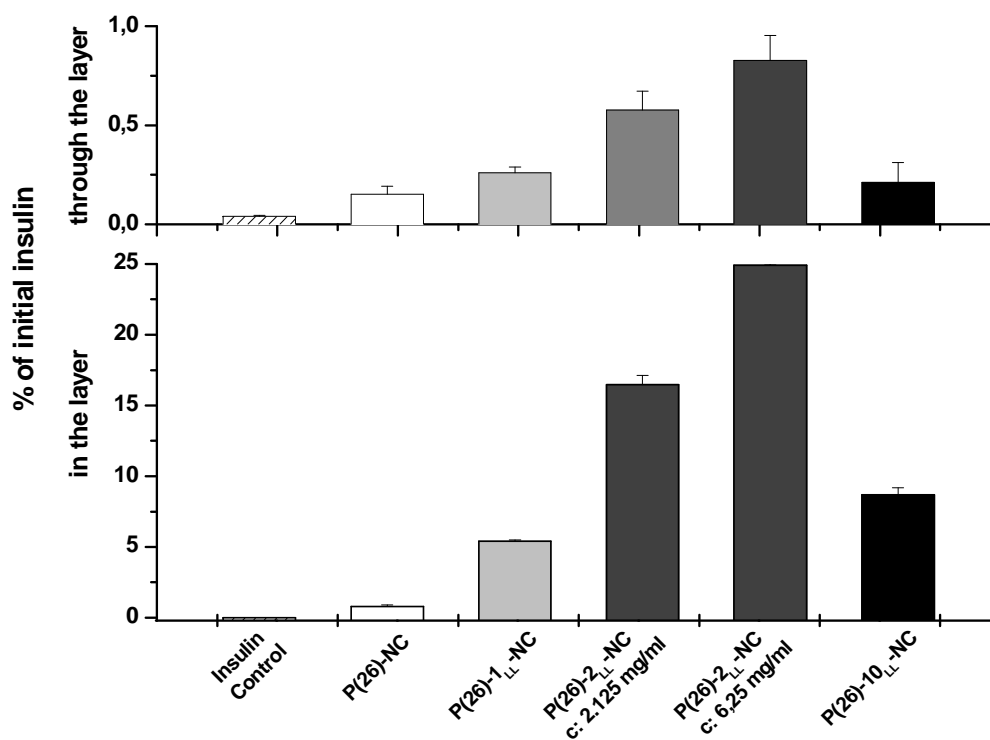


**Figure 8.** Transport studies of TRITC labelled insulin. Upper plot: Percentage of initial concentration of insulin found in the costar transwell® acceptor part. Lower plot: Percentage of initial concentration of insulin internalized in Caco-2 cell monolayers after 2,5 hours.

Although transport remained below 1%, it was demonstrated that all NC-formulations were able to significantly enhance the transport through as well as the uptake in Caco-2 cells compared to pure insulin. Semiquantitative visual information obtained from CLSM images are in accordance with the results of the transport experiments. For internalization we observed again a ranking dependent on amount of lactic grafting for NC, being highest for P(26)-2<sub>LL</sub>-NC with about 25% of the applied insulin dose internalized after 2.5 hours. The performance of the P(26)-10<sub>LG</sub> - NP preparation with 10% uptake and  $0,21 \pm 0,1\%$  transport, did not show considerable advantages in comparison to the complex formulations.

## 4.5. Conclusion

Colloidal carriers made of positively charged DEAPA polyesters revealed some interesting properties as drug delivery system for insulin. The comparison of permeability enhancing effects of nanocomplexes against a nanoparticle formulation, based on a high-grafted polymer version, showed no significant advantages for particles over complexes. However, nanocomplexes physico-chemical properties and interaction with Caco-2 monolayers varied strongly as a function of the polymer structural composition. The most effective variant possesses a combination of a hydrophilic backbone and hydrophobic side chains. On the other hand, this combination led to a higher amphiphilic, surfactant-like character of the molecule, which probably caused damages to membrane and tight junctions, as indicated by LDH release and TEER decrease. However, since these effects seemed to be reversible and NC with a higher lactide-grafting showed the best protection capabilities, the highest internalization and transport through Caco-2 monolayers, it may be assumed that these NC are suitable carriers for insulin to overcome mucosal absorption barriers.

## 4.6. References

- (1) F. J. Gomez-Peres, and J. A. Rull. Insulin therapy: current alternatives. *Arch. Med. Res.* **36(3)**: 258-272 (2005).
- (2) D. R. Owens, B. Zinman, and G. Bolli. Alternative routes of insulin delivery. *Diabetic Medicine* **20**: 886-898 (2003).
- (3) G. Pauletti, S. Gangwar, G. T. Knipp, M. M. Nerurkar, F. W. Okuma, K. Tamura, T. j. Siahaan, and R. T. Borchard. Structural requirements for intestinal absorption of peptide drugs. *J. Control. Rel.* **41**: 3-17 (1996).
- (4) G. P. Carino, and E. Mathiowitz. Oral insulin delivery. *Adv. Drug Del. Rev.* **35**: 249-257 (1999).
- (5) J. G. Still. Development of oral insulin: progress and current status. *Diabetes Metabolism: Res. Rev.* **18**: 29-37 (2002).
- (6) S. Clement, J. G. Still, and G. Kosutic. Oral insulin product hexyl-insulin monoconjugate (HIM2) in type 1 diabetes mellitus. The glucose stabilization effect. *Diabetes Technol Therapy* **4**: 549-566 (2002).
- (7) H. Chen, and R. Langer. Oral particulate delivery: status and future trends. *Adv. Drug Del. Rev.* **34**: 339-350 (1998).
- (8) A. T. Florence. The oral absorption of micro- and nanoparticulates: neither exceptional nor unusual. *Pharm. Res.* **14**: 259-266 (1997).
- (9) S. J. Milstein, H. Leipold, D. Sarrubi, A. Leone-Bay, G. M. Mlynek, and J. R. Robinson. Partially unfolded efficiently penetrated cell membranes – implications for oral drug delivery. *J. Control. Rel.* **53**: 259-267 (1998).
- (10) M. Simon, M. Wittmar, U. Bakowsky, and T. Kissel. Self-assembling nanocomplexes of insulin and water-soluble branched poly[(vinyl-3-(diethyl amino)propylcarbamate-co-(vinyl acetate)-co-(vinyl alcohol)]-graft-poly(L-Lactid): A novel carrier for transmucosal delivery of peptides. *Bioconjugate Chem.* **15(4)**: 841-849 (2004).
- (11) M. Simon, M. Wittmar, T. Kissel, and T. Linn. Insulin containing Nanocomplexes formed by self-assembly from biodegradable amine-modified poly(vinyl alcohol)-graft-poly(L-Lactide): Bioavailability and nasal tolerability in rats. *Pharm. Res.* *accepted 07/ 2005*
- (12) S. Dimova, Brewster M. E., M. Noppe, M. Jorissen, P. Augustijns. The use of human nasal in vitro cell systems during drug discovery and development. *Toxicol. In Vitro* **19(1)**: 107-122 (2005).
- (13) L. A. Dailey, E. Kleemann, M. Wittmar, T. Gessler, T. Schmehl, C. Roberts, W. Seeger, and T. Kissel. Surfactant-free, biodegradable nanoparticles for aerosol therapy based on the branched polyesters, DEAPA-PVAL-g-PLGA. *Pharm. Res.* **20(12)**: 2011-2020 (2003).

- (14) T. Jung, W. Kamm, A. Breitenbach, K. D. Hungerer, E. Hundt, and T. Kissel. Tetanus toxoid loaded nanoparticles from sulfobutylated poly(vinyl alcohol)-graft-poly(lactide-co-glycolide): evaluation of antibody response after oral and nasal application in mice. *Pharm. Res.* **18(3)**: 352-360 (2001).
- (15) M. Wittmar. Charge modified, comb-like graft-polyesters for drug delivery and DNA vaccination: Synthesis and Characterization of Poly(vinyl dialkylaminoalkylcarbamate-co-vinyl acetate-co-vinyl alcohol)-graft-poly(D,L-lactide-co-glycolide)s, Dissertation, Philipps University Marburg, 2004. <http://archiv.ub.uni-marburg.de/diss/z2004/0075/> (accessed 01/13/04).
- (16) R. J. Schilling, and A. K. Mitra. Degradation of insulin by trypsin and alpha-chymotrypsin. *Pharm. Res.* **8(6)**: 721-727 (1991).
- (17) E. Walter, and T. Kissel. Heterogeneity in the human intestinal cell line Caco-2 leads to differences in transepithelial transport. *Eur. J. Pharm. Sci.* **3**: 215-230 (1995).
- (18) I. Behrens, A. I. Pena, M. J. Alonso, and T. Kissel. Comparative uptake studies of bioadhesive and non-bioadhesive nanoparticles in human intestinal cell lines and rats: The effect of mucus on particle adsorption and transport. *Pharm. Res.* **19(8)**: 1185-1193 (2002).
- (19) I. Behrens, W. Kamm, A. H. Dantzig, and T. Kissel. Variation of peptide transporter (PepT1 and HPT1) expression in Caco-2 cells as a function of cell origin. *J. Pharm. Sci.* **93(7)**: 1743-1754 (2004).
- (20) L. A. Dailey, M. Wittmar, and T. Kissel. The role of branched polyesters and their modifications in the development of modern drug delivery vehicles. *J. Control. Release* **101(1-3)**: 137-149 (2005).
- (21) T. Jung, W. Kamm, A. Breitenbach, G. Klebe, and T. Kissel. Loading of tetanus toxoid to biodegradable nanoparticles from branched poly(sulfobutyl-polyvinyl alcohol)-g-(lactide-co-glycolide) nanoparticles by protein adsorption: a mechanistic study. *Pharm. Res.* **19(8)**: 1105-1113 (2002).
- (22) I. Chantret, A. Barbat, E. Dussaulx, M. G. Brattain, and Zweibaum A. Epithelial polarity, villin expression, and enterocytic differentiation of cultured human colon carcinoma cells : a survey of twenty cell lines. *Cancer Res.* **48(7)**: 1936-1942 (1988).
- (23) J. D. Joung, and F. H. Carpenter. Isolation and characterization of products formed by the action of trypsin on insulin. *J. Biol. Chem.* **236**: 743-748 (1961).
- (24) R. Jevprasesphant, J. Penny, R. Jalal, D. Attwood, N. B. McKeown, and A. D'Emanuele. The influence of surface modification on the cytotoxicity of PAMAM dendrimers. *Int J Pharm.* **252(1-2)**: 263-266 (2003).
- (25) D. M. Morgan, V. L. Larvin, and J. D. Pearson. Biochemical characterisation of polycation-induced cytotoxicity to human vascular endothelial cells. *J Cell Sci.* **94**: 553-559 (1989).
- (26) M. Sakai, T. Imai, H. Ohtake, and M. Otagiri. Cytotoxicity of absorption enhancers in Caco-2 cell monolayers, *J Pharm Pharmacol.* **50(10)**: 1101-1108 (1998).

- (27) M. G. Suhaida, I. B. Yahya, and M. Y. Darmawati. Preparation of naltrexone hydrochloride loaded poly (DL-lactide-co-glycolide) microspheres and the effect of polyvinyl alcohol (PVA) as surfactant on the characteristics of the microspheres, *Med J Malaysia* **59**: 63-64 (2004).
- (28) T. Shiomi, T. Tsuchida, and K. Imai. Surface tension of aqueous solutions of poly(vinyl alcohol) with pendant alkyl groups, *Interface Science* **99(2)**: 586-587 (1984).
- (29) S. Hayashi, C. Nakano, and T. Motoyama. The surface tension of aqueous solutions of poly(vinyl alcohol) esterified by fatty acids in homogeneous systems, *Journal of Japan Oil Chemists Society* **14(1)**: 24-26 (1965).
- (30) L. A. Dailey, E. Kleemann, M. Wittmar, T. Gessler, T. Schmehl, C. Roberts, W. Seeger, and T. Kissel. Surfactant-free, biodegradable nanoparticles for aerosol therapy based on the branched polyesters, DEAPA-PVAL-g-PLGA, *Pharm Res.* **20(12)**: 2011-2020 (2003).
- (31) Y. H. Lin, C. K. Chung, C. T. Chen, H. F. Liang, S. C. Chen, and H. W. Sung. Preparation of nanoparticles composed of chitosan/poly-gamma-glutamic acid and evaluation of their permeability through Caco-2 cells, *Biomacromolecules* **6(2)**: 1104-1112 (2005).
- (32) V. Dodane, M. A. Khan, and J. R. Merwin. Effect of chitosan on epithelial permeability and structure, *Int J Pharm.* **182**: 21-32 (1999).
- (33) N. G. Schipper, S. Olsson, J. A. Hoogstraate, A. G. deBoer, K. M. Varum, and P. Artursson. Chitosans as absorption enhancers for poorly absorbable drugs 2: mechanism of absorption enhancement, *Pharm Res.* **14(7)**: 923-929 (1997).
- (34) E. K. Anderberg, C. Nystrom, and P. Artursson. Epithelial transport of drugs in cell culture. VII: Effects of pharmaceutical surfactant excipients and bile acids on transepithelial permeability in monolayers of human intestinal epithelial (Caco-2) cells, *J Pharm Sci.* **81(9)**: 879-887 (1992).
- (35) M. P. Desai, V. Labhasetwar, G. L. Amidon, and R. J. Levy. Gastrointestinal uptake of biodegradable microparticles: effect of particle size, *Pharm Res.* **13**: 1838-1845 (1996).
- (36) P. Artursson, T. Lindmark, S. S. Davis, and L. Illum. Effect of chitosan on the permeability of monolayers of intestinal epithelial cells (Caco-2), *Pharm Res.* **11(9)**: 1358-1361 (1994).
- (37) I. Behrens, A. I. Pena, M. J. Alonso, and T. Kissel. Comparative uptake studies of bioadhesive and non-bioadhesive nanoparticles in human intestinal cell lines and rats: the effect of mucus on particle adsorption and transport, *Pharm Res.* **19(8)**: 1185-1193 (2002).

## **Chapter 5**

### Summary and Outlook

## Summary

In this work biodegradable DEAPA-PVAL-g-PLLA nanocomplexes (NC) were investigated as a colloidal peptide carrier system for non-invasive transmucosal insulin delivery.

**Chapter 1** describes the basic fundamentals of insulin therapy, current status, problems and future trends. The pathogenesis of diabetes mellitus and the different treatment options are discussed to give an understanding of the necessity for alternative non-invasive application systems. It was emphasized that epithelial barriers and enzymatic degradation prevent effective transmucosal insulin delivery.

The current status of the most promising industrial approaches for alternative delivery systems were highlighted. In addition, potential of colloidal biodegradable and bioadhesive polymeric carriers for oral, pulmonal or nasal application of insulin were discussed. The factors bioadhesivity and complexing-capability of polymers were considered with regard to literature. Reference was made to other fields where charge modified grafted polyester of these novel class were already successfully utilized for drug delivery. The objectives of this work were defined.

In **Chapter 2** the DEAPA-PVAL-g-PLLA polymers were characterized for their substitution degree of amine-groups and the extent of lactide grafting. It was possible to manipulate the hydrophilic-hydrophobic balance of these polyesters by factors such as molecular weight, PLLA chain lengths and degree of amine-substitution. Water solubility of these polymers allowed the spontaneous self-assembling with insulin to small nano-sized complexes with narrow size distribution without any mechanic emulsification procedures and without the use of surfactants.

The formulation of nanocomplexes made of polymers with varying structural composition were characterized for various physico-chemical characteristics, such as size distribution, surface charge and insulin association efficiency. Studies with isothermal titration calorimetry

demonstrated the influence of the structural architecture on binding constants. An increase in binding affinity, drug loading, zeta potential and a decrease of complex size could be correlated with a higher substitution degree of DEAPA groups and a higher lactic acid grafting of the backbone.

Systemic investigations of the complexation process, using nephelometric and light scattering techniques, allowed the evaluation of an optimal ratio of the binding partners. The complexes visualized by atomic force microscopy revealed a homogeneous particle collective with spheroidal complexes exhibiting an entangled internal structure.

In **Chapter 3** the suitability of insulin containing DEAPA-PVAL-g-PLLA nanocomplexes as a nasal insulin delivery system was studied under in-vivo conditions at wistar rats. We investigated two different types of NC to evaluate polymer composition influences.

Changes in blood glucose and insulin concentration were monitored in anaesthetized rats using a glucose meter and ELISA. The blood glucose response revealed a significant decrease of glucose concentration, which was accompanied by an increase of exogenous insulin concentration in rat blood. From the investigated two different NC options, the more amphiphilic variant with grafted lactic acid side chains was superior to the more hydrophilic backbone with no additional grafting. The pharmacological response observed in healthy rats was reproduced on streptozotocin induced diabetic rats, demonstrating in-vivo effectiveness in diseased subjects respectively. A significant increase in relative bioavailability was observed at higher polymer concentrations for the grafted variant.

The histological examination of the nasal mucosa with light microscopy showed no signs of toxicity on nasal morphology at the site of application after a single administration procedure. The results demonstrate that the NC significantly enhanced insulin absorption, suggesting that amphiphilic biodegradable comb-structured polymers could be a promising approach for nasal peptide delivery.

In **Chapter 4** the interaction of DEAPA-PVAL-g-PLLA nanocomplexes with enterocyte-like Caco-2 cells in terms of cytotoxicity, transport through and uptake in the cell layers was investigated.

The NC were compared against a nanoparticle formulation based on a higher grafted variant of DEAPA-PVAL-g-PLGA and prepared by a solvent displacement technique. The preformulated NP were loaded with insulin by surface adsorption. The comparison of permeability enhancing effects of nanocomplexes with the nanoparticle formulation, showed no significant differences. However, nanocomplexes physico-chemical properties and interaction with Caco-2 monolayers varied strongly as a function of the polymer structural composition. The most effective carrier possesses a combination of a hydrophilic backbone and hydrophobic side chains. On the other hand, this combination led to a higher amphiphilic, surfactant-like character of the polymer, which probably caused damages to membrane and tight junctions, as indicated by lactate dehydrogenase release and decrease of transepithelial resistance.

However, since these effects seemed to be reversible and NC with a higher lactide-grafting showed the best protection capabilities against trypsinic degradation, the highest internalization and transport through Caco-2 monolayers, it may be assumed that these NC are suitable carriers for insulin to overcome mucosal absorption barriers.

## Outlook

Branched polyesters consisting of poly(vinyl alcohol) (PVA) modified with amine structures and grafted with short chains of poly (lactic acid) (PLA) represent a new class of biodegradable polymers showing significant potential for the development of a variety of drug delivery vehicles. The amphiphilic character and the water solubility of this class provide advantages when dealing with sensitive drug molecules such as peptides.

In this work, nanocomplexes (NC) based on these polyesters, as colloidal carrier for insulin and factors critical for complexation and delivery of insulin to the mucosal tissue of the nose were investigated. The imitation of the physiological postprandial insulin secretion with non-invasive administration procedures is of great pharmaceutical interest. One of the main problems in this field is the finding of suitable insulin carrier systems. It is hoped, that the findings in this work may help to optimize and design a insulin delivery system for mucosal application required in the treatment of diabetes mellitus.

Moreover, further potential of the NC concept is based upon the potential transferability on other therapeutic important peptides. The modular design of the polymers allows for a structural engineering towards specific requirements, like complexation behavior or bioadhesion properties. These polymers are therefore a promising approach in the search for novel suitable excipients for peptide delivery systems in general. Further investigations are necessary to examine this potential.

## **Titel**

Insulin-Nanokomplexe gebildet durch Zusammenfügen mit aminmodifiziertem Poly(vinyl-alkohol)-graft-poly(L-lactid) für die nicht invasive mukosale Applikation: Herstellung, Charakterisierung und in vivo Untersuchungen

## **Zusammenfassung**

In dieser Arbeit wurden bioabbaubare DEAPA-PVAL-g-PLLA Nano-Komplexe als kolloidales Protein-Trägersystem zur nicht-invasiven, transmukosalen Insulin-Applikation untersucht.

**Kapitel 1** beschreibt die Grundlagen der Insulin-Therapie, den Forschungsstand, sowie Probleme und zukünftige Entwicklungen. Die Entstehung von Diabetes Mellitus und die verschiedenen Behandlungsmöglichkeiten werden vorgestellt, um die bestehende Notwendigkeit von alternativen, nicht-invasiven Applikationssystemen zu verdeutlichen. Es wurde herausgestellt das die Epithel-Barriere und der enzymatische Abbau eine effektive transmukosale Insulin-Aufnahme verhindern.

Der aktuelle Stand der vielversprechendsten industriellen Projekte für ein alternatives Darreichungssystem wird beschrieben. Darüberhinaus wird auf das Potential von kolloidalen bioabbaubaren und bioadhäsiven polymeren Trägern für orale, pulmonale und nasale Applikation für Insulin hingewiesen. Faktoren wie Bioadhäsivität und Komplexbildungsvermögen von Polymeren werden im Hinblick auf die Literatur erklärt. Es werden Beispiele aus anderen Bereichen angeführt, in denen Ladungs-modifizierte gepfropfte Polyester aus dieser neuartigen Klasse bereits erfolgreich eingesetzt wurden. Die Zielsetzungen dieser Arbeit werden definiert.

Im **Kapitel 2** werden DEAPA-PVAL-g-PLLA Polymere bezüglich ihres Substitutionsgrades und des Pfropfungsgrades charakterisiert. Es war möglich durch Einstellung von Faktoren wie Molekulargewicht, PLLA Kettenlänge und Amin-Substitution, das hydrophile-hydrophobe Gleichgewicht der Polyester zu beeinflussen. Die Wasserlöslichkeit dieser Polymere ermöglichte deren spontanes Zusammenfügen mit Insulin zu kleinen Komplexen im Nanometer-Bereich mit enger Größenverteilung, ohne Anwendung von mechanische Emulgierschritten und ohne Zusatz von Emulgatoren.

Die Herstellung der Nano-Komplexe aus Polymeren mit unterschiedlicher struktureller Zusammensetzung wurde im Hinblick auf Größenverteilung, Oberflächenladung und Insulin-Bindungskapazität beschrieben. Untersuchungen mit isothermaler Titrationskalorimetrie zeigten den Einfluß von Strukturmerkmalen auf die Bindungskonstante. Ein Anstieg der Bindungsaffinität, der Beladung, des Zetapotentials und eine Verringerung der Komplexgröße konnte mit einem höheren Substitutionsgrad von DEAPA-Gruppen und einem höheren Pfropfungsgrad des Rückgrates korreliert werden. Eine systematische Untersuchung des Komplexbildungsprozesses mit Hilfe von Trübungsmessungen und Streulichtmethoden, ermöglichte die Ermittlung von optimalen Verhältnissen der Bindungspartner. Die Komplexe wurden mit Hilfe von Rasterkraftmikroskopie dargestellt und zeigten ein homogenes Partikelkollektiv mit sphärischen Komplexen und einer knäuelartigen internen Struktur.

Im **Kapitel 3** wurde die Eignung von Insulin DEAPA-PVAL-g-PLLA Nano-Komplexen für die nasale Insulin-Applikation in-vivo an Wistar-Ratten untersucht. Es wurden zwei verschiedene Komplexvarianten untersucht, um den Einfluß der Polymerstruktur zu beurteilen. Änderungen der Glukose - und Insulinkonzentration im Blut der betäubten Ratten wurde mit Hilfe eines Blutzuckermessgerätes und ELISA verfolgt. Der Verlauf der Blutglukose zeigte einen signifikanten Abfall der Glukosekonzentration, begleitet von einer ansteigenden Konzentration exogenen Insulins im Rattenblut. Von den beiden untersuchten Komplextypen zeigte sich die amphiphile gepfropfte Variante, im Vergleich zu dem

hydrophilen Rückgrat ohne Pfropfung, als besser geeignet. Der pharmakologische Effekt, der an gesunden Ratten beobachtet wurde, konnte an Streptozotocin induzierten, diabetischen Ratten wiederholt werden und zeigte die in-Vivo Wirkung damit auch an der eigentlichen erkrankten Zielgruppe. Ein signifikanter Anstieg der relativen Bioverfügbarkeit wurde bei höheren Konzentrationen der gepfropften Variante beobachtet.

Nach einmaliger Applikation der Nano-Komplexe zeigten die histologischen Untersuchungen der nasalen Mukosa mit dem Lichtmikroskop keine toxischen Effekte auf das nasale Zellgewebe am Applikationsort. Die signifikante Insulin-Aufnahme mit Hilfe von Nano-Komplexen zeigt, dass amphiphile bioabbaubare und kammartig-verzweigte Polymere, einen vielversprechenden Ansatz für ein nasales Protein-Trägersystem darstellen.

Im **Kapitel 4** wird die Wechselwirkung von DEAPA-PVAL-g-PLLA Nano-Komplexen mit der Darmzelllinie Caco-2 im Hinblick auf Zelltoxizität, Transport durch und Aufnahme in die Zellschicht untersucht.

Die Nano-Komplexe wurden mit einer Nano-Partikel Formulierung verglichen, die aus einer stark gepfropften Variante von DEAPA-PVAL-g-PLGA mittels Solvent-Displacement-Verfahren hergestellt wurde. Die vorgefertigten Nano-Partikel wurden durch Adsorption von Insulin an die Partikeloberfläche beladen. Der Vergleich der Insulin-Aufnahme fördernden Wirkung zeigte keinen signifikanten Unterschied zwischen Partikel- und Komplex-Formulierung. Allerdings zeigten die physiko-chemischen Eigenschaften der Nano-Komplexe und deren Wechselwirkung mit Caco-2 Zellen eine starke Abhängigkeit von der Polymerstruktur. Die erfolgreichste Variante bestand aus einem hydrophilen Rückgrat und hydrophoben Seitenketten. Diese Kombination verstärkt jedoch den amphiphilen Charakter des Polymers und damit seine Oberflächenaktivität. Eine Eigenschaft die möglicherweise Schäden an der Membran und den Tight Junctions verursachte, wie durch LDH Freisetzung und den Abfall des transepithelialen Widerstandes angedeutet wurde.

Nicht zuletzt weil dieser Effekt reversibel war und Nano-Komplexe mit höherem Propfungsgrad den besten Schutz vor Trypsin-Abbau, die höchste Zellaufnahme und den höchsten Transport durch Caco-2 Zellen aufwiesen, scheint dieses Trägersystem für Insulin geeignet zu sein mukosale Aborptionsbarrieren zu überwinden.

## **Ausblick**

Verzweigte Polyester, bestehend aus Amin-modifiziertem Polyvinylalkohol mit gepfropften kurzen PLA-Ketten, stellen eine neue Klasse von bioabbaubaren Polymeren mit großem Potential für die Entwicklung von Arzneistoff-Trägersystemen dar. Der amphiphile Charakter und die Wasserlöslichkeit dieser Klasse bieten Vorteile im Umgang mit sehr empfindlichen, peptidischen Arzneistoffen.

In dieser Arbeit wurden Nano-Komplexe, basierend auf diesen Polyestern, als kolloidaler Träger für Insulin und die Faktoren, die für eine effektive Komplexierung und Zuführung zu den Schleimhäuten der Nase als kritisch angesehen werden, wurden untersucht. Die Nachahmung der physiologischen postprandialen Insulin-Ausschüttung mit Hilfe einer nicht-invasiven Applikationstechnik ist von großem pharmazeutischen Interesse. Eines der größten Probleme in diesem Zusammenhang ist die Auffindung geeigneter Trägersysteme. Es ist zu hoffen, daß die Ergebnisse dieser Arbeit bei der Entwicklung und Optimierung zukünftiger Insulin-Trägersysteme zur mukosalen Applikation hilfreich sind, welche einmal der Diabetes Behandlung dienen könnten.

Darüberhinaus besitzt das NC-Konzept weiteres Potential im Hinblick auf die mögliche Übertragbarkeit auf andere therapeutisch wichtige peptidische Arzneistoffe. Der modulare Aufbau der Polymere erlaubt die strukturelle Anpassung an spezielle Anforderungen, wie Komplexierungsverhalten oder bioadhäsive Eigenschaften. Die Polymere sind daher ein vielversprechender Ansatz für ein allgemeines Protein-Trägersystem. Weitere Forschung ist notwendig um diese Möglichkeiten zu untersuchen.

## **Appendices**

## Abbreviations

<b>AFM</b>	atomic force microscopy	<b>M<sub>w</sub></b>	molecular weight
<b>AMI</b>	aqueous mist inhaler	<b>MALLS</b>	multi angle laser light scattering
<b>ANOVA</b>	analysis of variance	<b>NC</b>	nanocomplexes
<b>AUC</b>	area under the curve	<b>NIDDM</b>	non-insulin-dependent diabetes mellitus
<b>CDI</b>	carbonyl di-imidazole	<b>NMP</b>	N-methyl pyrrolidone
<b>CLSM</b>	confocal laser scanning microscopy	<b>NMR</b>	nuclear magnetic resonance
<b>DAPI</b>	diamidino-phenylindole	<b>NP</b>	nanoparticles
<b>DEAPA</b>	diethyl-amino-propylamine	<b>NPH</b>	neutral protamine Hagedorn
<b>DMSO</b>	dimethyl sulfoxide	<b>PEC</b>	polyelectrolyte complexes
<b>DNA</b>	desoxyribonucleic acid	<b>pI</b>	point of isocharge
<b>DPI</b>	dry powder inhalers	<b>PLGA</b>	poly(D,L-lactic-co-glycolic acid)
<b>DS</b>	degree of substitution	<b>PLLA</b>	poly(L-lactic acid)
<b>ELISA</b>	enzyme-linked-immuno-sorbent assay	<b>pMDI</b>	pressurized meterd dose inhaler
<b>FCS</b>	fetal calf serum	<b>PBS</b>	phosphate buffered saline
<b>FDA</b>	food and drug administration	<b>PEO</b>	polyethylene oxide
<b>FITC</b>	fluorescein isothiocyanate	<b>PVA</b>	poly(vinyl alcohol)
<b>GALT</b>	gut associated lymphoid tissue	<b>SB</b>	sulfobutylated
<b>GIT</b>	gastrointestinal tract	<b>s.c.</b>	subcutaneously
<b>GPC</b>	gel permeation chromatography	<b>SDS</b>	sodium dodecyl sulfate
<b>HD</b>	Caco-2 cell line from Heidelberg	<b>TEER</b>	transepithelial electrical resistance
<b>H.E.</b>	hematoxylin and eosin	<b>TFA</b>	trifluoroacetic acid
<b>HIM</b>	hexyl-insulin-monoconjugate	<b>THF</b>	tetrahydrofuran
<b>HPLC</b>	high performance liquid chromatography	<b>TLCK</b>	tosyl-L-lysine chloromethyl ketone
<b>IDDM</b>	insulin-dependent diabetes mellitus	<b>TPCK</b>	tosylamide-phenylethyl-chloromethyl ketone
<b>ITC</b>	isothermal titration calorimetry	<b>TRIS</b>	tris(hydroxymethyl)aminomethane
<b>I.U.</b>	international units	<b>TRITC</b>	tetra-methyl-rhodamine isothiocyanat
<b>LDH</b>	lactate dehydrogenase	<b>WGA</b>	wheat germ agglutinin

## Publications

### Research Articles

**Insulin containing nanocomplexes formed by self-assembly from biodegradable amine-modified poly(vinyl alcohol)-graft-poly(L-Lactide): Bioavailability and nasal tolerability in rats**

M. Simon, M. Wittmar, T. Kissel, T. Linn  
Pharm. Res., 2005, **22(11)**, 1879-86

**Self-assembling nanocomplexes of insulin and water-soluble branched poly[(vinyl-3-(diethyl amino)propylcarbamate-co-(vinyl acetate)-co-(vinyl alcohol)]-graft-poly(L-Lactid): A novel carrier for transmucosal delivery of peptides**

M. Simon, M. Wittmar, U. Bakowsky, T. Kissel  
Bioconjugate Chem., 2004, **15(4)**, 841-849

**The Depolymerization of Chitosan: Effects on Physiocochemical and Biological Properties**

S. Mao, X. Shuai, F. Unger, M. Simon, D. Bi, T. Kissel  
Int. J. Pharm., 2004, **281**, 45-54

**Away with the needle. Noninvasive administration routes for insulin: improved quality of life for diabetics**

M. Simon, T. Kissel  
Pharm unserer Zeit, 2001, **30(2)**, 136-141

### Abstracts and Poster

**Protein delivery systems based on branched biodegradable polyesters**

T. Kissel, M. Simon, M. Wittmar  
Proceed. Intern. Symp. Control. Rel. Bioact. Mater., 2002, **29**, 160-162

**Self-assembling insulin-polymer complexes for peroral delivery: Interaction with Caco-2 cell monolayers, peptide transport and cytotoxicity**

I. Behrens, M. Simon, M. Wittmar, T. Kissel  
Proceed. Intern. Symp. Control. Rel. Bioact. Mater., 2002, **29**, 468-470

**Self-assembling insulin-polymer conjugates for mucosal delivery: Preparation and characterization**

M. Simon, M. Wittmar, I. Behrens, T. Kissel  
GPEN, September 13<sup>th</sup> - 15<sup>th</sup>, Uppsala, Sweden, 2000

# Curriculum Vitae

## Persönliche Daten

Michael Simon  
Apotheker  
geb. am 02. März 1973 in Warburg/Westfalen  
Staatsangehörigkeit: deutsch  
ledig

## Schulbildung

08/1979 - 07/1983      Grundschule in Ossendorf  
08/1983 - 06/1992      Gymnasium Marianum in Warburg - Allgemeine Hochschulreife

## Ersatzdienst

11/1991 - 11/1998      Katastrophenschutz, Deutsches Rotes Kreuz, Warburg

## Studium

10/1992 - 04/1997      Pharmaziestudium an der Philipps-Universität Marburg

## Pharmaziepraktikum

05/1997 - 10/1997      Neue Universitäts-Apotheke, Marburg  
11/1997 - 04/1998      Krankenhaus Eilbek, Hamburg

## Diplom

11/1999 - 07/2000      Diplomarbeit unter Leitung von Prof. Dr. T. Kissel, Marburg

## Promotion

08/2000 - 09/2003      Anfertigung vorliegender Dissertation unter Leitung von Prof. Dr. T. Kissel, Marburg

## Berufserfahrung

06/1998 - 10/1999      Apotheker in der Neuen Universitäts-Apotheke, Marburg  
08/2000 - 09/2003      Wissenschaftlicher Angestellter am Institut für Pharmazeutische Technologie und Biopharmazie der Philipps-Universität Marburg  
seit 10/2003            Laborleiter Pharmazeutische Entwicklung, LTS Lohmann Therapie Systeme AG, Andernach

